Université catholique de Louvain
Faculté d'ingénierie biologique, agronomique et environnementale
Département des Sciences du Milieu et de l'Aménagement du Territoire

Automated object-based change detection for forest monitoring by satellite remote sensing:

Applications in temperate and tropical regions

Baudouin Desclée

Mai 2007

Thèse présentée en vue de l'obtention
du grade de docteur en sciences agronomiques
et ingénierie biologique

Jury members:

President:	Pr. Bruno Delvaux (UCL, Belgium)
Supervisors:	Pr. Patrick Bogaert (UCL, Belgium)
	Pr. Pierre Defourny (UCL, Belgium)
Readers:	Dr. Frédéric Achard (JRC, Italy)
	Dr. Dominique Guyon (INRA, France)
	Pr. Benoît Macq (UCL, Belgium)
	Pr. Quentin Ponette (UCL, Belgium)

Tu trouveras bien plus dans les forêts que dans les livres.
(Saint Bernard)

Remerciements

La réalisation d'une thèse est une grande exploration scientifique et humaine remplie de découvertes et de bons moments mais également semée d'embûches et de passages complexes. Ce parcours du chercheur n'est pas une navigation en solitaire mais bien une aventure partagée et portée par de nombreuses personnes qu'il m'est difficile de rassembler entièrement dans ces quelques lignes.

Cette aventure a tout d'abord été rendue possible grâce à mes deux co-promoteurs, Pierre Defourny et Patrick Bogaert, qui m'ont donné l'occasion d'entreprendre et d'accomplir ce projet fascinant. Leur complémentarité aura été d'une grande richesse pour progresser dans ce travail et m'ouvrir à leurs différentes disciplines. Avec une bonne dose de rigueur, de persévérance et d'optimisme, ils m'ont été d'un grand soutien pour progresser dans mes questionnements scientifiques et mieux appréhender la complexité de la recherche. Pour tout cela, je tiens à les remercier chaleureusement.

Les différents membres de mon jury m'ont également apporté de nombreux et précieux conseils afin d'aboutir à cet ouvrage. Je remercie Quentin Ponette et Benoît Macq pour de riches discussions échangées durant ce doctorat ainsi que Dominique Guyon et Frédéric Achard qui ont rejoint cette équipe lors de la défense préliminaire.

De plus, j'exprime ma vive reconnaissance au Fonds National de la Recherche Scientifique (FNRS) qui, au travers d'une bourse du Fonds pour la formation à la Recherche dans l'Industrie et dans l'Agriculture (FRIA), m'a fait confiance dès le début et a accepté de soutenir financièrement ce projet de recherche.

Je tiens également à remercier les différentes personnes avec qui j'ai eu des collaborations enrichissantes pour mieux comprendre les processus étudiés mais également la réalité du terrain. Je pense particulièrement aux agents de la Division Nature et Forêts (DNF) qui m'ont guidé sur le terrain mais également à Marc Languy du WWF qui m'a partagé sa passion sur le fabuleux Parc des Virunga.

Mais ce parcours scientifique fut rendu agréable par la bonne ambiance qui règne dans la Faculté d'ingénierie biologique agronomique et environnementale et particulièrement chez les ENGE. Mélangeant richesse culturelle et convivialité, ce climat est source de grande motivation pour ce travail de longue haleine. Je remercie donc tous mes collègues pour avoir chacun contribué à cela, prolongeant parfois ces bons moments en dehors des portes du laboratoire. Je tiens également à exprimer ma reconnaissance en particulier à Carlos, Julien et Grégory pour les échanges scientifiques passionnants sur les forêts d'ici ou du Congo. Mon passage auprès de l'association des chercheurs de cette Faculté a été également source d'échanges multidisciplinaires passionnants et dont je remercie particulièrement Caroline et Thomas pour ces moments uniques.

Finalement, le soutien continuel de ses proches dans cette longue étape de vie est vraiment indispensable. Mes amis sont ici grandement remerciés pour m'avoir aidé à toujours garder le cap. Mais, je tiens surtout à remercier ma grande famille et spécialement mes parents pour leurs encouragements et leur aide précieuse.

Summary

Forest ecosystems have recently received worldwide attention due to their biological diversity and their major role in the global carbon balance. Detecting forest cover change is crucial for reporting forest status and assessing the evolution of forested areas. However, existing change detection approaches based on satellite remote sensing are not quite appropriate to rapidly process the large volume of earth observation data. Recent advances in image segmentation have led to new opportunities for a new object-based monitoring system.

This thesis aims at developing and evaluating an automated object-based change detection method dedicated to high spatial resolution satellite images for identifying and mapping forest cover changes in different ecosystems. This research characterized the spectral reflectance dynamics of temperate forest stand cycle and found the use of several spectral bands better for the detection of forest cover changes than with any single band or vegetation index over different time periods. Combining multi-date image segmentation, image differencing and a dedicated statistical procedure of multivariate iterative trimming, an automated change detection algorithm was developed. This process has been further generalized in order to automatically derive an up-to-date forest mask and detect various deforestation patterns in tropical environment.

Forest cover changes were detected with very high performances (>90%) using 3 SPOT-HRVIR images over temperate forests. Furthermore, the overall results were better than for a pixel-based method. Overall accuracies ranging from 79 to 87% were achieved using SPOT-HRVIR and Landsat ETM imagery for identifying deforestation for two different case studies in the Virunga National

Park (DRCongo). Last but not least, a new multi-scale mapping solution has been designed to represent change processes using spatially-explicit maps, i.e. deforestation rate maps. By successfully applying these complementary conceptual developments, a significant step has been done toward an operational system for monitoring forest in various ecosystems.

Contents

List of Figures

List of Tables

List of acronyms

ANN	Artificial Neural Networks
ATCOR	ATmospheric CORrection
AWiFS	Advanced Wide Field Sensor
BRDF	Bi-directional Reflectance Distribution Function
CBD	Convention on Biological Diversity
CE	Commission Error
CI	Criteria and Indicators
CLC	CORINE Land Cover
CVA	Change Vector Analysis
DEM	Digital Elevation Model
DMC	Disaster Monitoring Constellation
DN	Digital Number
DNF	Division Nature et Forêts
DOS	Dark Object Subtraction
DRCongo	Democratic Republic of Congo
ENGE	unité d'ENvironnemétrie et de GEomatique
FNRS	Fonds National de la Recherche Scientifique
FRIA	Fonds pour la formation à la Recherche dans l'Industrie et dans l'Agriculture
ETM	Enhanced Thematic Mapper
FAO	Food and Agriculture Organization
GCP	Ground Control Point

GIS	Geographic Information System
GLM	Generalized Linear Model
GMES	Global Monitoring for Environment and Security
GPS	Global Positioning System
HRVIR	Haute Résolution Visible et InfraRouge
IRS	Indian Remote Sensing
ISODATA	Iterative Self-Organizing Data Analysis Technique Algorithm
LCCS	Land Cover Classification System
LISS	Linear Imagine Self scanning System
MAD	Multivariate Alteration Detection
MDDV	Modified Dense Dark Vegetation
MKT	Multitemporal Kauth-Thomas
MMC	Multispectral Multi-date Classification
MMU	Minimum Mapping Unit
MPCA	Multitemporal Principal Component Analysis
NDMI	Normalized Difference Moisture Index
NDVI	Normalized Difference Vegetation Index
NDWI	Normalized Difference Water Index
NGO	Non-Governmental Organization
NIR	Near-InfraRed
OB	Object-Based
OE	Omission Error
OS	Object Signature
PC	Principal Component
PCA	Principal Component Analysis
PIF	Pseudo Invariant Feature
RGB	Red-Green-Blue (color composite)
RMA	Reduced Major Axis

RMSE	Root Mean Square Error
SAA	Sun Azimuth Angle
SFM	Sustainable Forest Management
SMA	Spectral Mixture Analysis
SMAC	Simplified Method for Atmospheric Correction
SPOT	Système Probatoire pour l'Observation de la Terre
6S	Second Simulation of the Satellite Signal in the Solar Spectrum
SRTM	Shuttle Radar Topography Mission
SWIR	Short-Wave InfraRed
SZA	Sun Zenith Angle
TM	Thematic Mapper
TOA	Top-Of-Atmosphere
TOC	Top-Of-Canopy
UNEP	United Nations Environment Programme
UNESCO	United Nations Educational, Scientific and Cultural Organization
UNFCCC	United Nations Framework Convention on Climate Change
VAA	View Azimuth Angle
VZA	View Zenith Angle
WWF	World Wide Fund for nature

Introduction

Monitoring the forests

Forest ecosystems, which cover a third of all terrestrial land areas, have always been crucial for fulfilling many functions including ecological, socio-economic and cultural aspects. Recently, these ecosystems have received considerable attention due to their importance in the global carbon balance and their biological diversity. The worldwide concerns about forest have been reflected into several international conventions such as the UN Framework Convention on Climate Change (UNFCCC) and the subsequent Kyoto Protocol, the Convention on Biological Diversity (CBD) and also into principles of Sustainable Forest Management (SFM).

The important role of forest in global carbon fluxes has been emphasized by the climate change issue. Whereas forest absorbs and stores carbon dioxide over an extended period of time, loss of forest affects climate by releasing this carbon back into the atmosphere. Most of the emissions during the past 20 years are due to fossil fuel burning, the rest (10 to 30%) is predominantly due to land-use change, especially deforestation (IPCC, 2001). However, this amount of carbon emission is still uncertain due to the lack of spatially explicit and consistent information on change in forest area (DeFries et al., 2002; FAO, 2001). Biodiversity loss is another important global issue as the biological diversity of forests is the richest one of all terrestrial ecosystems. However, the reduction of biodiversity is linked to its sensitivity to numerous changes such as climate and land-use changes (Sala et al., 2000). A new international target has been adopted at the CBD Conference of the Parties in 2002 which is to achieve by 2010 a significant reduction of the current rate of biodiversity loss at global, regional and national levels. Some indicators including the forest area and its change have been identified for measuring progress towards this target (Balmford et al., 2005). Concepts of sustainable development have also been applied to forest ecosystems for combining forest management with conservation of all types of forests. In order to assess the quality of forest management by an independent third-party, forest certification was introduced in 1993. Forest certification has the advantage to share the aim of promoting SFM and to assess its implementation by Criteria and Indicators (CI) (Rametsteiner and Simula, 2003). These CI facilitate international reporting and provide a framework for international agreements while reflecting national differences in characteristics and descriptions of forests (Hall, 2001). To study and reduce further environmental degradation, as well as to monitor progress to sustainable development, these indicators of environmental status have to be continuously assessed.

The world's forest covers a large variety of vegetation types ranging from boreal to tropical moist forests and from managed to undisturbed primary forests. Characteristics of forest ecosystems are very different between temperate and tropical regions. The number of tree species in temperate forests is far less important than in tropical forests. However, the diversity of living conditions defined by topography, climate and soil conditions is higher in temperate regions (Kasischke et al., 2004). The forest succession dynamic is also different between these two biomes with fast regeneration in tropical regions compared to longer time period in temperate forests. While both forest ecosystems are concerned by global issues, they also have specific problems due to their different history and context.

Temperate forest has long been subject to human influences, and patterns of significant anthropogenic deforestation date back to the Middle Ages. Currently, the forest area is stable in these regions and even increase slightly (FAO, 2006). The current challenge in temperate forest is thus focused on its multifunctionality for reconciling economical (timber extraction, paper, bioenergy), environmental (water and soil protection, nature conservation) and social (recreation) aspects. As there is a growing demand for fulfilling all these various functions, the different forest stakeholders claim for more participatory processes thus requiring more transparent land-use planning. Moreover, rapid and accurate assessments of forest damage due to several causes like fires and storms are also needed for forest stakeholders and decision makers. The monitoring of forest conditions is indeed a headline of the Global Monitoring for Environment and Security (GMES) program. Forest monitoring tools are thus required for providing up-to-date information necessary for forest management, decision-making and damage assessment.

Tropical forest is a very crucial ecosystem because it cover half of the total world's forest area and represent the largest terrestrial reservoir of biodiversity. During the 1990's, forest degradation and conversion into other land-uses have reached an alarming high rate (Achard et al., 2002; FAO, 2001). In addition of having an impact at global scale, deforestation also induces important consequences at local scale, i.e. damages to soil and water resources, changes in microclimate and socio-economic impacts. The reduction of deforestation processes is difficult due to the combination of several prevailing causes which include agricultural expansion, wood extraction and infrastructure extension (Geist and Lambin, 2002). Although deforestation rate is decreasing in some places (FAO, 2006), many efforts are still required to apply SFM principles in order to have a better integration of the social, nature conservation and economical aspects. Up-to-date measurements of forest extent and forest cover changes are essential for quantifying more precisely forest degradation. Precise mapping of forest changes is also needed for decision-making in order to monitor specific management, e.g. nature conservation, on priority areas as well as for reporting forest status for international conventions.

Forest cover changes and remote sensing

Forest ecosystems are continuously in a changing state given the successive stages of vegetative growth characterizing the forest succession. These natural changes are generally progressive and do not modify forest cover in a important way. However, man-made and natural disasters can affect this succession, causing rapid changes or disturbances. These changes are generally applied on forest stands which are smallest management units of trees with similar composition, age and spatial distribution. The most drastic change is the clear-cut, i.e. the complete removal of canopy cover. When the forest is converted to another land-use, this forest clearing is referred as deforestation implying a long-term or permanent forest cover loss (FAO, 2000). The reverse change is the recovery of the forest cover after a temporary state with no forest cover and is called forest regrowth or reforestation. Other forest changes, e.g. thinning or disease, also have an impact on forest conditions but such disturbances are more subtle. As these last changes modify only slightly the forest cover, they were not taken into account as change in this study. The only forest cover changes considered in this research are forest clearing and regrowth.

Satellite remote sensing provides frequent and quantitative information for monitoring forest in a cost-efficient way. Several studies have demonstrated the close link between spectral reflectance observed from satellite image and forest characteristics (Gerylo et al., 2002; Gholz et al., 1997; Jakubauskas and Price, 1997). Changes in forest cover thus affect the remotely sensed signal. However, the variations of the multispectral reflectance induced by forest cover change should be higher than those from other multitemporal noise sources such as atmosphere, seasonnality and sensor calibration. Based on these assumptions, change detection methods aim at analysing two or more satellite images acquired at different dates for identifying forest cover changes. Different change detection techniques have been developed for identifying land-cover changes (Lu et al., 2004c; Coppin et al., 2004). They can be broadly grouped into three categories, namely visual interpretation, pixel-based and object-based approaches. First, land-cover changes can be detected by skilled analysts by comparing multi-date images and visually delineating areas affected by changes. Second, in order to be more objective and repeatable, pixel-based techniques use digital analysis of satellite images for comparing multi-date pixel values independently of their neighbours. Third, object-based approaches have been applied in change detection for analysing objects, i.e. contiguous pixels grouped together. Thanks to recent advances in image segmentation, this last category of techniques becomes more attractive for improving the efficiency of change detection.

Large-scale forest monitoring can be based on different satellite data which are characterized by their spatial resolution. In order to provide global or regional information about forest cover changes, several studies have been based on coarse to moderate spatial resolution satellite images (Di Maio Mantovani and Setzer, 1997; Hansen and DeFries, 2004; Anderson et al., 2005; Morton et al., 2005; Carreiras et al., 2006). However, these data are inappropriate to detect small changes in fragmented landscapes related to agriculture extension and shifting cultivation, one of the main causes of deforestation. High spatial resolution imagery was found better to grasp small forest changes widely distributed over the landscape. Precise change measurement in forest cover should thus require images from satellite sensors such as Landsat TM, ASTER or SPOT-HRVIR. Whereas high cost, large data volume and low frequency of data acquisition were a problem in the past (Malingreau and Tucker, 1988), these satellite imageries are now accessible in increasing quantity and variety. Moreover, the extent of images acquired by new sensors has increased and becomes as large as 600 km for DMC and 740 km for AWiFS. Satellite image data sets are also provided at global scale such as the GeoCover Landsat mosaic. Operational forest monitoring should thus rely on automated procedures for analysing this continuous and large flow of high spatial resolution satellite images.

Different strategies can be chosen for estimating changes based on high resolution satellite images, either using a sampling procedure or adopting a wall-to-wall mapping. While the first approach produces robust change estimates without information about the spatial distribution, the latter has the advantage to cover exhaustively the whole region of interest and provide geographical distribution of changes (Stehman, 2005). Despite wall-to-wall mapping appears very promising given the increasing satellite data availability, the operational costs and the difficulty to represent change detection results still remain important challenges (Loveland and DeFries, 2004). While the first issue can be reduced by more processing automation, the second one requires new approaches for producing more spatially-explicit change map relevant for different purposes such as decision-making, management and field planning.

Objective and outlines of the thesis

This research aims at developing and evaluating an automated change detection method using high resolution satellite images for monitoring forest cover changes. The first research objective is the automation of the whole process of forest change detection in order to allow rapid analysis of large volume of remote sensing data. The generic aspect of the approach is also a research objective in order to detect forest change in different ecosystems, namely temperate and tropical, and from different data acquired from various satellite sensors. A third objective is to represent forest change detection results in a meaningful and efficient way to support decision-making and forest management. These three objectives are adressed by taking most advantages of the new capabilities offered by the recent advances of object-based techniques.

This thesis is structured in four chapters corresponding to papers published, submitted or still in preparation for scientific journals. *Chapter 1* reviews existing change detection methods developed or applied over forest ecosystems. Focused on techniques using high resolution satellite images, this synthesis groups techniques into three different categories of change detection approaches including visual interpretation, pixel-based and object-based methods. These approaches are divided into key steps for assessing their assets and weaknesses and screening out appropriate elements for the development of an automated forest change detection.

The spectral reflectance dynamics over the forest stand cycle is investigated in *Chapter 2* for characterizing its temporal evolution and identifying spectral changes related to forest cover changes, namely forest clearing and regrowth. Change detection is introduced by the way of multi-date analysis of the multispectral signal and the potential of each spectral band and vegetation index is assessed for detecting the two considered forest cover changes. This per-parcel analysis is focused on conifer stands in temperate forests, given its high reflectance variation over the forest cycle. The spectral reflectance dynamics signal of different change types is analysed for different image temporal resolution in the perspective of generic change detection.

In *Chapter 3*, the automated object-based change detection algorithm is designed, described and applied over temperate regions. This algorithm combines image segmentation into objects and then statistical analysis of their multi-date spectral reflectance behaviour. It relies on the characterization of the spectral variations related to forest cover changes described in Chapter 1 for the same study area. However, all forested lands including both coniferous and deciduous stands, namely areas included into an existing forest mask, are considered for the methodology evaluation. A specific performance assessment is also introduced for evaluating the real improvements of the proposed approach vs. a pixel-based one. Performances of both change detection methods are assessed over Belgian temperate forests to take advantage of the better knowledge of forest changes and of the availability of reference data.

The developed method is then generalized in *Chapter 4* for detecting deforestation over tropical regions and for improving its automation. A step of forest mask update is integrated at the beginning of the approach in order to produce automatically an up-to-date delineation of forest area from any existing forest map and two images acquired at different dates. The robustness of this methodology is then assessed for different deforestation patterns, different time periods and various satellite data thanks to two sources of reference data. This study also investigated the potential of multiscale object-based approach for improving the representation of change detection results and combining different information about deforestation processes into deforestation rate maps.

Finally, the main findings of this research are summarized and the remaining challenges of the forest change detection are discussed in *Conclusions and Perspectives*.

Chapter 1

Review of forest change detection techniques

Abstract

This chapter reviews the literature on the techniques using optical satellite images for forest change detection. Given that the methods are becoming more and more numerous and complex, a new categorisation is proposed to summarize the different approaches from visual interpretation to pixel-based and object-based methods. The different techniques are described and compared in order to assess their degree of automation and their flexibility.

1.1 Introduction

Since early days of earth observation systems, various techniques of change detection have been developed for forest monitoring using high resolution optical remote sensing. These approaches are focused on the identification of forest cover change, described by Geist (2006), including among others forest clearing, regrowth, damage and disease. Different reviews have been proposed in the literature for summarizing and comparing these different approaches (Singh, 1989; Coppin and Bauer, 1996; Lu et al., 2004b; Coppin et al., 2004). However, as new change detection methods are still designed and with the recent development of image segmentation applications, change detection approaches are regrouped into three categories: (1) visual interpretation, (2) pixel-based and (3) object-based methods. This review attempts to summarize the different key steps of each approach (Figure 1.1) in order to assess their degree of automation and their flexibility. It is worth noting that all steps are not required for all methods depending on the change types of interest and on the change detection algorithm.

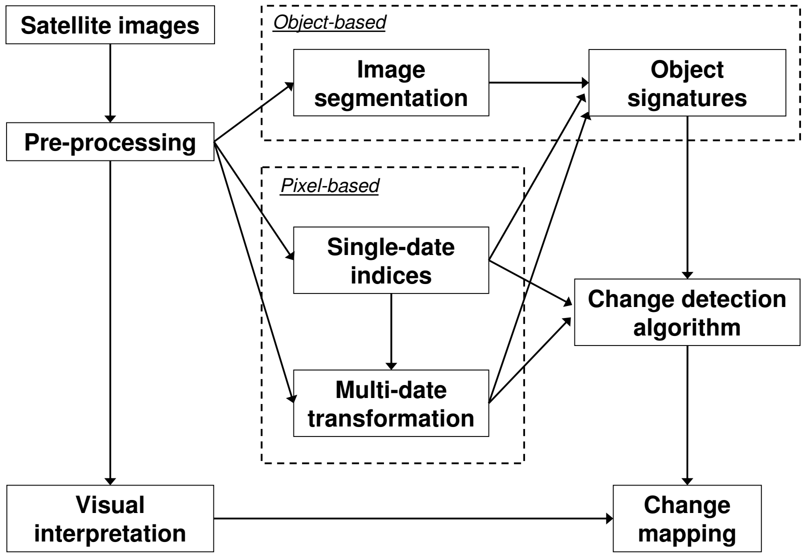

Figure 1.1: Overview of key steps for different change detection methods.

1.1.1 Image acquisition

The selection of appropriate satellite images is very crucial for change detection. With the development of earth observation systems, a large variety of satellite data is now accessible. High resolution optical imagery is most often considered as the most adequate remote sensing data for forest monitoring (Collins and Woodcock, 1999). This category includes satellite imagery acquired from sensors such as SPOT-HRVIR, Landsat TM or ETM, IRS-LISS and ASTER which have a spatial resolution from 5 to 30 m. New sensors, i.e. DMC, can acquire high resolution data (32 m) over a wide swath (600 km per orbit) which makes it well adapted for large-scale change detection.

The timing of the image acquisitions should be closely related to the seasonality of the study area. Near-anniversary images are preferred for reducing the seasonality effect. They are generally selected at the phenological peak season in order to achieve the maximum vegetation cover. Whereas the availability and variety of high resolution satellite images has increased, some regions, particularly the tropical ones, still suffer from difficult atmospheric conditions, drought and other non-seasonal disturbances which often limit the choice of image acquisition dates.

The time interval between images acquisition often depends on data availability. However, the selection of the appropriate interval should be closely linked to the temporal behaviour of the change of interest. Only few authors have studied the impact of temporal frequency on forest change detection. Using vegetation indices, Wilson and Sader (2002) recommended interval between image acquisition less than 3 years for monitoring forest harvesting. Based on normalized difference moisture index (NDMI) and tasseled cap Wetness, Jin and Sader (2005a) distinguished clear-cut which can be detected with image acquisition interval up to 5 years from small harvest requiring a 1 or 2-year interval. Comparing change detection results using 3, 7 and 10-year intervals for detecting clear-cut, Lunetta et al. (2004) found that 3-year interval between image acquisition provides the best results based on tasseled cap Brightness and Greenness.

1.1.2 Pre-processing

The whole change detection process relies on the quality of satellite images to deal with real land-cover change. This quality is ensured by several pre-processing steps which include (1) geometric correction, (2) radiometric and atmospheric correction, and (3) masking.

Precise geometric correction is mandatory for a strong spatial correspondence of multi-date images. Misregistration errors should be below the pixel size in order to reduce the presence of false detection. Although polynomial corrections were commonly performed before, orthorectification using Ground Control Points (GCPs) and a Digital Elevation Model (DEM) becomes more popular and is required since parallax effect is of the same order of magnitude as the pixel size. The higher spatial resolution and the orientation capabilities of recent sensors have increased this effect thus rendering more complex its correction. New automated image registration procedure is still sought but until now, such system has not reached the high precision required for performing change detection.

Radiometric correction reduces unexpected differences between multi-date images due to sensor calibration, Bi-directional Reflectance Distribution Function (BRDF) and geometry of acquisition. This can be performed at different levels from calibration to relative correction (image normalization). Radiometric calibration converts Digital Number (DN) of raw image into Top-Of-Atmosphere (TOA) reflectance thanks to calibration parameters using sensor calibration coefficient. Although this operation reduces the impact of sensor calibration effect, relative correction can also be applied in order to better match images acquired at different dates. The relative radiometric corrections approaches include the Pseudo Invariant Features (PIF) method, the ridge method and the automatic normalization method. Schott et al. (1988) used PIF's, namely temporal stable features, and a reference image for reducing differences between multi-date images. Normalization is performed on a band-by-band basis using the visually selected PIF's with reduced major axis regression between the reference image and another one (Schott et al., 1988). The ridge method identifies invariant pixels based on density function of pixels between two images (Song et al., 2001). The linear normalization function is defined by visual interpretation of the density ridge. Instead of selecting PIFs visually, an automatic normalization method has been developed by Canty et al. (2004) based on Multivariate Alteration Detection (MAD) (Nielsen et al., 1998). For most of change detection studies which aims at detecting drastic changes, relative radiometric corrections are unnecessary (Song et al., 2001). However, some corrections can improve the change detection results and are particularly required for identifying subtle changes. For characterizing early successional forest patterns, the automatic normalization method of Canty et al. (2004) was found efficient for reducing the differences between multitemporal images (Schroeder et al., 2006).

Absolute atmospheric corrections have been proposed to convert TOA reflectance into Top-Of-Canopy (TOC) reflectance based on the composition of the atmosphere at the image acquisition time. These methods range in complexity from Dark Object Subtraction (DOS) (Chavez Jr., 1996; Song et al., 2001), Modified Dense Dark Vegetation (MDDV) (Liang et al., 1997; Song et al., 2001) to Second Simulation of the Satellite Signal in the Solar Spectrum (6S) (Vermote et al., 1997). Based on radiative transfer model of the atmosphere, this last method requires the availability of measurements for vapour, water content, ozone and optical thickness. Simplified procedures as Simplified Method for Atmospheric Correction (SMAC) or ATmospheric CORrection (ATCOR) were found more operational. However, according to Song et al. (2001), these atmospheric corrections can be omitted for certain change detection method like image differencing when based on an algorithm that does not assume zero value for stable classes. While atmospheric corrections are not necessarily required, cloud screening is a mandatory step of pre-processing. This can be done either by visual delineation (Wilson and Sader, 2002) or preliminary classification (Greenberg et al., 2005) or combination of both (Hayes and Sader, 2001).

Masking out features irrelevant for the change detection study, e.g. water bodies or other land-cover types having no interest for the study, is generally required before applied the change detection algorithm. Requested for analysing only forested areas, forest mask can be derived from a land cover classification (Hayes and Sader, 2001; Jin and Sader, 2005a; Guild et al., 2004) based on the first satellite image of the image pair. In order to reduce the time-consuming interpretation required for this classification, forest mask can also be extracted from other data sources such as existing forest map (Häme et al., 1998). However, such maps are rarely produced at the same date as the beginning of the change detection period and thus already introduce error in change detection results.

1.2 Visual interpretation

Visual interpretation using single or multi-date images requires human expertise (computer-assisted or not) for delimiting and labelling zones that are considered as changed. This method can make full use of an analyst's experience and knowledge. Texture, shape, size and patterns of the images are key elements for identification of land cover change through visual interpretation (Lu et al., 2004b). Although this technique is time-consuming and requires skilled analysts, visual interpretation is still widely used (Anttila, 2002; Asner et al., 2002; Franklin et al., 2000; Sunar, 1998). Currently, there is no automatic image processing able to grasp the high complexity of land cover changes made by the combination of several factors such as the stage or the size of the change area. That is why change maps produced for large-area projects with many land cover changes classes like CORINE Land Cover (CLC) 2000 (Büttner et al., 2002) or Forest Resources Assessment (FAO, 2001) are still based on this technique. In order to control the precision of the polygon delineation, the Minimum Mapping Unit (MMU) has been introduced for defining the minimum size of polygon that can be drawn.

1.3 Pixel-based methods

Digital pixel-based methods aim to offer objective and repeatable procedures for identifying land-cover change. These approaches are referred as pixel-based methods given that every pixel is compared from one date to another independently from their neighbours. Each pixel-based method are characterized by a specific combination of three key steps, namely single-date indices, multi-date transformation and change detection algorithms.

1.3.1 Single-date indices

Single-date indices are derived from each satellite image of the multi-date data set. The single-date term underlines the absence of temporal information at this stage. Single-date indices include the reflectance of the different spectral bands or a combination of them (predefined or based on image statistics), or also the result of single-date land-cover classification. In change detection, a combination of different spectral bands into indices is often preferred instead of directly analysing reflectance values for different reasons. First, it reduces data redundancy between spectral bands and processing time for the analysis due to data volume reduction. Second, it facilitates the direct interpretation of the change types. However, it is important to first assess the expected improvement using these indices instead of individual spectral bands. Required for the post-classification comparison, land-cover classification can also be considered as a single-date index. Finally, single-date indices can be summarized in six groups: (1) spectral reflectance, (2) vegetation index, (3) principal component, (4) tasseled cap component, (5) endmember fraction and (6) land-cover class.

Spectral reflectance is the primary source of information for change detection. Many techniques directly use reflectance value from the different spectral bands, but only few studies have compared the contribution of each spectral band in change detection performances. Lu et al. (2005) found that the Short-Wave InfraRed (SWIR, landsat TM5) band provided the best change detection results, followed by the Red band (landsat TM3) for land-cover changes in tropical regions.

Vegetation indices have been widely applied in change detection. These variables related to green leaf biomass were found useful for distinguishing vegetation from other surfaces. The Normalized Difference Vegetation Index (NDVI) has been the most popular index in change detection due its close relationship with leaf biomass and its simplicity of computation and interpretation (Hayes and Sader, 2001; Michener and Houhoulis, 1997; Sader and Winne, 1992; Volcani et al., 2005). Another vegetation index, the Normalized Difference Moisture or Water Index (NDMI or NDWI), is more sensitive to changes in water content (Hardisky et al., 1983). This last index was found less affected to atmospheric effects than NDVI (Gao, 1996). Wilson and Sader (2002) found better accuracy using NDMI than NDVI for detecting forest harvest. Other studies have combined several vegetation indices in order to improve the detection capability (Coppin et al., 2004). Various indices have been developed but no single vegetation index can be considered as better than the others in all change detection cases (Lyon et al., 1998; McDonald et al., 1998). However, by reducing data redundancy, vegetation indices can also be less sensitive for detecting vegetation changes than the original reflectance values (Chavez and MacKinnon, 1994; Lu et al., 2005).

Principal Components (PC) are obtained by linear transformation of spectral bands into a new coordinate system. Principal Component Analysis (PCA) reduces the number of spectral bands to fewer PC's which account for most of the variance from the original multispectral images. To monitor the degraded areas caused by gold miners, Almeida-Filho and Shimabukuro (2002) applied a PCA separately on each of the 6 Landsat TM images. The third PC of each image was selected for performing the change analysis due to the enhancement of degraded areas relative to surrounding savanna vegetated terrain. According to Cakir et al. (2006), the first Principal Component (PC1) corresponds to sharp contrast between vegetation and non-vegetation features. The main problem of PCA is the information reduction to one or two PC empirically chosen for the representation of the change of interest. Moreover, this technique is based on the statistical properties of the satellite data and is thus scene-dependent.

Tasseled cap components produced by the Kauth-Thomas transformation are considered as a global vegetation index. The derived components are in fact a particular PCA which optimises the monitoring of each stage of growing vegetation (Kauth and Thomas, 1976). Crist and Cicone (1984) have derived band coefficients for producing three main components from Landsat TM, namely Brightness, Greenness and Wetness. Used in several change detection studies (Jin and Sader, 2005a; Franklin et al., 2002; Lunetta et al., 2004; Healey et al., 2005), these band coefficients are not scene-dependent but they are sensor-specific.

Spectral Mixture Analysis (SMA) aims at decomposing the reflectance into proportions of different pure spectral signatures or *endmember fraction*. Initially developed for coarse resolution images, SMA approach has been also applied in change detection for identifying subtle changes. Adams et al. (1995) and Roberts et al. (1998) applied SMA based on four endmembers (green vegetation, non-photosynthetic vegetation, soil and shade) to analyse forest land-cover change. Changes are detected by comparing the endmember proportions between multitemporal images (Asner et al., 2003; Greenberg et al., 2005; Lu et al., 2004a). This approach can detect more finer changes but the critical steps of SMA is the time-consuming selection of reference endmembers which can be derived either from the image or from the field.

Classification can be performed independently on each image to convert it into thematic map for further comparison. The process can be done by different ways (unsupervised or supervised) depending on the *a priori* knowledge of the study area. Several approaches are commonly used from simple algorithm (e.g. maximum likelihood) (Currit, 2005; Petit et al., 2001) to more advanced classifiers such as Artificial Neural Networks (ANN) (Gopal and Woodcock, 1996) or fuzzy classification (Deer, 1998). This process provides detailed land-cover information but its application on each image is region-specific.

1.3.2 Multi-date transformation

The multi-date transformation is an intermediate step in the change detection process for combining the spectral and temporal information from all satellite images. Different techniques can compare images acquired at different dates for producing multi-date change index analyzed by the change detection algorithm. These transformations include (1) image differencing, (2) change vector analysis, (3) multitemporal principal component analysis, (4) multitemporal Kauth-Thomas transformation, (5) multivariate alteration detection, (6) chi square transformation and (7) generalized linear models.

The simplest technique is the *image differencing* corresponding to the difference between the values of the same pixel at two different dates. When appropriate radiometric and atmospheric corrections have been applied, the distribution mean tends to zero. The differencing is generally performed on vegetation indices (Coppin et al., 2004; Jin and Sader, 2005a; Lyon et al., 1998; Michener and Houhoulis, 1997; Townshend and Justice, 1995) or tasseled cap components (Cohen et al., 1998; Coppin et al., 2001; Jin and Sader, 2005a). Other studies have subtracted the PC1 from the two images (Cakir et al., 2006; Lu et al., 2005). Image differencing can be also applied on endmember fraction images derived from SMA (Lu et al., 2004a; Rogan et al., 2002). Image differencing is rarely applied on all spectral bands given the difficulty of combining the change detection results from each difference band. Lu et al. (2005) compared the performance of each spectral band using image differencing as well as the combination of them by a majority rule. They found that change detection using the combination of all spectral bands provided the best accuracy, even better than based on NDVI. Image differencing is widely applied in change detection in many different regions given its easy of use and its straightforward character.

Change Vector Analysis (CVA) measures the displacement of a pixel from date-1 to date-2 in the multidimensional space defined by the different spectral bands. Two outputs are derived from each change vector: the magnitude and the direction of the vector. The magnitude, calculated by the Euclidean distance between the two positions, measures the intensity of the change in surface reflectance. The direction, depending on the relative values of the axis coordinates, gives information about the type of change. The CVA method was first developed by Malila (1980) using Brightness and Greenness components for detecting changes in northern Idaho forests. Using the same indices, Lunetta et al. (2004) facilitated the visualization of change vector in the Cartesian Brightness-Greenness space. The extension of CVA to three input bands required an appropriate definition of change direction angles. Extended CVA techniques measured absolute angular changes and total magnitude of tasseled cap components (Brightness, Greenness, and Wetness) (Allen and Kupfer, 2000; Cohen and Fiorella, 1998; Nackaerts et al., 2005). Finally, CVA technique was also applied over all spectral bands only for deriving the change magnitude (Häme et al., 1998). The main advantage of this technique is to simultaneously identify several types of change. However, change directions are often hard to interpret.

The *Multitemporal Principal Component Analysis* (MPCA) is based on the same principle as the PCA described in Section 1.3.1 except that it is applied on the complete multi-date data set. It is expected that one or more multitemporal principal components can be directly related to land-cover changes (Byrne et al., 1980). The main difficulty of this approach is the selection of the components of interest which is mainly done by visual interpretation (Chavez and Kwarteng, 1989; Michener and Houhoulis, 1997; Muchoney and Haack, 1994). Collins and Woodcock (1996) have selected the significant components for forest mortality prediction using a stepwise regression procedure. As MPCA transformation relies on the statistical distributions of the multi-date dataset, this technique is quite image pair-dependent.

Multitemporal Kauth-Thomas (MKT) transformation is the generalization of the Kauth-Thomas transformation for multi-date data (Collins and Woodcock, 1996). The MKT approach produces six main components from a multi-date dataset including the mean (the stable components) and the difference (the change components) of the three tasseled cap components between the two images. Combined with image differencing, the MKT approach was found superior to MPCA due to the physically-based variables produced by MKT compared to the image-dependent components derived by PCA (Rogan et al., 2002).

The *Multivariate Alteration Detection* transformation is an extension of traditional canonical correlation analysis (Nielsen et al., 1998). This transformation generates a set of mutually orthogonal difference images of decreasing variance having the same dimension as the original multispectral images. According to Nielsen et al. (1998), this transformation is invariant to linear scaling of the input data and can use different data types. However, this approach has not been assessed for real change detection applications.

Generalized Linear Models (GLM) were used by Morisette et al. (1999) for combining different change indices such as spectral band differences or tasseled cap differences into a model. The model can be based on different link functions and the best explanatory variables are selected by a stepwise regression method. The appropriated GLM is applied on the enhanced multi-date data set and produces maps of change probability and variability. The main difficulty of this approach is the selection of appropriate models which thus reduces its generalization to other regions.

A *Chi square* transformation is proposed by Ridd and Liu (1998) for combining all spectral bands of image difference into one single change image. The change index is obtained by computing the Mahalanobis distance between the difference value of each pixel and the difference mean for all pixels in the multidimensional space defined by the number of spectral bands. This method is based on the assumption that only a small proportion of the image is changed. A disadvantage of this technique is that change observed in a specific spectral band might not be readily identified in the change image but its flexibility allows its application over various environments.

1.3.3 Change detection algorithms

The crucial step of the whole process is the change detection algorithm. These algorithms which include post-classification comparison, thresholding and classification make the final decision for distinguishing change and no-change features. Preliminary steps were only required for optimizing the input data for the algorithm in order to better discriminate change classes. Whereas thresholding only gives a binary change/no-change response, post-classification comparison and classification provide information about the change types.

Post-classification comparison

The most widely used change detection algorithm is the post-classification comparison which analyses independently produced classified images (Currit, 2005; Deer, 1998; Gopal and Woodcock, 1996; Miller et al., 1998; Petit et al., 2001). This technique provides detailed change trajectories between the two images. Moreover, the independent classification processes reduce the impact of multitemporal effects due to atmosphere or sensor differences (Lu et al., 2004b). However, its main drawback is the impact of classification errors. In fact, the accuracy of the change map is, in the worth case, the product of the accuracy of the two independent classifications. For example, the change map produced by two images classified with 80% overall accuracy would have only 64% overall accuracy (Singh, 1989). In fact, the real rate of change is most often largely lower than the error combination of the two classifications. Finally, this approach is time consuming given that it requires twice complete classifications of the whole scene.

Thresholding

For many approaches relying on direct multi-date analysis, a critical step is the selection of appropriate threshold boundaries between change and no-change pixels (Franklin et al., 2002; Greenberg et al., 2005; Häme et al., 1998; Jin and Sader, 2005a; Jha and Unni, 1994; Le Hégarat-Mascle and Seltz, 2004; Skakun et al., 2003). Given that threshold values are scene-dependent, they should be calculated dynamically based on the image content. However, the thresholds can be determined by three approaches: (1) interactive, (2) statistical and (3) supervised. In the first approach, thresholds are interactively determined visually or by trial and error tests. The second approach is based on statistical measures from the histogram of multi-date change indices. Using image differencing, the threshold selection is commonly based on a normal distribution characterized by its mean m and its standard deviation σ. Values outside the level of confidence determined by $[m - x\sigma, m + x\sigma]$ are considered as changes, where x is the number of standard deviations from the mean determined *a priori*. Third, the supervised approach derives thresholds based on a training set of change and no-change pixels. Techniques for selecting appropriate thresholds are based on the modelling of the signal and noise (Radke et al., 2005; Rogerson, 2002; Rosin, 2002). Whereas thresholds are usually set at equal distance from the change index mean, Cakir et al. (2006) proposed to find different and optimal values for low-end and high-end thresholds. Based on the fuzzy theory, optimized thresholds are determined by using both cumulative producer's and user's accuracies for each change classes. The main advantage of thresholding techniques is their simplicity and ease of interpreting results. Moreover, they allow fast processing of large image data volume. However, they are generally based only on one change index due to difficulty to combine thresholding over several bands, thus assuming that change information is concentrated into this index.

Classification

Classification is the direct analysis of the multi-date dataset for detecting and characterizing areas of change. The multi-date dataset can be either the different single-date indices stacked together (Jolly et al., 1996; Sader et al., 2001; Woodcock et al., 2001) or the change indices derived from the multi-date transformation (Cohen and Fiorella, 1998; Coppin and Bauer, 1994; Healey et al., 2005; Heikkonen and Varjo, 2004; Lunetta et al., 2004; Rogan et al., 2002). Change is expected to show statistics significantly different from no change, so that they can be grouped in specific classes. Like for single-date classification (see Section 1.3.1), different methods have been used for multi-date classification going from common algorithm (Cohen and Fiorella, 1998; Coppin and Bauer, 1994) to more advanced classifiers such as decision trees (Rogan et al., 2003) and ANN (Woodcock et al., 2001). Sader et al. (2001) have developed the "RGB-NDVI" method based on an unsupervised classification over the NDVI of 3 dates for detecting forest harvest. Multi-date classification is an easy-to-use and simple technique given that all images are analysed in one single operation. However, this approach is applied on an *ad hoc* basis and cannot thus be directly extended to other areas. For each new region, the appropriate way to analyse the multi-date image must be found in order to produce high detection performances. Moreover, the classes corresponding to changed areas are difficult to label because of their number and their diversity.

1.4 Object-based methods

Object-Based methods have been proposed to combine the contextual analysis of visual interpretation with the quantitative aspect of pixel-based approaches. Indeed, different pixel-based studies have emphasized the necessity to incorporate inter-pixel dependency for improving change detection results (Rosin, 2002; Bruzzone and Prieto, 2000a). Instead of analysing pixels independently of their location, similar contiguous pixels are grouped into objects. Although the object delineation remains crucial, a limitation of object-based approach is the definition of the MMU. Defined initially to control the visual interpretation process (Saura, 2002), this parameter defines the minimum object size that can be analysed as calculated by its number of included pixels. While first object-based approaches have been based on parcels derived from a Geographic Information System (GIS), the recent advances in segmentation algorithms has increased the interest of these techniques for remote sensing applications.

1.4.1 GIS-data

Forest stand map included in GIS database is an important data source in forest management for planning field operations. The combination of these GIS data with remote sensing was found useful to reduce the spectral noise of pixel-based approach and integrate shape and context aspects into parcel-based analysis. While forest stand delineation has already been combined with satellite images for precise forest mapping (Kayitakiré et al., 2002), it has also been applied for detecting forest disturbances and updating forest information using multi-temporal image data set (Coppin and Bauer, 1995; Heikkonen and Varjo, 2004; Varjo, 1996; Walter, 2004). Spectral information inside each object defined by stand boundaries is summarized and analysed through different change detection algorithms. While this approach takes advantage of multisource information, its performance greatly depends on the geometric accuracy of both data. Indeed, pre-defined boundaries are not always coherent with satellite images and these inconsistencies can induce errors in the final results.

1.4.2 Image segmentation

The objects can also be directly delineated from satellite image thanks to image segmentation algorithms. Image segmentation is the division of satellite image into spatially continuous and spectrally homogeneous regions or objects. While many image segmentation algorithms have been developed in pattern recognition science for several decades (Fu and Mui, 1981; Haralick and Shapiro, 1985; Pal and Pal, 1993), they were only rarely applied in remote sensing applications due to their complexity and difficulty to process large satellite images. Recently, such algorithms have been considerably improved and integrated in remote sensing (Soille and Pesaresi, 2002). Indeed, the analysis of very high resolution satellite images has required to find alternatives from traditional pixel-based classification. These new tools now becomes adequate for many different operational applications in remote sensing but still rarely applied in change detection.

Different segmentation algorithms exist and can be regrouped into two main categories, namely edge-based and region-based. Edge-based segmentation methods detect edges between different regions which sharply contrast and thus define objects delineated by these edges. These approaches are very numerous (Davis, 1975) and they include a first step of edge detection. They generally relie on the computation of an intensity gradient and use edge detecting operators (e.g. Canny, Sobel). Snakes or active contour models are a specific edge-based technique which adjusts arbitrary boundaries until it matches an object of interest (Kass et al., 1988). Finally, supplementary processing steps are required to combine edges into edge chains that correspond better with borders in the image and form a closed object.

Region-based segmentation methods can be divided into region growing, merging and splitting. The most popular technique is the region growing which groups pixels starting from seed pixels and ending when a pre-defined threshold is achieved. The grouping criterion is the homogeneity or a combination of size and homogeneity. The process is repetitive by defining new seeds at each iteration until all pixels are included into objects. In region merging and splitting techniques, the image is divided into subregions and these regions are merged or split based on their properties (Blaschke et al., 2004). Watershed algorithms are also region-based methods and effects the growth by simulating a flooding process, which progressively covers the region (Vincent and Soille, 1991). Watershed transformation generally produces an over-segmented result, with many irrelevant regions. A region merging algorithm could merge these regions but requires a long computational time. Some studies have also combined region-based and edge-based techniques in order to improve their efficiency (Munoz et al., 2003).

Different operational tools have implemented these segmentation techniques. However, their comparison is quite complex due to their variety and the lack of standard for quantitatively assessing them. Meinel and Neubert (2004) have qualitatively compared different existing segmentation tools provided in accessible software for remote sensing applications. They found that among the fast processing techniques, eCognition software produced high quality segmentation results which were also reproductible even if image size is modified.

Change detection has still achieved very little applications using object-based approach while these segmentation tools have known a growing development in many other remote sensing applications. Some attempts have been done for integrating image segmentation and change detection process but these methods have either not been applied and assessed in real change detection applications (Hall and Hay, 2003; Niemeyer, 2006) or did not provide satisfactory results (Saksa et al., 2003).

1.5 Change mapping

Results from change detection include the change map and the derived area estimates. The change map is composed of categorical values which correspond to change classes. The number of classes can be limited to 2 classes (change and no-change) or extended to several change trajectories (the different "from to" classes). A transition matrix is produced by pixel-to-pixel matching of two landcover classifications and provides detailed change trajectories and their corresponding affected areas. The change representation is difficult given that change is generally rare and includes many change trajectories. Many change classes may thus cover a small portion of the study area. Moreover, many studies have pointed out the problem of noise in remote sensing data which induces strong "salt and pepper" effects in the change map. Indeed, each pixel is analysed independently of its neighbours. Whereas recent studies propose to integrate spatial inter-pixel dependency in a post-processing step (Bruzzone and Prieto, 2000a; Nielsen et al., 1998), many change detection methods are still using filter to smooth out isolated change pixel.

The accuracy assessment of change map is crucial for evaluating the quality of change detection results. More complex than for classical thematic map, this procedure have to rely on specific statistical sampling designs and analysis technique (Biging et al., 1998). Except for the kappa coefficient, most accuracy indices are affected by the disproportion of reference data points for the change and the no-change category (Nelson, 1983). Fung and LeDrew (1988) also recommended kappa coefficient for determining optimal thresholds for change detection image. However, reliable change detection accuracy assessments are rather rare due to the difficulty of finding historical reference data and independent from the process of analysis. Finally, very few techniques have been designed for evaluating object-based change detection approach.

1.6 Method comparison

The comparison of change detection methods is rather complex for several reasons. First, each method focuses on specific changes of interest which are different from one study to another. Second, these approaches are based on different sets of satellite images having their own properties such as time interval and study region. Third, given that change indices are generally different from one study to another, change detection methods cannot be directly compared. Only few studies have quantitatively compared change detection methods. For detecting tropical forest clearing and regrowth on a 3-image dataset, highest performances were achieved using the multi-date NDVI classification, also called RGB-NDVI, compared to NDVI differencing and PCA (Hayes and Sader, 2001). With the recent complex techniques, change detection methods become more difficult to benchmark and results appear to be site and data-specific. The comparison is thus done by modifying only one step: the single-date index, the multi-date transformation, or the change detection algorithm. Comparing several change detection approaches for detecting forest changes, both Lu et al. (2005) and Nackaerts et al. (2005) clearly recommended to combine image differencing from all spectral bands for achieving the best results. Guild et al. (2004) have compared hybrid methods by changing only the multi-date transformation. Using tasseled cap components, the simple multi-date unsupervised classification was found better than the two other methods using multi-date unsupervised classification based either on multi-date PCA or on image differencing.

1.7 Conclusions

The variety of forest change detection techniques has been reviewed and classified into three categories. Many approaches, mainly classification, have been developed for *ad hoc* studies using a specific combination of single-date index and multi-date transformation. These methods are generally difficult to replicate directly in other environments. Moreover, several techniques rely on the statistical properties of the satellite images and thresholds for distinguishing change from no-change areas are thus scene-dependent. Whereas there is a growing need for more automation, very few reviewed approaches can be considered as automated. Classification approaches which are rather labour-intensive and region-specific are thus not appropriate for automated change detection. Thresholding algorithms are found more appropriate than classification approaches for rapidly processing massive data volume over various regions. However, pixel-based studies have emphasized the necessity to incorporate inter-pixel dependency for improving the accuracy of change detection results. With the recent advances in image segmentation, object-based offers new opportunities for change detection analysis in order to improve their performances and automation.

Chapter 2

Characterizing spectral reflectance dynamics of conifer stand cycle in a change detection perspective

Abstract

Change detection based on satellite remote sensing relies on the comparison of multispectral reflectance acquired at different dates. A major problem in forest change detection is to separate the signal change related to forest conversion from other sources of noise. Besides the radiometric calibration, the atmospheric and BRDF corrections, the most difficult source of signal change is the ever-changing state of a forest stand from the regrowth to the mature age. This research aims at characterizing spectral reflectance over the whole forest succession in order to quantify the reflectance dynamics and to identify the most appropriate spectral signal for a robust change detection approach. From a large sample of spruce stands, spectral trajectories of forest cycle were derived for Green, Red and NIR reflectances and the NDVI. These trajectories were found typical for spruce stands and consistent between satellite images acquired at 3 and 8-year intervals. Based on multi-date comparison using image differencing, the combination of all spectral bands was proved more discriminant than any single spectral band or NDVI. Two forest changes, namely the clearing and the regrowth, have been distinguished based on multivariate analysis for different temporal resolutions up to 8-year interval. Finally, this study emphasized the need of a better characterization of changes of interest for defining appropriate forest monitoring systems.

2.1 Introduction

Forest change detection remains a challenging issue for remote sensing because most of the forests correspond to an ever-changing state change. However, two forest cover changes show a different order of magnitude in all forest ecosystems: the clearing and the regrowth. Whereas clearing is the removal of a mature forest, regrowth corresponds to the recovering of forest from bare soil to closed canopy cover. Monitoring these two forest changes is essential for operational carbon accounting systems which model carbon cycle dynamics (Kurz et al., 2002) and for ecological habitat assessment. Moreover, information about these changes are also required for evaluating the sustainability of forest management (Hall, 2001). Forest monitoring systems able to detect both change types are thus needed for providing up-to-date status of forest conditions.

Several change detection based on satellite remote sensing, methods have been developed for identifying forest changes over large areas. However, these studies are rather *ad hoc* because they generally rely on prior classifications based on various indices derived from the original spectral bands. Vegetation indices such as Normalized Difference Vegetation Index (NDVI) have often been applied in forest monitoring due to their ease of use and their relation with vegetation biomass (Hayes and Sader, 2001; Sader, 1995; Wilson and Sader, 2002). Other indices such as Brightness, Greenness and Wetness components obtained by tasseled cap transformation have been widely used for detecting forest changes in many studies (Cohen et al., 1998; Coppin et al., 2001; Guild et al., 2004; Franklin et al., 2002; Healey et al., 2006). However, these indices are sensitive to time period between satellite images (Franklin et al., 2005). Using NDVI, Wilson and Sader (2002) recommended an interval between image acquisition less than 3 years. Based on NDMI and Wetness, partial and clear cuts were detectable up to respectively 2 and 5-year interval (Jin and Sader, 2005b). According to Lunetta et al. (2004), monitoring vegetation changes using Brightness and Greenness required time periods up to 3 or 4-year interval between image acquisition. However, the image temporal frequency is often determined by the availability of satellite data (Coppin and Bauer, 1996). Robust approaches are needed for analysing multi-temporal spectral signal and detecting changes over different available temporal resolution, instead of relying on recommended time intervals.

Quantitative models have been developed in order to link spectral reflectance with forest age to monitor the progressive forest evolution. Forest inventory variables including stand age have been also derived from SPOT and Landsat images using multivariate regression (Jakubauskas and Price, 1997; Gerylo et al., 2002; Sivanpillai et al., 2006). Artificial neural network approaches were found efficient for predicting coniferous forest age by taking into account the nonlinear relations between stand age and spectral reflectance (Jensen et al., 1999; Kimes et al., 1996). Other models retrieving forest structure variables have been developed using image texture analysis from very high resolution images (Kayitakiré et al., 2006). Whereas these models were focused on closed canopy forest, other studies focused on early succession, i.e. from bare soil to closed-canopy. Wulder et al. (2004) estimated the age of lodgepole pines during the regeneration using a stepwise multivariate regression model from both spectral reflectance and Wetness. However, as these models focused on the changes of forest state, they rarely cover the whole forest succession, i.e. the different stages from bare soil to mature forest. Different descriptive studies investigated the relationship between conifer succession and spectral reflectance either on early succession or on following succession stages. During early succession, reflectance rapidly decreases in all spectral bands, except for Near-Infrared (NIR) band which increases (Pussa et al., 2005). Red and SWIR bands were found more sensitive to vegetation density than other spectral channels in the first stage of forest succession (Häme, 1991; Horler and Ahern, 1986). In the following succession stages, all spectral bands reach a plateau after the canopy closure except for NIR band which still has an unclear trajectory (Jensen et al., 1999; Fiorella and Ripple, 1993; Nilson and Peterson, 1994; Nilson et al., 2003). Causes of this reflectance variation are numerous and complex but canopy shadow (Spanner et al., 1990) and crown shape (Rautiainen et al., 2004) seem to have an important impact. Better characterization of forest spectral trajectories over the whole succession is thus needed for improving the distinction between major forest cover changes like clearing and regrowth and natural forest reflectance variation.

The objective of this research is the analysis of spectral reflectance dynamics over a conifer stand cycle in order to identify the most appropriate spectral information for forest change detection. These dynamics are characterized over the whole forest succession, i.e. from bare soil to mature forest, for a large set of conifer stands. Using SPOT HRVIR images, this per-parcel study quantifies the effect of the two main forest cover changes with regards to the overall signal range observed over the forest stand cycle. Finally, multi-date image differencing is used to characterize the reflectance change observed over the same stands at different dates in order to define a robust change detection approach.

2.2 Geographical area and sample stands

The geographical area covers more than 180,000 ha located in Eastern Belgium, the Hautes Fagnes region (Figure 2.1). The forest that covers 40% of the total area includes both deciduous and coniferous stands, the last being dominant. This study was focused on coniferous forests, primarily composed of Norway spruces (*Picea abies* (L.) Karst.), for analysing a large number of stands with an equal representation of each successional stages. Covering more than 1,750 ha, a sample of 650 spruce stands, dispersed over the study region, has been selected for the analysis of forest stand cycle. These stands, with mean area of about 2.8 ha, are located on relatively flat areas with elevation ranging from 300 to 610 m. The stand age distribution of the sample is illustrated in Figure 2.2 for the year 2003. This large sample has been extracted from a forest inventory of the state-owned forests for including only monospecific (spruce) and homogeneous (without gaps) stands and covering all successional stages. This forest inventory has been provided in GIS vector format including stand properties, such as species composition and date of the last planting. Forest stands were visually delineated with a MMU of less than 0.1 ha from a mosaic of aerial photographs and stand characteristics were collected on the field and updated in 2003. These digital and orthorectified natural colour aerial photographs were acquired at 1:20,000 scale between 1997 and 1998.

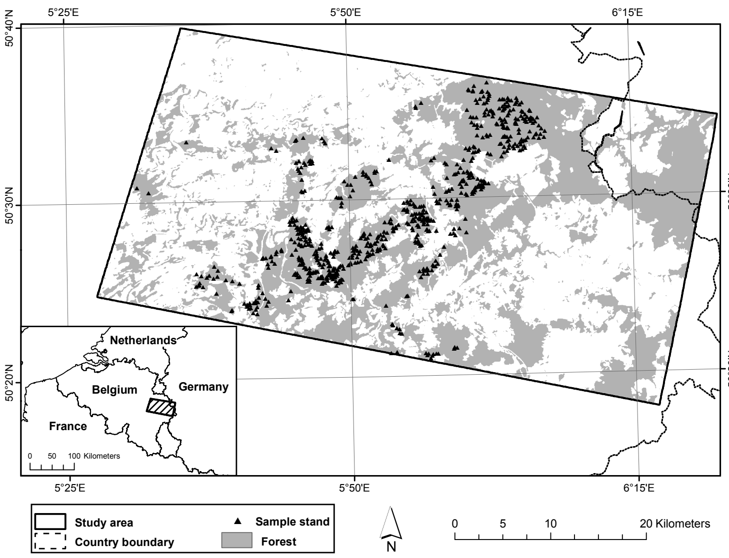

Figure 2.1: Geographical area of the study with the location of the sample spruce stands.

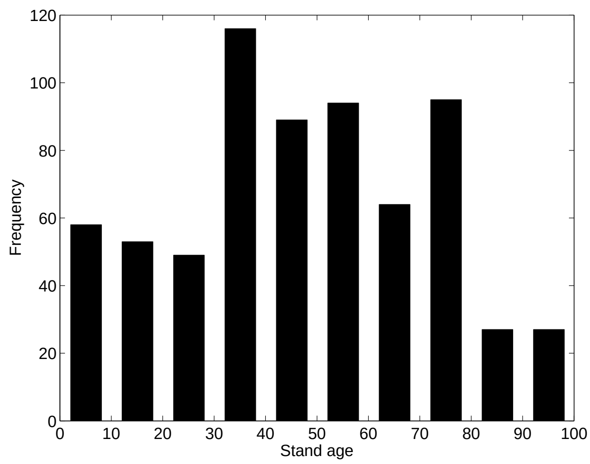

Figure 2.2: Stand age distribution of the sample of spruce stands in 2003 ($n = 650$).

In the study area, forest management of spruces is mainly based on monospecific and even-aged stands. The stand is the minimal forest management unit with homogenous species composition. While forest succession is generally used for the natural evolution of unmanaged forest, this term here corresponds to the forest stand cycle and refers to the different growing stages in managed forest driven by timber harvesting and silvicultural treatments. Based on the Uotila and Kouki (2005) classification, forest succession of managed spruce stands is characterized by the following stages: (1) bare soil, (2) regeneration, (3) sapling, (4) young and (5) mature. After the bare soil resulting of a clear-cut, the regeneration is usually done by plantation (natural regeneration was not observed on sample stands). The canopy tends to be closed after 10 to 15 years when trees reach about 3 m height. Tree grows in height till 14 m (top height) during the sapling stage before having the first thinning at about 25 to 35 years and an age between 60 and 80 years, depending on the soil fertility. Several thinnings are then performed during young and mature stages. Finally, the harvest is completed when trees reach 30 to 35 m height. While these practices can slightly vary, they were similar for most of the stands in the study area. These successional stages, except for young stage which is similar to mature one, are illustrated in Figure 2.3 by a sequence of aerial photographs acquired in August 1997.

2.3 Satellite images and ancillary data

Three SPOT-HRVIR images were acquired in 1992, 1995 and 2003 over the study area. Acquisition parameters are given in Table 2.1. Near-anniversary dates were selected during the summer season. The spatial resolution of multispectral images is 20 m for the two first images and 10 m for the 2003 image. For all images, three spectral bands, i.e. Green, Red and NIR, were available with an additional SWIR band (1.58-1.75 μm) for the 2003 image. The parameters characterizing the geometry of acquisition include the View Zenith Angle (VZA), the View Azimuth Angle (VAA), the Sun Zenith Angle (SZA) and the Sun Azimuth Angle (SAA).

Pre-processing was applied on the three satellite images, including orthorectification and normalization. First, a coregistra-

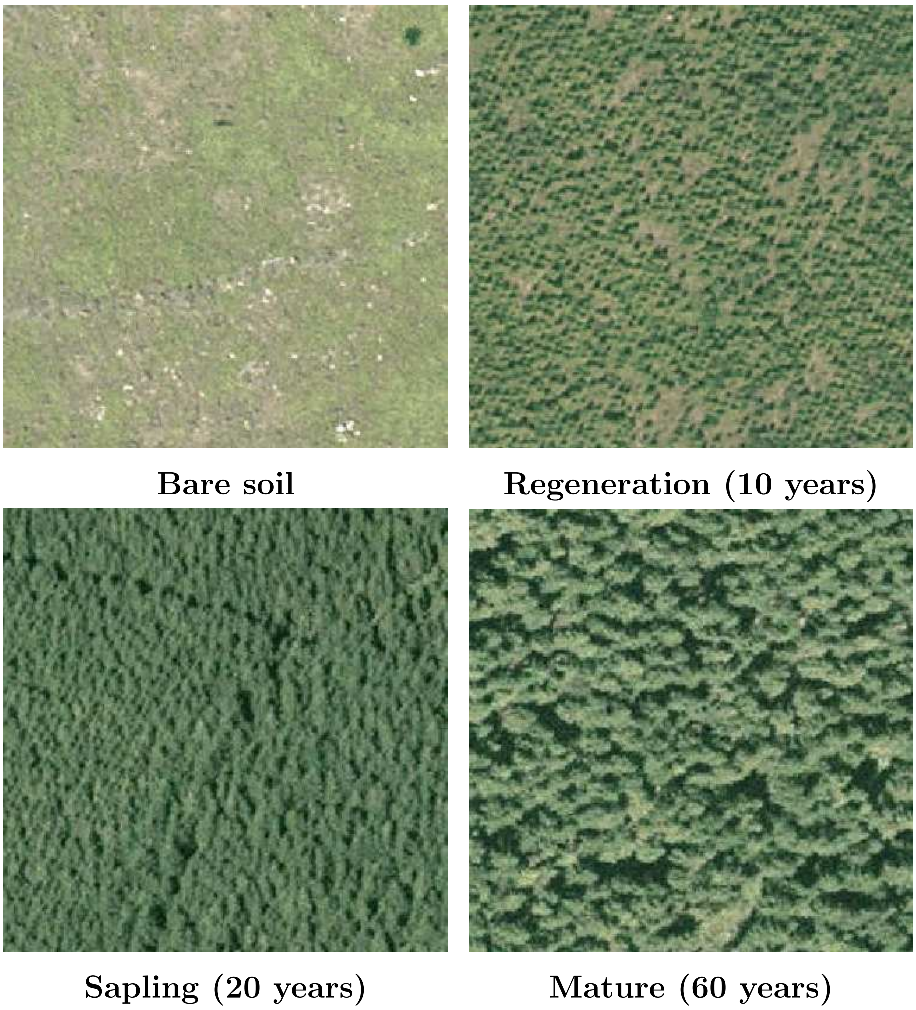

Figure 2.3: Stages of forest cycle of different spruce stands (stand age in brackets) illustrated by extracts of natural color aerial photographs acquired in August 1997.

Table 2.1: Acquisition parameters of the SPOT satellite images (Angles in degrees).

Image	Acquisition date	Sensor	VZA	VAA	SZA	SAA
XS92	7 Aug 1992	SPOT-2	13.4	285.9	34.9	163.2
XS95	24 Jul 1995	SPOT-3	22.3	100.2	33.5	147.4
XS03	14 Sep 2003	SPOT-5	25.8	101.9	48.9	158.1

tion between the three images was carried out with high precision to avoid misregistration errors. Depending on the satellite image, a set of 18 to 26 common Ground Control Points (GCP) spread over the whole study area were selected from aerial photographs. Orthorectification using a DEM was then applied on each image. This DEM was interpolated by bilinear interpolation from contour lines of the 1:50,000 topographic maps. The Root Mean Square Errors (RMSE) were respectively 0.51, 0.66 and 0.39 pixels. Given that this error is about half the pixel size, the effect of misregistration errors on change detection results can be considered as limited (Dai and Khorram, 1998). Moreover, as each image was resampled thanks to bilinear interpolation, the effect of a shifted boundary was expected to be reduced. Second, radiometric corrections between multidate images were performed in two steps: (1) radiometric calibration and (2) radiometric normalization. Radiometric calibration consists in the conversion of DN from raw image into TOA radiance and into TOA reflectance based on the calibration parameters of the satellite sensor. Then, the radiometric normalization aims at matching multidate images to a reference image using PIFs and RMA. The automatic radiometric normalization based on multivariate alteration detection developed by Canty et al. (2004) was selected because it automatically selects PIFs from two images and normalize them. Based on the PIFs, parameters are derived from the linear relationship between each SPOT image and the SPOT 2003 reference image using ordinary least squares regression analysis. The NDVI was derived from the TOA reflectance channels (NIR and Red) respectively for each image where

$$NDVI = \frac{(NIR - Red)}{(NIR + Red)} \tag{2.1}$$

Two image differences were computed from the two pairs of images. The 3 and 8-year difference images were derived from XS95 minus XS92 and XS03 minus XS95.

2.4 Data analysis

The per-parcel analysis was performed in extracting parcel boundaries of the selected stands from the vector data layer. A buffer of 20 m, corresponding to the largest pixel size, was subtracted from each polygon in order to reduce possible edge effects. Stand age was computed by the difference between the image acquisition date and the stand planting date provided by the forest inventory. Based on this buffered stand delineation, summary statistics were extracted from the reflectance of each satellite image (XS92, XS95 and XS03) as well as the image difference (XS95-XS92 and XS03-XS95) including stand reflectance means for the different spectral bands (Green, Red, NIR and SWIR) as well as for NDVI. These statistics were combined with the stand age provided by the forest inventory for constructing the different trajectories. Standard deviations of the stand reflectance averages were also computed for each period of 3 years to describe their distribution.

For multi-date analysis, the unchanged forest state has been compared to the two types of forest cover change, namely clearing and regrowth. Their distinction was based on the planting date provided by the GIS inventory and visually checked on the corresponding satellite images. While the period between harvesting and plantation can slightly vary, it was assumed that an interval of 2 years was typical for the study area. Forest clearing corresponds to the change from mature forest to bare soil, i.e. when the harvesting occurs during the time interval between both images. The forest regrowth corresponds to the recovery of canopy from bare soil to closed-canopy forest, i.e. when the plantation takes place during images interval. Unchanged forest corresponds to forest where no important forest cover change has occurred.

2.5 Results

2.5.1 Spectral trajectories of forest cycle

Figure 2.4 summarizes the temporal trajectories of forest stand cycle for the different spectral bands extracted from the 2003 image. While the chronosequence of forest succession usually starts at the bare soil stage, the mature stage is repeated at the beginning of the trajectory in order to better characterize the impact of forest clearing. The general trend of these trajectories is a reflectance increase due to forest clearing and then a decrease during the subsequent growing stages. However, while the reflectance of all visible and SWIR bands decrease right after the clear-cut, the NIR reflectance increase significantly during the early regrowth stage and decreases only 6 years later.

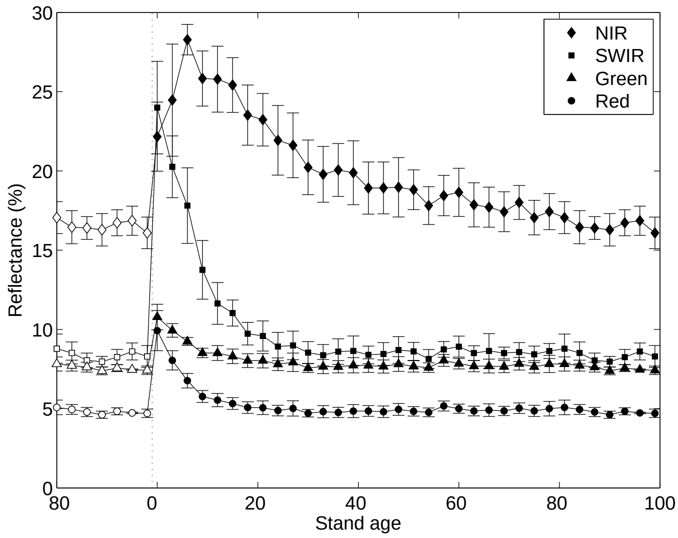

Figure 2.4: Spectral trajectories of forest cycle for spruce stands derived from the 2003 SPOT image. Each point corresponds to the mean reflectance value from all stands within a 3-year interval around the considered stand age while error bars refer to one standard deviation interval. The white symbols correspond to the repetition of the stands at mature stages.

The drastic removal of the forest cover due to clear-cut, i.e. the forest clearing, leads to an increase in all spectral bands but with different intensity according to the wavelengths. This effect is of gradual importance for Green, NIR, Red and SWIR bands. The result of forest clearing is the bare soil with some cutting debris showing reflectance rather higher than vegetation in all spectral bands. While the soil properties can have a significant effect on bare soil reflectance, its impact is generally limited for low organic matter and moisture contents (Guyot et al., 1989).

The reflectance for visible and SWIR bands rapidly decreases asymptotically during the transition from bare soil to closed canopy, i.e. the forest regrowth, due to the development of the vegetation and the proportion reduction of visible bare soil. These reflectances reach the value of a mature forest after 15 years when the canopy is completely closed, i.e. when the effect of underground vegetation on reflectance is negligible. In Green and Red bands, the reflectance decreases due to the leaf pigment absorption including the chlorophyll which reduces mainly Red reflectance. The same trend was observed for the SWIR band due to higher vegetation water content.

While different studies have confirmed that the reflectance decrease for visible and SWIR bands, several authors could hardly characterize the NIR successional trajectory (Häme, 1991; Fiorella and Ripple, 1993; Jensen et al., 1999; Nilson et al., 2003). In this study, its reflectance first increases during the canopy closure to reach its maximum around 6 years and then decreases regularly until the mature stage corresponding to a plateau around 50 years. This particular bell-shape trajectory can be explained by several factors. First, the proportion between young and old needles can have an important influence on the NIR reflectance as needles of the current year have significant higher NIR reflectance compared to older needles (Guyot et al., 1989; Middleton et al., 1997). Second, canopy roughness has also a decreasing influence on NIR reflectance due to the increase of shaded crowns. Its impact depends on the geometry of image acquisition and on canopy roughness which both determine the shadows fraction of the remote sensed signal (Asner and Warner, 2003; Song et al., 2002). Finally, the evolution of the crown shape can have an impact on the reflectance. According to Ishii and McDowell (2002), the crown structure is changing from conical profile for young conifers to cylindrical shape for old ones, thus reducing NIR reflectance.

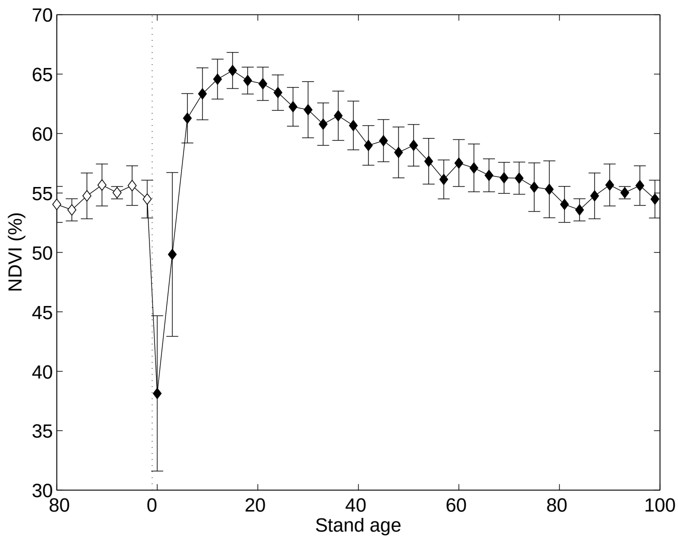

Figure 2.5: NDVI trajectory of forest cycle for spruce stands derived from the 2003 SPOT image. Each point is the mean reflectance value from all stands within a 3-year interval around the considered stand age while error bars refer to one standard deviation interval. The white symbols correspond to the repetition of the stands at mature stages.

As a consequence of Red and NIR temporal profiles, the relationship between NDVI and stand age shows three distinct phases during forest stand cycle (Figure 2.5). From the mature stage, the NDVI drops drastically when a clear-cut occurs. During the forest regrowth, the NDVI rapidly rises to reach its highest value at 15 years. Its value decreases very slowly afterwards to reach the plateau of mature forest value around 40 years. While the link between this index and the vegetation biomass is confirmed for the beginning of the trajectory, the regular decrease of NDVI for closed-canopy forest should be related to the decreasing trajectory of NIR band. As a result of this particular shape, some stages between 3 and 6 years have the same reflectance value as a mature forest which is quite problematic for change detection.

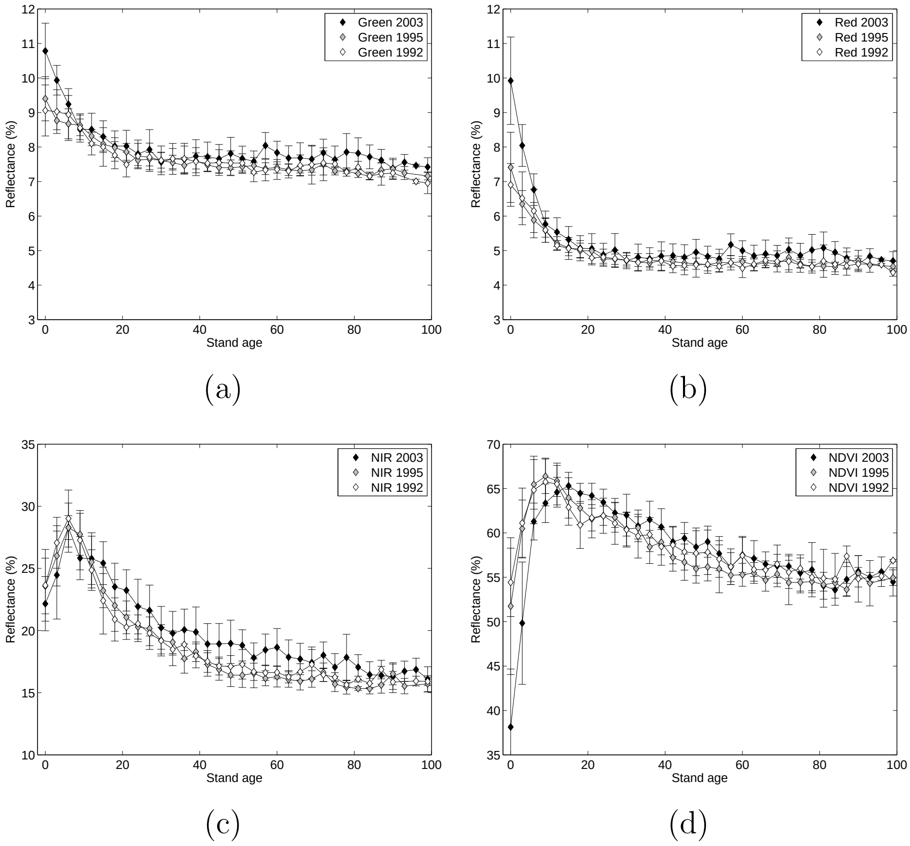

Figure 2.6: Successional trajectories for Green, Red and NIR reflectances as well as for NDVI of spruce stands from SPOT images acquired in 1992, 1995 and 2003. Each point is the mean reflectance value from all stands within a 3-year interval around the considered stand age while error bars refer to one standard deviation interval.

Based on three images acquired in 1992, 1995 and 2003, successional reflectance and NDVI trajectories were compared together in order to confirm the results obtained from the 2003 image (Figure 2.6). These trajectories were found very similar for the three images and can be considered typical for spruce stands with similar management practices. However, the SWIR pattern could not be repeated as it was not provided in the two first images due to SPOT sensor differences.

2.5.2 Detection of forest clearing and regrowth

The two different forest cover changes were then analysed using multi-date images combined thanks to image differencing. Based on the stand age classification described in Section 2.4, the change classes have been characterized using the NDVI and then the combination of Red and NIR mean stand values for different time period, namely 3 and 8-year interval (respectively 1995 minus 1992 and 2003 minus 1995).

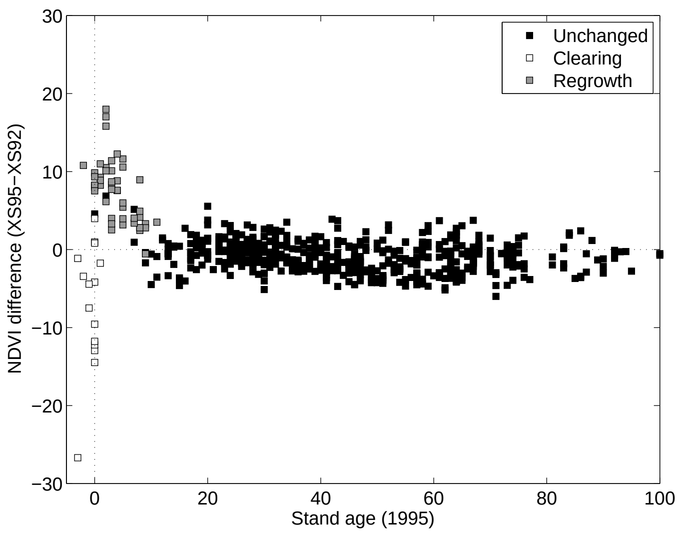

Figure 2.7: Relation between NDVI difference means for 3-year time interval and stange age in 1995 for the sample of spruce stands characterized by different types of forest cover changes.

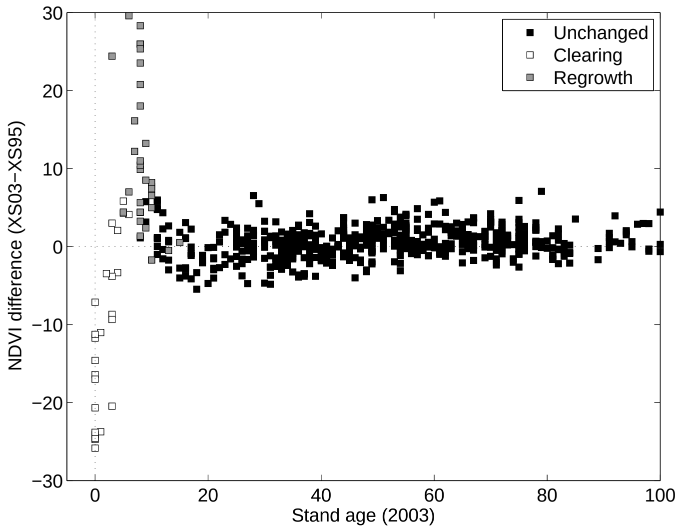

Figure 2.8: Relation between NDVI difference means for 8-year time interval and stange age in 2003 for the sample of spruce stands characterized by different types of forest cover changes.

Figures 2.7 and 2.8 show the relation between NDVI differences and stand age for 3 and 8-year time periods. While the NDVI difference is centred on the zero value for unchanged forest, forest clearing generally induced negative values and positive ones for forest regrowth. But these also highlight the confusion of certain stands affected by forest clearing with unchanged forests when using only this index.

The combination of Red and NIR differences is first illustrated for the 3-year difference image in Figure 2.9. Unchanged stands are centered on zero values for both Red and NIR differences, but the variation of NIR difference values is higher than for the Red band. Both Red and NIR differences are positive for forest clearing as a logical consequence of the increase of reflectance in all spectral bands due to forest harvest. The forest regrowth is characterized by negative Red differences whereas NIR differences are still positive. As observed in Figure 2.4, these spectral changes are related to the different behaviours between the decrease in Red reflectance and the increase in NIR reflectance during early succession. Similar trends were also observed for the 8-year difference image (Figure 2.10). However, the intensity range of difference values is higher for the 8-year than for 3-year period due to the longer time interval. Moreover, the inter-image differences observed between NIR trajectories in Figure 2.6c were higher between the years 1995 and 2003 than between 1992 and 1995.

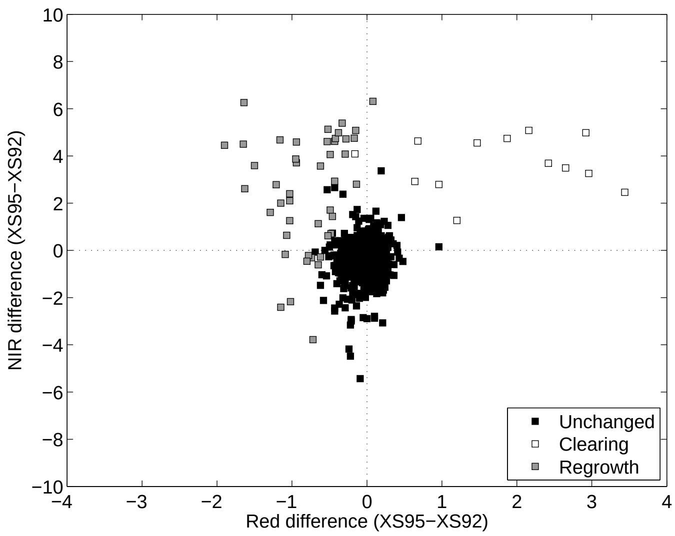

Figure 2.9: Relation between NIR and Red reflectance difference means for each spruce stand derived from 3-year interval SPOT images for different types of forest cover change.

2.6 Discussion

The spectral reflectance and NDVI dynamics were successfully characterized over the whole forest cycle for temperate conifer stands. They combine the different stages of forest cycle and include both important forest cover change (clearing and regrowth) and forest state change when canopy cover is closed. The limited study region in temperate region could limit the generalization of the derived trajectories. But similar trajectories have been derived over other regions. First, the relationships between reflectance and stand age

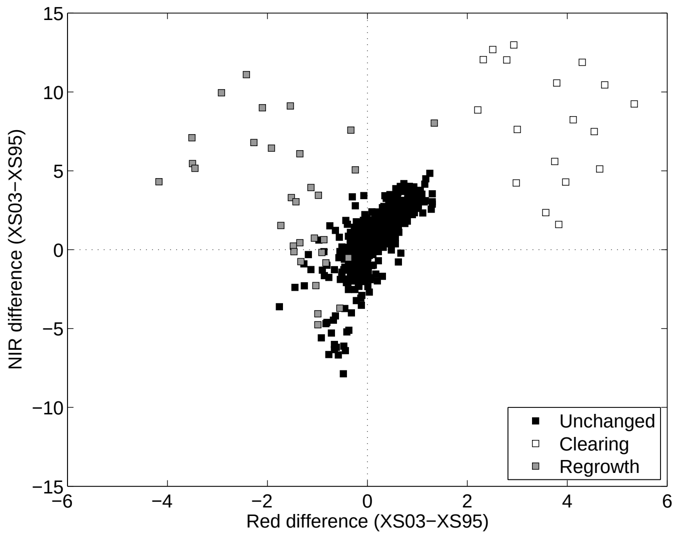

Figure 2.10: Relation between NIR and Red reflectance difference means for each spruce stand derived from 8-year interval SPOT images for different types of forest cover change.

computed by a model developed by Häme (1991) over a pine stand provided similar trajectories in boreal forests. This model simply combines the reflectance of the different elements observable by remote sensing and their respective proportions in terms of cover. Second, the same relationships were derived for tropical forests by Steininger (1996) and Lucas et al. (2002). The NIR trajectory also showed a bell-shape curve but faster spectral reflectance dynamics were observed (NIR peak at about 5 years old) for tropical forests.

These trajectories were found also consistent between satellite images acquired at different dates, though the absolute values could be affected by different external effects such as atmosphere, topography, phenology, sensor calibration and geometry of acquisition. Song and Woodcock (2003) have assessed these effects using multitemporal Landsat images but they concluded that they were difficult to correct given that they are all combined. Schroeder et al. (2006) reduced spectral differences of early forest succession stands between multi-date data using automatic normalization. The same technique was successfully applied in this study for reducing differences due to sensor calibration, geometry of acquisition and atmospheric effects.

For change detection based on multi-date analysis, the selection of appropriate spectral bands or vegetation indices is crucial. The combination of Red and NIR bands was found very efficient for change detection based on different temporal resolution. These two bands are indeed complementary for detecting forest changes. The NDVI was found also interesting for change detection with short time interval (less or equal to 3 years) thanks to its important drop in value at bare soil stage. However, after 3 years of growth, the NDVI value can be similar than mature forest stage one. The SWIR band should be even more appropriate than the Red one because the reflectance difference between bare soil and mature stands is higher. Its importance has already been proved by Jolly et al. (1996) for detecting clear cut areas in multi-date classification. However, the impact of SWIR band was not assessed in this study due to the lack of this spectral band in the first two images.

Spectral trajectories of forest cycle are very useful for selecting the most appropriate spectral bands for change detection depending on the change of interest. This research was focused on two forest changes, including clearing and regrowth. Other forest disturbances, such as diseases or decline, could also be detected if they induce reflectance variation larger than the forest natural growth variability. Moreover, less drastic change, such as natural regeneration, could also be detected using all spectral bands instead of one spectral band or NDVI.

The per-parcel analysis of forest spectral reflectance dynamics is a first step toward object-based approach for detecting changes. While the boundary of forest stand was here derived from GIS-data based on visual delineation, objects could be directly derived from the satellite image using image segmentation approach. Wulder et al. (2004) have efficiently combined both GIS-data and image segmentation for deriving stand age of lodgepole pines. Such trajectories could be also useful for several applications such as automatic forest map updating as well as regeneration monitoring.

Forest monitoring should be linked to the forest management and its related silvicultural treatments. During the study period, spruce stands were mainly planted by artificial regeneration. However, the recent evolution in silvicultural practices promotes the natural regeneration. This change in silvicultural practices will result in harder detection of forest clearing as the removal of forest canopy will not concern the whole stand area.

2.7 Conclusions

This study has highlighted the high spectral reflectance dynamics for conifer stands during the whole forest cycle. Variations in spectral reflectance are mainly due to important forest cover changes, namely forest clearing and regrowth. The evolution of NIR reflectance during forest cycle has been found to have a bell-shape reflectance trajectory, thus inducing a particular trajectory for NDVI. These trajectories derived from a large sample of spruce stands were found also consistent between satellite images acquired at different dates.

The detection of these forest cover changes through multi-date comparisons has been assessed using image differencing for two time periods, namely 3 and 8-year intervals. Each spectral band has a change type discriminant potential but they have a decreasing discriminant potential from NIR, Red to Green bands. Using these three spectral bands together (multivariate) was found more efficient for whatever time period than using a single one or the NDVI (univariate).

Focused on conifer stands in temperate regions, these results can be extended to other ecosystems as similar relationships between forest age and reflectance were found for boreal and tropical regions. This suggests incorporating the potential of multivariate analysis into generic change detection approaches. Moreover, while SWIR reflectance cannot be used in this study, its trajectory close to the Red band one with higher amplitude suggests its high potential for change detection. Finally, it could be useful to derive spectral trajectories for other change types in order to extent the detection approach to these changes and propose a change type labelling in various forest environments.

Chapter 3

Forest change detection by statistical object-based method *

Abstract

Forest monitoring requires more automated systems to analyse the large amount of remote sensing data. A new method of change detection is proposed for identifying forest cover change using high spatial resolution satellite images. Combining the advantages of image segmentation, image differencing and stochastic analysis of the multispectral signal, this OB-Reflectance method is object-based and statistically driven. From a multi-date image and a forest mask, a single segmentation using region-merging technique delineates multi-date objects characterised by their reflectance difference statistics. Objects considered as outliers from multitemporal point of view are successfully discriminated thanks to a statistical procedure, i.e. the iterative trimming. Based on a chi-square test of hypothesis, abnormal values of reflectance differences statistics are identified and the corresponding objects are labelled as change. The object-based method performances were assessed using two sources of reference data, including one independent forest inventory, and were compared to a pixel-based method using the RGB-NDVI technique. High detection accuracy ($> 90\%$) and overall Kappa (> 0.80) were achieved by OB-Reflectance method in temperate forests using three SPOT-HRVIR images covering a 10-year period.

*Adapted from Desclée, B., Bogaert, P. and Defourny, P. (2006). Forest change detection by statistical object-based method. *Remote Sensing of Environment*, **102**, 1–11.

3.1 Introduction

Forest ecosystems have never been so affected by human pressure than currently (FAO, 2001). The rapid conversion or degradation of forest environments is thus of important international concern. Forest monitoring mainly focuses on detecting and estimating the land conversion rate and, more recently, on assessing carbon stocks in the forest ecosystem. Operational systems for monitoring and updating forest maps are thus needed for many applications such as forest management, carbon budgeting and habitat monitoring (de Wasseige and Defourny, 2004; Foody, 2003; Sader et al., 2001).

Satellite remote sensing is widely used to detect forest change and update existing forest maps. Many change detection techniques have been developed since the early days of earth observation. However, because of the enormous amount of remote sensing data to analyse, operational monitoring systems require more automated methods. An efficient change detection procedure should be objective, easy to use, and should require a limited number of parameters for extracting changes. Indeed, the huge amount of work that has been done in change-thresholding of the histograms of vegetation-difference-images clearly warrants the reduction of human intervention in the process (Bruzzone and Prieto, 2000b; Fung and LeDrew, 1988; Jin and Sader, 2005a; Le Hégarat-Mascle and Seltz, 2004). By using an automated procedure, this time-consuming human interpretation could thus be limited to the class labelling of the identified changed areas. However, in spite of increasing demand connected with international concern about forest, very few automatic algorithms have been proposed in the literature (Rogan and Chen, 2004). Taking advantages of object-based techniques, two methods have already been developed but they suffered of low detection performances. The first one is the unsupervised technique of Häme et al. (1998) which is based on change vector analysis. By analysing groups of pixels to reduce the "salt and pepper" effect, this technique does not take advantage of image segmentation. The second one is based on a presegmentation step coupled with an unsupervised ISODATA classification (Saksa et al., 2003). This technique failed to correctly extract clear-cut areas because the segmentation and the clustering algorithm were not appropriate (MMU too large and classification based on object difference means).

This research aims to develop a new method to extract land cover changes in forest by taking advantages of image segmentation, image differencing and stochastic analysis of the multispectral signal. Using high spatial resolution images and a forest mask, this method was sought to be scene-independent and easy-to-use. This study also aims to test this new approach on a multi-year SPOT-HRVIR data set and to compare its performances to the pixel-based method using the RGB-NDVI technique.

3.2 Study site and data

As the study site and the data have been already described in Sections 2.2 and 2.3, the reader can start at Section 3.3 for avoiding repetitive readings. However, it is important to notice that the whole forest land is taken into account for this change detection analysis.

The study site covers more than 180.000 ha and is located in Eastern Belgium. The forest that covers 40% of the total area includes both deciduous and coniferous stands, with the last type being dominant. Land cover changes are more frequent and cover larger areas in conifer stands because they are rather monospecific and have a shorter exploitable age. Whereas different forest management systems coexist, many clear-cuttings occurred in coniferous stands on areas ranging from 0.1 to more than 10 ha. After this forest removal, the forest regeneration can either rely on natural recolonisation or young tree plantation. The distinction between these two regeneration techniques is not possible using the available remote sensing data.

Three cloud-free multispectral SPOT-HRVIR images were acquired over a decade and are considered as our multi-date dataset. Near-anniversary dates during the phenological peak season were selected in order to reduce the seasonality effect. The acquisition dates for these images were August 7th 1992 (XS92), July 24th 1995 (XS95) and September 14th 2003 (XS03), respectively from SPOT-2, -3 and -5 satellites. The difference in the spatial resolution between images (20 m for the first two and 10 m for the last one) was corrected by bilinear interpolation resampling of the last image (XS03) to 20 meters. Moreover, because the SWIR band was only available for the last acquisition, this spectral band was not used in the study. The 3 spectral bands, respectively Green, Red and NIR, were combined for the 3 dates in a 9-band multi-date dataset.

Ancillary data included a forest inventory data layer, GIS topomaps, aerial photographs, the 1990 CORINE Land Cover (CLC) map and a DEM. The 2003 updated forest inventory of the state-owned forest was provided in GIS vector format including stand properties, such as the species composition and the date of the last planting. Forest stands were delineated from aerial photographs with a MMU of less than 0.1 ha and stand characteristics were collected on the field. This independent data source was used as reference for the accuracy assessment. Topographic maps 1:10,000 scale were used for the field survey. A set of digital and orthorectified aerial photographs 1:20,000 scale acquired in 1997-1998 was also available for the selection of very precise GCPs for accurate coregistration and validation. The CLC map, as produced by classification of Landsat images in 1990, served as a coarse independent forest mask which was then visually improved. Finally, a 30 m DEM was resampled at 20 m by bilinear interpolation for the orthorectification of the satellite images.

Two pre-processing steps were required for a meaningful comparison of the satellite images. First, a coregistration between the three images was carried out with high precision to avoid misregistration errors inducing false change alerts. Depending on the satellite image, a set of 18 to 26 GCPs spread over the whole study area were selected from aerial photographs. Orthorectification using the DEM was then applied on each image. The RMSE were respectively 0.51, 0.66 and 0.39 pixels. Secondly, as significant radiometric differences between images (due to geometry of acquisition and sensor calibration) could prevent the comparison of absolute reflectance values in multitemporal analyses (Häme, 1991), the radiance of images was radiometrically corrected into TOA reflectance using the calibration parameters of SPOTimage (Lillesand et al., 2004). In order to apply the RGB-NDVI method, the NDVI was calculated from the TOA reflectance channels (NIR and R) respectively for each image (Equation 2.1). From the 3 satellites images, two multi-date dataset were produced: (i) the 3 NDVI bands, and (ii) the 9 TOA reflectance channels.

3.3 Object-based methodology

The proposed change detection method is object-based and statistically driven. This technique, presented in Figure 3.1, includes 3 steps resulting in the production of change maps. First, the multi-date segmentation partitions the whole multi-year image into objects. Second, the object multi-date signatures are extracted from each object to characterize the object spectro-temporal behaviour. Third, the multivariate iterative trimming is a statistical procedure to identify changed objects based on theirs object signatures.

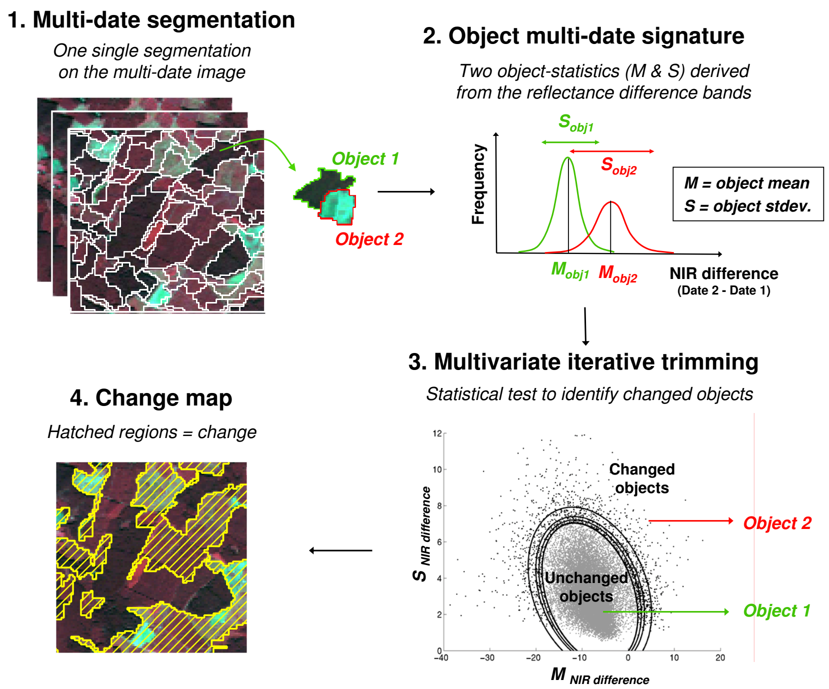

Figure 3.1: General principles of the Object-Based change detection method using Reflectances (OB-Reflectance).

Over the time span covered by a sequence of satellite images, the change detection algorithm aims to distinguish "changed objects", corresponding to areas with forest cover change (clearing and regrowth), from "unchanged objects" (i.e., regular growth of closed-canopy forest). The proposed algorithm relies on three basic assumptions: (i) changes are rare and concern a small part of the total study area, (ii) unchanged objects exhibit similar reflectance differences and (iii) changes induce large surface reflectance variation and abnormal reflectance differences. Assuming these hypotheses hold, the algorithm measures for each object the surface reflectance variation over time and compares it between objects. Object exhibiting abnormal reflectance change over time can thus be statistically identified and labelled as changed areas. It is worth noting that the proposed basic assumptions are most often respected for forested areas, even if the change proportion clearly depends on the time interval between observations as well as on the region size. As a confirmation of the second assumption, Liang et al. (1997) and Coppin and Bauer (1994) take advantage of unchanged forests as stable targets for radiometric calibration between multi-date images.

3.3.1 Multi-date segmentation

Image segmentation is the process of partitioning an image into groups of pixels that are spectrally similar and spatially adjacent, by minimizing the within-object variability compared to the between-object variability. The object delineation has been achieved using a general segmentation algorithm based on homogeneity definitions, in combination with local and global optimization techniques, as implemented in the e-Cognition commercial software (Baatz and Schäpe, 2000). The segmentation algorithm is a region-merging technique which fuses the objects according to an optimization function given by Equation 3.1, with

$$w_{\mathrm{sp}} \sum_{\mathrm{nb}} w_b \sigma_b + (1 - w_{\mathrm{sp}}) \left(w_{\mathrm{cp}} \frac{l}{\sqrt{\mathrm{np}}} + (1 - w_{\mathrm{cp}}) \frac{l}{\mathrm{lr}} \right) \leq h_{\mathrm{sc}} \qquad (3.1)$$

where nb is the number of spectral bands, σ_b is the within-object standard deviation for the spectral band b, l is the object border length, np is the number of pixels and lr is the shortest possible length given the rectangle bounding the pixels (although each band b can potentially have a specific weight, referred to as w_b, the same weight has been considered for all bands in this study). This function also includes three kinds of user-defined parameters or weights. The spectral parameter w_{sp}, trades between spectral homogeneity vs. object shape. The compactness parameter w_{cp}, trading compactness vs. smoothness, adjusts the object shape between compact objects and smooth boundaries. Finally, corresponding to the threshold of heterogeneity, the scale parameter h_{sc} controls the size properties of the produced objects.

Traditionally, the segmentation process has only been applied to one single satellite image (Flanders et al., 2003; Mäkelä and Pekkarinen, 2001; Wulder et al., 2004). In this study, objects are defined in a single operation from the whole set of spectral bands using all sequential images together. This approach, hereafter denoted as multi-date segmentation, relies on spatial, spectral and temporal information to delineate suitable objects, so that pixels that are spectro-temporally similar in a nb-dimensional space are grouped together, where nb refers to the number of different spectral bands for the set of sequential images.

3.3.2 Object multi-date signature

In order to compare the multi-date evolution of the spectral signal, the reflectance of the three sequential (dates 1, 2 and 3) satellite images were subtracted pairwise for all pixels belonging to the same object. Thus, two image differences were computed from the successive observations, i.e. dates 2-1 and dates 3-2.

For each object delineated by the previous multi-date segmentation, the distribution of the reflectance difference values was summarized by a multi-date signature. This signature includes two descriptive statistics, i.e. the mean (M) and the standard deviation (S), corresponding respectively to a measure of surface reflectance difference and heterogeneity. As these differences are computed for each band, the multi-date signature X_{ij} of each object can be defined as a vector, with

$$X_{ij} = (M_{ij1}, ..., M_{ijb}, S_{ij1}, ..., S_{ijb})' \tag{3.2}$$

where i refers to the object, j (with j=1 or 2) to the image difference considered, and b to the number of spectral bands.

3.3.3 Multivariate iterative trimming

Using the vectors as defined in Equation 3.2, changed objects from the unchanged ones were separated by a statistical analysis using an iterative trimming procedure. Trimming is defined as the removal of extreme values that behave like outliers. The common purpose of this procedure is to reduce the sensitivity to outliers for many parameter estimates, such as the sample mean and variance (Kotz et al., 1988). In the case of a Gaussian distribution, the trimmed mean is a robust estimation of the mean that is not affected by outliers. According to Bickel (1965), this estimator is efficient under a variety of circumstances. More details about this technique can be found in Huber (1972), Hoaglin et al. (1983) and Lee (1995). It is worth noting that the trimming procedure is applied here in a slightly different context. While typically used to eliminate abnormal values, these values need to be kept in our context, as the corresponding objects are classified as changed.

The object reflectance differences over time are similar for undisturbed forest because the local forest heterogeneity is efficiently smoothed out by the combination of image differencing and image segmentation. Assuming that observed differences are due to various uncontrolled factors, the distribution of the multi-date signature parameters for unchanged objects could be reasonably approximated by a Gaussian distribution (this assertion will be validated for both M and S statistics from the results of the analysis). These limited modifications of the temporal reflectances are also expected to sharply contrast with the high and heterogeneous reflectance modifications (respectively on M and S statistics) in the case of forest cover change. As the segmentation do not always produce pure objects, the S statistic is very crucial for detecting objects partially changed. The statistical values for changed objects thus tend to be located mainly in the head and tail of the distribution, so that they behave like outliers with respect to those for unchanged objects.

In this study, the trimming procedure was performed in its multivariate version, that takes simultaneously into account the different object statistics appearing in each vector X_{ij}. The combination of several variables by way of multivariate analyses strengthened the analysis. Using simultaneously the object standard deviation of reflectance difference in addition to the object mean of reflectance difference for all spectral bands, the capability of detecting changes increases, as e.g. these changes may affect the various spectral bands to different extents. As proposed above, let us assume that for unchanged objects, X_{ij} is Gaussian distributed with mean vector m_j and covariance matrix $\sum_j$, so that we can define

$$C_{ij} = (X_{ij} - m_j)' \sum_j^{-1} (X_{ij} - m_j) \sim \chi^2(2b) \tag{3.3}$$

where C_{ij} is the square of the Mahalanobis distance for the object i and the image difference j. Given that all C_{ij} are chi-square distributed with $2b$ degrees of freedom, we can thus write that

$$P(C_{ij} < \chi^2_{1-\alpha}(2b)) = 1 - \alpha \tag{3.4}$$

i.e., for a chosen probability level $1 - \alpha$ (with $1 - \alpha = 0.99$, for example), we can identify a value $\chi^2_{1-\alpha}(2b)$ that C_{ij} will only exceed with probability α. If α is chosen to be small, a simple hypothesis test at the $1 - \alpha$ confidence level consists of identifying any C_{ij} value that exceeds this threshold as a potentially outlying value, so that in our context the corresponding object i is flagged as changed. This procedure is similar to the approach applied by Ridd and Liu (1998) using a pixel-based approach, which proved to be efficient to detect changes in an urban environment. The confidence level $1-\alpha$ can be optimized to the application at hand thanks to a training data set.

Clearly, applying Equation 3.3 can only be done if one knows the corresponding m_j and $\sum_j$. These can be initially estimated directly from the whole set of corresponding X_{ij} vectors, but as this set is precisely expected to contain outlying values, this could lead to poor estimates. We thus propose to use Equations 3.3 and 3.4 in an iterative approach. Initial estimates $\hat{m}_j$ and $\hat{\sum}_j$ are computed from the whole set of objects, and a first trimming is applied. From the set of objects flagged as unchanged, new estimates $\hat{m}_j$ and $\hat{\sum}_j$ are obtained, and trimming can be applied again. This iterative procedure is stopped when no new objects are flagged as changed. Instead of extracting changed objects in a single step from poor initial estimates $\hat{m}_j$ and $\hat{\sum}_j$, the selection of outliers thus becomes finer at each new iteration. An illustration of the iterative procedure results is given in Figure 3.2, where only a single band has been used for the sake of simplicity; as the number of iterations increases, the corresponding confidence ellipses shrink progressively until no more additional changed objects are identified.

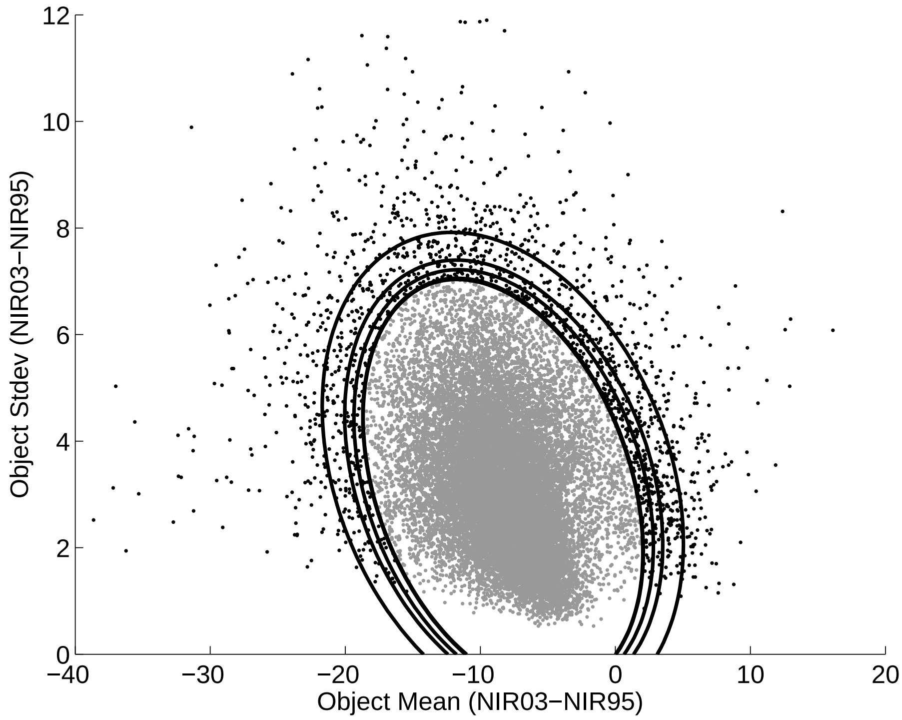

Figure 3.2: Detection of changed objects from two statistics describing the reflectance difference (XS03-XS95) for the NIR spectral band, i.e. the mean (Object Mean) and standard deviation (Object Stdev). The iterative process is illustrated by the ellipses drawn for iterations 1, 2, 3 and 13 (out of 13 iterations). Points outside the smallest ellipse (iteration 13) are all considered as changed objects.

As described above, the whole procedure was only applied on a single image difference. It was, however, repeated respectively for both image differences and the results were combined, in the sense that an object detected as an outlier in at least one of the statistical tests was considered as "changed" for the whole change detection process.

3.4 Experimental design

The proposed Object-Based (OB) methodology was tested on the SPOT-HRVIR images in order to assess its performance using only the NDVI series on one hand (OB-NDVI) and using all of the 9 reflectance bands on the other hand (OB-Reflectance). These results were compared to a robust pixel-based method, i.e. the RGB-NDVI (Sader et al., 2001) and an extension of this technique, the Multispectral Multi-date Classification (MMC).

3.4.1 Object-based change detections

The multi-date segmentation was carried out from the 9 TOA reflectance bands of the SPOT images using equal weights for all bands. The segmentation parameters w_{sp} and w_{cp} of Equation 3.1 were equal set at 0.5 to produce objects which are expected to correspond to forest stands. In the first parameter, spectral and shape criterions have been selected to have the same importance in order to obtain spectrally homogenous objects while irregular or branched objects are avoided. The second parameter is selected to equally balance between compactness and smoothness as there are generally both crucial in forest stand delineation. The h_{sc} was set at 5 to obtain image segmentation with a minimum object size of 0.5 ha, or 12 pixels of the SPOT-HRVIR image. This corresponds to a trade-off between the minimum size of change object which could be detected and the number of pixels per object required to compute robust summary statistics.

To compare their respective change detection performances, two separate datasets were prepared: (i) NDVI differences and (ii) TOA reflectance differences. The NDVI differences were computed from the two NDVI paired images, i.e. NDVI95–NDVI92 and NDVI03–NDVI95. For each object obtained from the multi-date segmentation, M and S statistics were extracted from each NDVI difference image, so that for each object i and image difference j, we could define the corresponding vector $X_{ij} = (M_{ij}, S_{ij})'$. The iterative trimming procedure was applied to each image difference and the results of these 2 analyses were combined. Whereas the confidence level is generally set at 0.99 in statistical tests, a preliminary optimization of this parameter was completed to maximize the overall accuracy of the change detection algorithm. The appropriate confidence level was thus selected thanks to an optimization step based on a training set of 1230 objects. These objects, different from the reference data, have been visually selected and interpreted in order to include the different change types, namely clearing and regrowth, at different time and for both deciduous and coniferous stands. For the NDVI data set, the confidence level 1–α was selected by an optimization step and the optimized value was defined equal to 0.975 (see section 3.5.3). This approach will be named hereafter Object-Based method using NDVI (OB-NDVI).

Similarly, the same protocol was applied to the reflectance difference dataset (OB-Reflectance) from the two multispectral images differences XS95–XS92 and XS03–XS95, where each image difference includes 3 difference bands, i.e., the NIR, Red and Green. For each object i and difference image j, the corresponding vector is thus $X_{ij} = (M_{ij1}, M_{ij2}, M_{ij3}, S_{ij1}, S_{ij2}, S_{ij3})'$. The trimming procedure was run separately for each image difference and the results obtained separately for the 2 image differences were combined. The optimized confidence level 1–α was defined equal to 0.99 for OB-Reflectance.

3.4.2 Pixel-based change detections

Using the 3 NDVI bands of the multi-date SPOT dataset, the RGB-NDVI technique of Sader et al. (2001) was applied to produce change maps. The unsupervised ISODATA clustering algorithm (Richards, 1993) produced 45 multitemporal classes which were interactively labelled in binary format (change vs. no-change) based on the visual interpretation of the color composites without using validation dataset.

Similarly, this technique was extended to a more general classification, namely MMC, using the Green, Red and NIR bands of the three SPOT images, i.e. 9 bands. The unsupervised ISODATA classification also subdivided 45 classes interactively labelled into change or no-change.

3.4.3 Accuracy assessment

Among the various accuracy assessment methods presented by Biging et al. (1998) and Foody (2002), the change detection error matrix was chosen and computed for each change map. According to Zhan et al. (2002), 4 accuracy indices derived from this error matrix are required to compare these change detection methods. The *overall accuracy* is the proportion of changed and unchanged elements (objects or pixels) that are correctly classified by the method. The *detection accuracy* is the proportion of correctly detected changed elements. The *omission error* is the proportion of omitted changed elements, while the *commission error* is the proportion of falsely detected unchanged elements. κ analysis (Cohen, 1960) uses the overall Kappa and the per-class Kappa statistic, which is a measure of accuracy or agreement based on the difference between the error matrix and chance agreement (Rosenfield and Fitzpatrick-Lins, 1986).

The comparison between different category of change detection techniques requires three types of validation approach: (i) a polygon-wise validation for the object-based method, (ii) a pixel-wise for the pixel-based method and (iii) a polygon-wise for the pixel-based method. First, for a polygon-based mapping output, any pixel-based accuracy assessment would tend to underestimate the map accuracy (Biging et al., 1998). The proposed object-based method was thus evaluated in a polygon-wise way. Each object randomly selected for the accuracy assessment was compared to the corresponding forest parcel of the validation dataset. The change label (change or no-change) was compared to the change attribute of the reference data. Given that the selected MMU is 0.5 ha, an object is validated as changed if more than 0.5 ha of its area is covered by a change forest stand of the validation dataset. Second, as the multi-date classification is a pixel-based change detection method, it was evaluated by a pixel-wise assessment. Third, in order to directly compare the two change detection methods, the change maps obtained by multi-date classification were assessed not only pixel-wise but also polygon-wise, following the example of Zhan et al. (2002). For the polygon-wise assessment of the pixel-based method, the change attribute of each object from the multi-date segmentation was derived from the area of the changed pixels. If this changed area is higher than the MMU defined at 0.5 ha, the polygon is classified as changed.

Two sources of reference data were considered as complementary for the method assessment. The first reference dataset was based on the visual interpretation of each one of the 1000 objects randomly selected out of the about 22,000 objects processed by the algorithm. From the false color composite of each date, each of the 1000 objects was interpreted as changed or unchanged. The second reference dataset consists of approximately 325 randomly selected objects where forest inventory information was available. Not based on these satellite images, this independent dataset strengthened the accuracy assessment. Because of random selection, changed vs. unchanged samples were not evenly distributed and the proportions of changed objects were equal to 33% for visual interpretation and 20% for forest inventory.

3.5 Results

Four change maps have been produced based on the 4 change detection techniques, namely RGB-NDVI, OB-NDVI, MMC and OB-Reflectance. From the performances indices assessment, the method comparison has been done separately for each input data, namely the NDVI and the reflectance. Depending of the change detection objectives, the proposed object-based method can been tuned by a preliminary optimization step, presented for OB-Reflectance in Section 3.5.3. An example of the OB-Reflectance change map is presented in Figure 3.3 beside the corresponding multi-year images.

3.5.1 Methods comparison using NDVI

Table 3.1 shows the accuracy assessment results based on four performance indices computed from OB-NDVI and RGB-NDVI change maps using both validation approaches and both reference dataset. The overall accuracy of both change maps was similar (about 83%) but the high proportion of unchanged objects made this index less appropriate to evaluate the change detection algorithm. The detection accuracy which is a more informative index to assess the change detection performances was much higher for OB-NDVI (65%) than

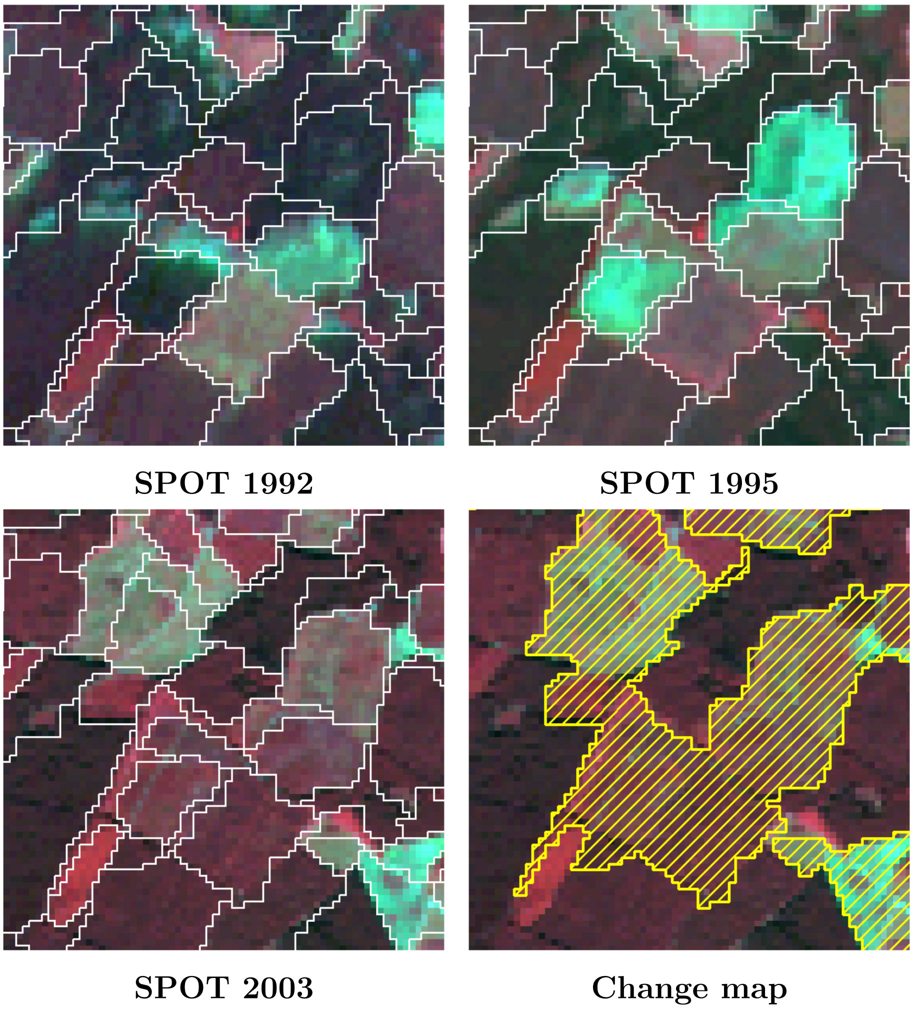

Figure 3.3: False color composite subsets (RGB=NIR-Red-Green) of each image of the SPOT time series (1992-1995-2003) overlaid by the multi-date segmentation result. Bright objects are clear-cuts while regions in reddish grey are regenerating areas. The hatched regions on the change map correspond to detected changed objects by the OB-Reflectance method.

for RGB-NDVI (51%). The efficiency of this algorithm was also reported by the omission error (35% vs. 49%) and the commission error (18% vs. 29%). For the polygon-wise validation, the RGB-NDVI detection accuracy was higher whereas the overall accuracy was lower. For the change class, the Kappa statistic was higher for OB-NDVI (0.52) than for RGB-NDVI (0.40), and the overall kappa's were respectively 0.61 vs. 0.49. The independent reference dataset derived from the forest inventory confirmed these results. The detection accuracy was still higher for the object-based method (66% vs. 49%).

Table 3.1: Performance indices for both change detection methods using NDVI, as estimated by two validation approaches, i.e. polygon-wise and pixel-wise, and two sources of reference data, i.e. visual interpretation (n=1000) and forest inventory database (n=325, between brackets).

Change detection method	OB-NDVI	RGB-NDVI	RGB-NDVI
Validation approach	Polygon-wise	Polygon-wise	Pixel-wise
Detection accuracy (%)	64.6 (66.2)	64.3 (58.8)	50.6 (49.2)
Omission error (%)	35.4 (33.8)	35.7 (41.2)	49.4 (50.8)
Commission error (%)	18.1 (26.2)	39.0 (56.0)	28.6 (32.6)
Overall accuracy (%)	83.7 (88.0)	74.8 (75.7)	82.7 (86.6)
Kappa : Change class	0.52 (0.58)	0.45 (0.43)	0.40 (0.41)
Kappa : No-change class	0.73 (0.67)	0.42 (0.29)	0.62 (0.60)
Overall Kappa	0.61 (0.62)	0.44 (0.35)	0.49 (0.49)

3.5.2 Methods comparison using reflectance

Table 3.2 summarizes the validation results for both change detection methods using all calibrated reflectance channels, i.e. OB-Reflectance and MMC. While the performances of the pixel-based method remained about the same as when using NDVI, the object-based accuracy was improved using reflectances. Indeed, the OB-Reflectance overall accuracy was as high as 93% whatever the validation source. Similarly, the detection accuracy was found higher than 91% for the proposed technique, while omission and commission errors were reduced. The MMC commission errors were low (16%) but can be considered as a logical consequence of the 51% omission errors. The polygon-wise validation of the MMC again provided detection accuracy better than the pixel-wise. The increase in commission errors was offset by the decrease in omission errors, so the overall accuracy remains about the same. The two per-class κ were similar for the OB-Reflectance (0.87 vs. 0.81) whereas the κ for the change class was lower than the no-change class for MMC (0.41 vs. 0.79). The OB-Reflectance overall kappa was much higher than using the MMC method. The independent reference dataset derived from the forest inventory also confirmed these results. The OB-Reflectance detection accuracy was still higher (91% versus 63%).

Table 3.2: Performance indices for both change detection methods using reflectances, as estimated by two validation approaches, i.e. polygon-wise and pixel-wise, and two sources of reference data , i.e. visual interpretation (n=1000) and forest inventory database (n=325, between brackets).

Change detection method	OB-Reflectance	MMC	MMC
Validation approach	Polygon-wise	Polygon-wise	Pixel-wise
Detection accuracy (%)	91.5 (91.2)	54.9 (70.6)	49.4 (62.7)
Omission error (%)	8.5 (8.8)	45.1 (29.4)	50.6 (37.3)
Commission error (%)	13.0 (21.5)	24.7 (32.4)	15.9 (17.8)
Overall accuracy (%)	92.7 (92.9)	79.3 (86.8)	85.1 (90.9)
Kappa : Change class	0.87 (0.88)	0.41 (0.62)	0.41 (0.57)
Kappa : No-change class	0.81 (0.73)	0.63 (0.59)	0.79 (0.78)
Overall Kappa	0.84 (0.80)	0.50 (0.61)	0.54 (0.66)

3.5.3 OB-Reflectance optimization

Due to its statistical design, the object-based method can be optimized according to the purpose of the change detection. Indeed, the alpha parameter (α) in the statistical test defines the confidence level 1-α and can be tuned either to maximize one of the performance indices or to balance both of them. From the subset of 1230 objects (different from the validation set), the four detection performance indices were computed for different α values using the OB-Reflectance (Figure 3.4). For α=0.002 up to 0.05, the omission error decreased whereas the commission error logically increased. The detection accuracy increased with α, reaching 100% accuracy for α=0.05. In this case, the commission errors were high (about 52%) corresponding to many false change alerts. Whereas the overall accuracy was still the same for α=0.002 up to 0.02, the detection accuracy variation was about 20%. Using the reflectance, the highest overall accuracy combining both errors was reached for α=0.01.

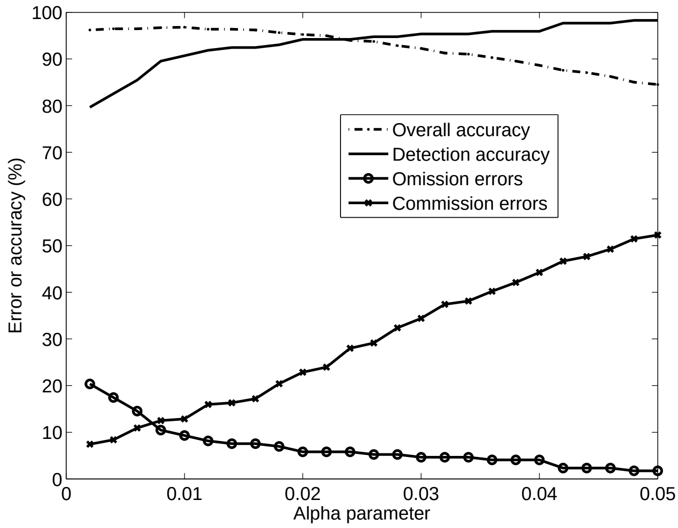

Figure 3.4: Evolution of 4 performance indices as a function of the alpha parameter (α) defining the confidence level (1-α) for the OB-Reflectance method.

These tuning capabilities allow the user to customize the change detection method with respect to the project objectives. For forest map updating that includes a field visit of the changed areas, the detection accuracy would be maximized so that a high α value, e.g. α=0.03, should be preferred. The selection of the confidence level value could be tuned depending of the human resources available for field surveys. In contrast, the maximisation of the overall accuracy of the change detection algorithm should be preferred for other applications. For example, the forest change for carbon stocks studies can be estimated by this change detection technique using an alpha value (α) below 0.01 to balance omission and commission errors.

3.6 Discussion

As outlined above, the proposed OB-Reflectance method combines the advantages and strengths of three methodological aspects; i.e. image segmentation, image differencing and statistical testing.

Through the object-based approach, the initial multi-date segmentation process insures the quality of the multispectral data to be submitted to iterative trimming. Indeed, the object delineation combined the spectral, temporal and spatial information to create consistent units of interest for statistical analysis. The object-based analysis is expected to be less sensitive to slight misregistration errors than traditional pixel-based analysis methods as this effect is supposed to affect only the object border and thus could be smoothed out at the object level. The processing time for detecting change is also reduced given that there are much fewer objects than pixels. Moreover, the object boundaries derived directly from the satellite images are more consistent for change detection than using GIS data which sometimes have non-reconcilable boundaries when overlaid on these images. Based on these objects, the subsequent statistical analyses are thus more robust and the change detection performances are increased. It is worth noting that the objects defined by the multi-date segmentation do not necessarily correspond to real stands on the field. In particular, the selection of only one segmentation scale for the analysis constrains the object size and may sometimes prevent the delineation of either very large stands or spatially limited changes. However, this multi-date segmentation was found to be better than a combination of independent segmentations on each image, that easily leads to over-segmentation with sliver polygons.

The multi-date image comparison was performed using image differencing. Many change detection studies have been based on the single vegetation index NDVI to reduce the differences in illumination and topographic effects (Hayes and Sader, 2001; Lyon et al., 1998; Wilson and Sader, 2002). While reflectance differencing is a well-known technique for change detection, the comparison of these reflectance differences by way of iterative trimming makes this approach very robust, even without accurate radiometric calibration. Moreover, due to the sun synchronous character of the SPOT satellite, topographic effects are supposed to be constants between images. It should be noted however that, after the cloud coverage screening, the method assumes that atmospheric effects are homogeneous over the whole study area. Heterogeneous atmospheric effects may require a preliminary stratification of the region or indeed, corrections of these effects (Song et al., 2001).

The use of a statistical procedure makes the method scene-independent. The multi-date reflectance is considered as very homogeneous for unchanged objects which are very numerous compared to changed ones. The detection of these rare objects having abnormal multi-date reflectance is done thanks to the combination of both statistics, M and S, from the object multi-date signature. Whereas only the object mean (M) is computed in several object-based methods (Saksa et al., 2003; Wulder et al., 2004), the addition of the object standard deviation (S) was found to be very efficient. Indeed, when an object is partially changed, the object standard deviation S allows its discrimination in the iterative trimming test. Moreover, the comparison of algorithm performance in this study illustrated that the most relevant input data for change detection is the whole set of spectral channels (NIR, Red and Green) rather than a combination of these channels in the NDVI. Changed objects are better identified when the spectral band number increases as a land cover change could affect only one spectral band.

The change detection results of the proposed method were found higher than many studies reported in the literature. Indeed, the OB-Reflectance method has achieved an overall accuracy of 93% and an overall kappa of 0.84. The particular unsupervised multi-date classification developed by Häme et al. (1998) was found less efficient for change extraction (respectively 66% and 0.21). Hayes and Sader (2001) have assessed three different methods using the same performance indices: PCA method (74% and 0.69), NDVI differencing (82% and 0.79) and RGB-NDVI (85% and 0.83). Using change vector analysis, Lunetta et al. (2004) achieved quite good performances (86% and 0.55). High results (92% and 0.87) were obtained by Rogan et al. (2003) using classification trees which can be considered as scene-dependent. For the RGB-NDVI method, the performance achieved by this study corresponds to those from the literature (Hayes and Sader, 2001). They were even higher (83% and 0.49) than the 64% and 0.29 achieved by Wilson and Sader (2002, Table 8) using 3 NDVI bands.

The comparison between object-based and pixel-based is a difficult task. Using both polygon-wise and pixel-wise validations, the analysis of our performance showed two particular trends. First, the polygon-wise validation of the multi-date classification provides lower overall accuracy than the pixel-wise. In the polygon-wise validation, objects with pixels classified as 'changed' covering an area larger than the MMU are considered as changed. So, omission errors are reduced whereas commission errors are more numerous, thus reducing the overall accuracy. This polygon-wise validation is thus not suitable for accuracy assessment of a pixel-based method except for the sake of comparison between pixel-based and polygon-based method. Secondly, the overall accuracy is slightly higher using forest inventory as reference whereas commission errors are more frequent for all detection methods. The increase of false change alerts can be explained by the larger proportion of unchanged forest stands in the forest inventory. Indeed, the comparison of these changed/unchanged proportions thanks to chi-square test of Pearson has showed a significant bias between the two data sources. This can be related to the quality of both data and above all to the updating of forest inventory data.

This approach has proved to be very efficient for forest change extraction and offers the advantage of being an automated procedure. Indeed, no predefined threshold for reflectance difference channels was required in this analysis. There were only two parameters to be set by the user: (i) the scale parameter h_{sc} and (ii) the confidence level 1-α of the statistical test. The first was based on the MMU expected from the change analysis. The second relied on the proportion of changed vs. unchanged objects. Although the default parameter settings already provide satisfactory results, the fine-tuning capabilities offered by the method allow the user to optimize it with respect to the considered application. In our study, this level of confidence was tuned at 0.99 for the OB-Reflectance by an optimisation procedure on overall accuracy.

Whereas most of the change detection studies cope with change extraction and change labelling analyses, this study was focused mainly on the extraction of change regions. From change detection results, the visual interpretation can be focused on the rare changed objects to determine the type of forest cover change. Moreover, the performance of extraction can be assessed independently of the change labelling. It is important to mention that all types of forest changes, namely clear-cutting and reforestation, were detected using the same processing algorithm and that no very precise measurement of their size or shapes have been done. Finally, forest cover changes in both deciduous and coniferous stands were successfully detected over the study area whereas they have different spectral responses to forest disturbances.

3.7 Conclusions

The object-based change detection method proposed here proved to be very efficient to identify forest land cover changes in both deciduous and coniferous stands. A detection accuracy higher than 90% and an overall kappa higher than 0.80 were achieved using a SPOT multi-date dataset covering a 10-year time span. This technique can be considered scene-independent in the sense that no predefined threshold for reflectance difference channels of the multi-date image was required. Moreover, the fine-tuning capabilities of a single algorithm parameter allow the user to customize the change detection technique according to its specific objectives. The change detection results achieved by the object-based method were higher than pixel-based methods, regardless of the validation data source.

Given its scene-independent property and its sound statistical formulation, the proposed object-based method can be easily extended to other kinds of data, other regions, or even for monitoring surface changes in non-forested areas. Other experiments using different sensors in various environments are needed in order to extent this very promising method for land surface monitoring and map updating.

Whereas this study was focused mainly on the extraction of change regions without distinction about the nature of these changes, it could be very useful to address the problem of change type classification inside the procedure itself. Further theoretical developments are still needed for this. Improving the exact delineation of detected changed stands is another aspect that could also be helpful to develop in the future, especially if the aim is to obtain quantitative assessments about the change area.

Chapter 4

Mapping tropical deforestation rate by automated object-based approach*

Abstract

Local, national and international organizations need up-to-date and accurate deforestation maps for environmental reporting and land management. The availability of large volumes of high resolution satellite imagery has recently increased the needs for automated processing methods able to detect tropical forest changes. An object-based method is proposed to map deforestation rate based on high resolution satellite images and any existing forest map. This process takes advantage of the efficiency of multi-date and multiscale segmentation and of an iterative statistical approach for change detection. In order to assess its robustness, the proposed method was implemented and tested on two very different situations corresponding to two sectors in and around the Virunga National Park (DRCongo). The overall accuracies of the deforestation maps were respectively equal to 79 and 87% based on visual interpretation of both satellite images and airborne video data. Finally, mapping deforestation rate thanks to a multiscale change interpretation was found relevant for decision makers. This quantitative and spatially-explicit way of representing change detection results describes simultaneously deforestation intensity, location and extent.

*Adapted from Desclée, B., de Wasseige, C., Bogaert, P., Defourny, P. and Languy, M., Mapping tropical deforestation rate by automated object-based approach: case studies in the Virunga National Park (DRCongo). *International Journal of Applied Earth Observation and Geoinformation*, submitted.

4.1 Tropical deforestation mapping

Remote sensing is crucial for producing deforestation maps thanks to its synoptic view and temporal resolution. Since early days of earth observation, satellite images acquired at different dates are compared using change detection methods for identifying areas of change. As deforestation is defined by the temporary or permanent clearance of forest for agriculture or other purposes (Lanly, 1982), deforestation mapping must focus on forest which was converted into another land-cover. Two types of forest change information can be derived, namely deforestation estimate and deforestation map (Stehman, 2005). In order to cover continental or sub-continental areas while keeping costs and delivery time reasonable, deforestation estimates are provided based on sampling (FAO, 2001; Duveiller et al., 2007). Deforestation mapping has the advantage to provide both a complete spatial coverage of land cover change information. Only few studies provide land cover change map in addition to the overall transition matrix (Alves et al., 1999; Steininger et al., 2001; Turner et al., 2001). However, the deforestation process could be better described by mapping together different information, i.e. extent, location and intensity.

Among the different change detection methods reviewed by Lu et al. (2004b), post-classification comparisons are generally used for deforestation mapping. This technique greatly depends on the accuracy of each forest map derived either from visual interpretation (Roy and Tomar, 2001) or from digital classification (Tucker and Townshend, 2000; Sanchez-Azofeifa et al., 2001; Zhang et al., 2005). More straightforward, other change detection techniques are based on a simultaneous visual analysis of multitemporal images (FAO, 2001; Achard et al., 2002). Lu et al. (2005) compared different change detection methods for moist tropical regions and found that image differencing was an efficient method for detecting different types of land-cover changes. However, the multi-date unsupervised classification using either NDVI (Hayes and Sader, 2001) or tasseled cap components (Guild et al., 2004) have been found most accurate for detecting deforestation processes. Although these pixel-based methods produced good results, they are greatly affected by "salt and pepper" effects due to the high spectral variability which characterizes tropical regions. Indeed, forest spectral variability was found dependent on both canopy roughness and geometry of observation (de Wasseige and Defourny, 2002) while heterogeneous atmospheric conditions, including frequent hazes, induce noise in surface reflectance measurement. Moreover, the contextual information, namely the spatial information between the values of proximate pixels, is not taken into account. New approaches using parcel-based image analysis were found efficient for forest mapping (Kayitakiré et al., 2002; Dorren et al., 2003; Flanders et al., 2003). Initially based on stand delineation from GIS, these techniques can now rely on image segmentation to group pixels with similar values into objects for reducing local spectral variability and incorporating contextual information. These objects can be derived at different scales thus allowing multiscale analysis.

Forest change detection based on direct multi-date analysis generally requires a preliminary forest delineation to focus the monitoring only on forested areas (Coppin and Bauer, 1996). This forest mask can be derived from a land cover classification (Hayes and Sader, 2001; Guild et al., 2004) based on the first satellite image of the image pair or be extracted from other data sources such as existing forest map (Häme et al., 1998), as done in Chapter 3. However, these forest limits, e.g. from Africover land cover maps, are often not accurate enough for change detection analysis which relies on the spatial resolution of the satellite images. Despite the very variable accuracy of existing forest maps, they should still serve as preliminary forest information. Dedicated techniques to update or adjust these initial forest masks are thus required.

This research aims at developing and testing an object-based method to detect deforestation and produce deforestation rate maps based on high resolution satellite images and any existing forest map. This process should take advantage of image segmentation and change detection for ensuring its automation and its use over various regions. Its robustness is tested for complex deforestation patterns – recent or old, large or very fragmented –in African forests, over different time periods – 1 and 5 years – and combining data from different sensors – SPOT and Landsat. This research also proposes a new way of representing deforestation process by combining extent, location and intensity information on a single map, namely deforestation rate map.

4.2 Study areas

The Virunga National Park is a protected area located across the equator at the east of the Democratic Republic of Congo (DR-Congo) and bordering Uganda and Rwanda (Figure 4.1). It is a site of exceptional biological and ecological value due to its geodiversity and its considerable altitudinal range (from 680 m to 5100 m) over a limited area, i.e. 7900 km^2. This area is crucial for the conservation of a large range of ecosystems and the protection of numerous endemic species. Although it was the very first African national park to be established in 1925 and declared as a World Heritage Site by UNESCO in 1979, it is currently one of the most threatened (Languy and de Merode, 2006). The main causes of pressure on the park are (i) the demographic explosion around the park increasing the demand for agricultural land, food and fuelwood, (ii) its valuable forest products, (iii) its location at the crossing of trans-border access roads and, (iv) its unstable situation due to conflicts leading to crisis, population displacement and illegal resources mining. The installation of refugee camps in and around the park from 1994 to 1996 induced severe degradations on the flora and above all on mammals. Nowadays, the park is still in a critical situation due the contrasts between eastern and western regions of this protected area in terms of soil richness and population density.

Two sectors, the Semliki and the Mikeno sectors, were selected due to their very different vegetation types and degradation patterns, including respectively small encroachments and large clear-cuttings. First, the Semliki sector includes lowland tropical forest on both side of the Semliki river where different forest degradations occurred. The extension of the agricultural activities of the people living near the park leads to degradation distributed in small patches within the forest. In contrast with shifting cultivation practices where forests may recover after several years thanks to natural regeneration, the clear-cut parcels in the Semliki area are not left over and natural vegetation cannot regenerate. Second, the Mikeno sector covers a gradient of mountain vegetation ranging from the mid-altitude mountain forest to afro-alpine vegetation on top of the extinct volcanoes. The mid-altitude mountain forest recently suffered from an exceptional and sudden intensive illegal clear cutting between June and July 2004 (de Wasseige et al., 2005). A forest block of several hundred of hectares disappeared in less than two months and several other smaller forest patches were severely degraded. No forest regeneration has been observed on any of both sites during the study period.

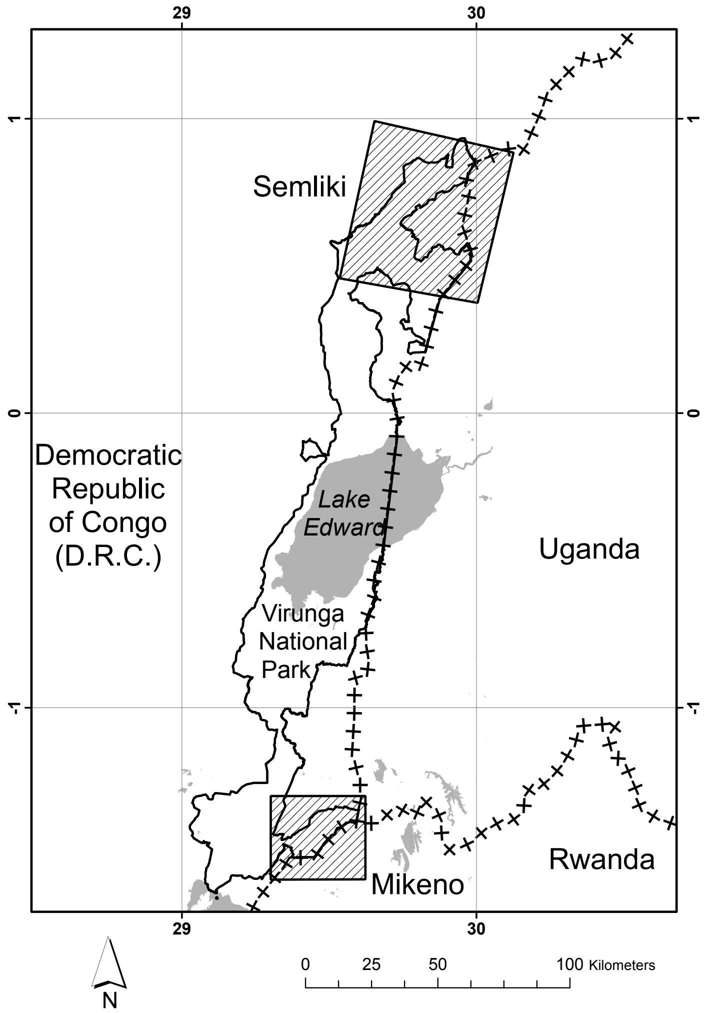

Figure 4.1: Location of the study areas including Semliki and Mikeno sectors of the Virunga National Park (grid in decimal degree).

4.3 Data pre-processing

Four high resolution satellite images were acquired and pre-processed. For the Semliki sector, images were acquired on April 1, 2000 and on February 11, 2005 respectively by SPOT-4 and -5 satellites. For the Mikeno sector, images were acquired on January 31, 2003 and July 3, 2004 respectively by Landsat-7 and SPOT-5 satellites. The pre-processing of these images included three steps: geometric corrections, cloud screening and image differencing. The images pairs were coregistered for each sector based on a set of 6 to 14 well distributed GCPs and orthorectified using the 90 m SRTM DEM. For each image, the RMSE was below the pixel size. All images were resampled by bilinear interpolation to 10 m resolution in order to harmonize the pixel size to the finest spatial resolution of SPOT-5 images. Clouds, shadows and regions with highly rugged terrain were masked out from the dataset based on visual screening of clouds and shadows and altitude DEM thresholding. Finally, the DN values of the 4 spectral bands, including Green, Red, NIR and SWIR bands, were subtracted for each pair of successive images. Two image differences were produced, one on the Semliki sector (2005 minus 2000) and the other on the Mikeno sector (2004 minus 2003).

Ancillary data include Africover land cover maps of DRCongo, Uganda and Rwanda, used as first coarse forest mask, and airborne video for independent accuracy assessment over the Semliki sector. These land cover maps were produced by visual interpretation of digitally enhanced 30 m Landsat TM color composites (Bands 4-3-2) (Latham, 2001). The land cover classes were defined according to the FAO/UNEP international standard Land Cover Classification System (LCCS) (Di Gregorio, 2005). Over the study region, these maps were produced using satellite images acquired in 2001 and 1999 respectively for the Semliki and Mikeno sectors. The set of airborne video was acquired by WWF over the Semliki sector from a video recorder linked to a Global Positioning System (GPS). These natural color digital video were collected in April 2004 mainly in vertical but sometimes in tilted position. A set of 60 airborne video frames was extracted for the accuracy assessment. These images of 1 to 5 m spatial resolution were coregistered using 4 or 5 GCP's derived from the 2005 SPOT image.

4.4 Methodology

The object-based and automated deforestation detection method includes three main steps (Figure 4.2): (1) multi-date and multi-scale segmentation, (2) forest mask update and (3) deforestation detection. First, the segmentation delineates objects from two satellite images acquired at different dates for two segmentation scales, providing objects (scale-1) and super-objects (scale-2). Objects correspond to the processing units and are characterized by Object Signatures (OS) derived from single-date image 1 and multi-date image difference (respectively OS1 and OS21). Second, starting from any existing forest map, the forest mask update relies on a no change detection approach and on forest/non-forest classification in order to produce an updated forest mask. The related statistical analyses are respectively based on OS21 and OS1 signatures. Finally, the deforestation detection then distinguishes deforested objects from forest objects based on OS21 signatures to produce the deforestation map. These results are then aggregated at the super-object scale for mapping deforestation rates.

The main assumptions of this deforestation detection method are that (i) under the initial forest mask, the numerous regions which exhibits similar reflectance differences correspond to unchanged forests, i.e. undisturbed between the time period, (ii) the stratification of the study area into large homogeneous regions reduces the variety of forest types, (iii) in a given stratum, all forested areas can be delineated based on the spectral properties of a sample of local unchanged forests, and (iv) deforestation concerns a small part of all forested areas and induces large surface reflectance variation in multi-date analysis compared to unchanged forests. Based on the key steps of object-based approaches defined in Figure 1.1, this methodology takes advantage of the strong key points of the object-based change detection method proposed in Chapter 3, namely the multi-date segmentation and the change detection algorithm based on iterative trimming.

4.4.1 Multi-date and multiscale segmentation

The multi-date and multiscale segmentation consists in partitioning an image into objects and super-objects which group spatially

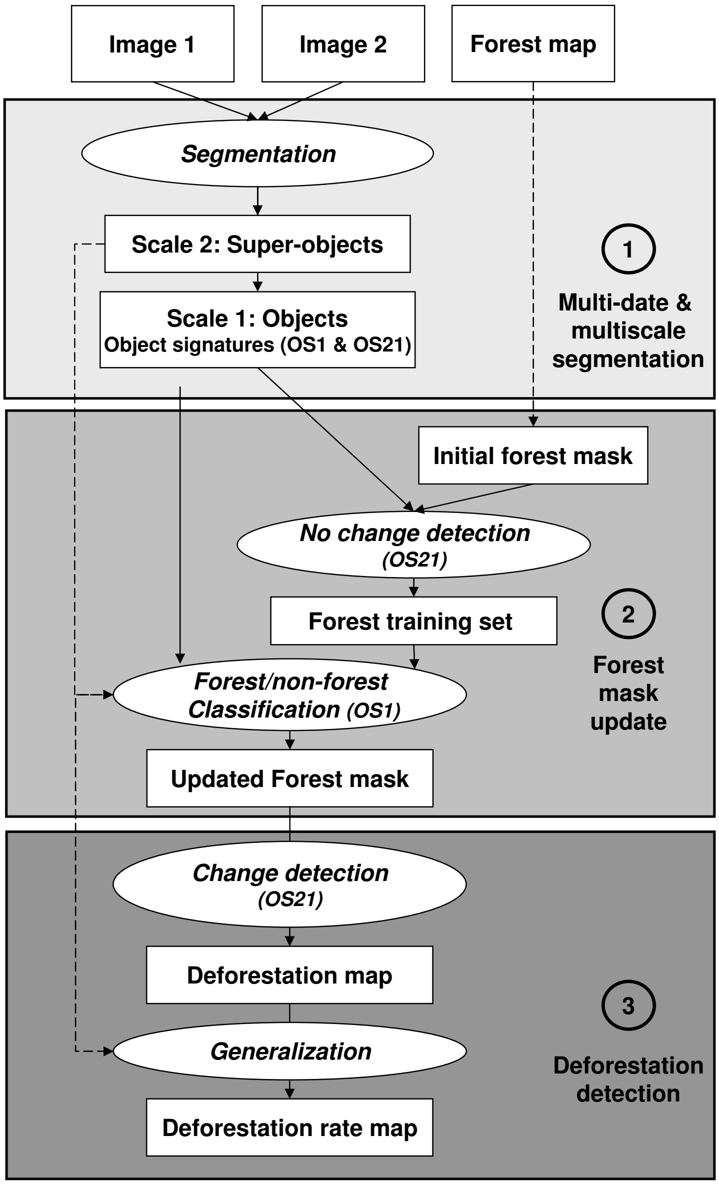

Figure 4.2: Overview of the deforestation detection method. The 3 main steps are the multi-date and multiscale segmentation, the forest mask update and the deforestation detection.

connected pixels that are spectrally and temporally similar at two different scales, i.e. different spatial dimensions. The interest of the multiscale approach is to focus the analysis on little objects in order to achieve high spatial precision while larger objects, the super-objects, are needed for defining strata of homogeneous forest types and generalizing the results over large regions. The resulting objects are the cornerstone of the approach because they are consistent processing units for both forest mask update and deforestation detection analysis. This makes more robust the method by combining results over the same units of interest and avoids sliver polygons which could result from the combination of different segmentations. For the subsequent analysis, each multi-date object is characterized by its object signature which combines several summary statistics. These ones are derived from the spectral reflectance value – single-date or multi-date — of each pixel belonging to the object.

The multi-date image that combines satellite images over the same location at two different dates is segmented using eCognition tool (Baatz and Schäpe, 2000). Segmentation is based on an optimization function including three parameters, namely spectral, compactness and scale. The spectral parameter, trading spectral homogeneity vs. object shape, is required to obtain either very spectrally homogenous objects or to avoid irregular and branched objects. The compactness parameter, trading compactness vs. smoothness, adjusts the object shape between compact objects and smooth boundaries. Finally, the scale parameter that controls the object size is selected so that the minimum object size matches the minimum elementary unit to analyse. By varying this parameter, different segmentation scales can be produced, each characterized by its own mean object size.

Two segmentation scales, providing objects nested into super-objects, are achieved from the multi-date data set made of 2 satellite images with 4 spectral bands respectively. The first scale delineates the objects and computes object signatures for each of them. Single-date Object Signatures of image-1 (OS1) are obtained by averaging spectral values for all the pixels belonging to a given object. Multi-date Object Signatures (OS21) are made of object's mean and standard deviation for each spectral band of the difference image (image-2 minus image-1). Segmentation parameters were selected for obtaining spectrally and temporally homogeneous objects, equally balancing between smoothness and compactness and matching the smallest forest change size (about 2 ha). The super-objects of the second segmentation scale are derived from the fusion of similar and adjacent objects. Different parameter values for the scale-2 object delineation were selected by visual assessment in order to obtain larger super-objects for the Mikeno sector than the Semliki one (mean size of respectively 500 and 2000 ha) as the size of the deforested patches is very different.

4.4.2 Forest mask update

An object-based classification method was developed to derive or update the forest mask from any already existing forest map. The basic idea is that forest maps, even outdated, are useable as coarse forest mask to initialize a no change detection algorithm as long as the majority of the forested area is still correct. The forest extent initially corresponds to the forest and woodland classes of the Africover land cover database (Latham, 2001). Forest is defined as forested land with closed canopy, which have canopy cover of more than 65% according to the LCCS definition. Non-forest includes all other land cover classes such as cropland, savanna, fallow and water bodies. The updated forest mask is obtained in two automated steps, (i) an selection of forest training set and, (ii) the stratified forest/non-forest classification of image 1. Given the extent and the forest type diversity of the study area, several strata corresponding to large homogeneous regions were defined from the super-objects. Each stratum, equal to one super-object, is then processed separately.

The selection of forest training sets aims at identifying a representative sample of forest objects based on the first method assumption. All objects covered by the existing forest mask are considered for the selection of forest training set. This selection is achieved by comparing object multi-date signatures (OS21) in order to screen out changed forest objects. Objects showing multi-date signature close to OS21 distribution average are classified as unchanged forest using a no change detection procedure based on a multivariate iterative trimming algorithm. Trimming is defined as the removal of extreme values that behave like outliers, as expected for changed forest objects. Based on a chi-square test, this algorithm identifies changed objects having abnormal multitemporal behaviour analysing the OS21 signatures. The iterative trimming procedure is performed with a confidence level equal to 99%. Objects with signature within the confidence interval of the last iteration are selected as forest training areas for the classification of image 1.

The stratified forest/non-forest classification labels objects into forest and non-forest classes. The discrimination is based on the spectral similarity between the OS1 of the object to label and the average OS1 computed from all the forest training set retained for a given stratum defined by a super-object. The spectral similarity is derived by the Mahalanobis distance (Richards, 2006) computed from the 4 variables corresponding to the 4 spectral bands of image 1. As these distances are chi-square distributed, objects with OS1 within the confidence interval defined for a confidence level of 99.9% are then classified as forest. The others are labelled as non-forest and masked out for the subsequent analysis. As a summary, the following sequence is thus performed for each super-object: (i) extraction of the local forest training set, (ii) computation of the Mahalanobis distance for each object with regards to the training set average values in 4-bands space, (iii) object labelling into forest and non-forest classes based on the defined confidence interval. Finally, the results of all super-objects are combined to produce the updated forest mask.

4.4.3 Deforestation detection

The deforestation detection identifies changed objects belonging to the updated forest mask. The approach is similar to the one described for the selection of the forest training set but the algorithm searches for objects showing large multi-date surface reflectance variation. The statistical process is performed on the multi-date signature (OS21) with a confidence level equal to 99.9%. Because of the forest high spectral heterogeneity, this value is superior to the 99% used for the forest mask update in order to be less sensitive to the forest intrinsic variability. Moreover, only the NIR and SWIR difference images are used because of higher atmospheric effects in the visible bands. Changed objects are only classified as deforestation if they were initially labelled as forest. The resulting deforestation map thus distinguishes three classes, namely non-forest, unchanged forest and deforestation.

The deforestation rate map is produced by computing the object area belonging to each class within each super-object (scale-2) and by aggregating adjacent super-objects with similar deforestation rates. The categorical approach of objects is converted into continuous value at super-object scale ranking from 0 to 100% of deforestation rate. Super-objects also delineate deforestation fronts which are rather indicative than being rigorously geographically correct. Clouds and shadows, which are masked out from the deforestation detection analysis, are sometimes included into super-objects but their areas are not taken into account into the deforestation rate computation. The annual deforestation rate is obtained by dividing the deforested area (the deforestation intensity) by the forested area defined by the updated forest mask and the time period. It is important to notice that this index is computed and represented over the super-object extent while it is based on the initial forested area.

4.4.4 Accuracy assessment

The robustness of the accuracy assessment is ensured by a stratified random sampling supported by different reference data sources. The accuracy of deforestation map was assessed by visual interpretation of 180 objects using either satellite image or airborne video frame. The advantage of the latter source is its acquisition which is independent from the deforestation detection process. The sampling was based on a equal distribution between each class, namely non-forest, unchanged forest and deforestation, and a weighted representation between each reference data source (one third using airborne video frame, two thirds using satellite image). As no airborne video was available on the Mikeno sector, the sample was only stratified according to the classes. Four performance indices were derived from the confusion matrix: overall accuracy, overall kappa and for the deforestation class, Omission and Commission Errors (respectively OE and CE). Based on the number of objects and their corresponding areas, these indices were derived from the overall results, the deforestation map, and also separately for the results of two different steps, i.e. the forest mask update and the deforestation detection. The performances between both steps as well as their respective contributions to errors in the deforestation class can thus be compared.

4.5 Results

4.5.1 Deforestation maps and accuracy

Two deforestation maps were produced using the proposed method and were assessed with reference data over the Semliki and Mikeno sectors. A sample of the Semliki deforestation map zooming on an active front (Nyaleke-Mavivi region) and the corresponding satellite images acquired in 2000 and 2005 are presented in Figure 4.3. The overlay of deforested areas over the 2005 satellite image shows the fragmented deforestation patterns.

For the Semliki sector, the deforestation map's overall accuracy was estimated between 81 and 87% and the overall kappa between 0.71 and 0.73, showing little difference between well classified objects and the proportion of their corresponding areas (Table 4.1). The updated forest mask reached an overall accuracy of 85 to 89% whereas the deforestation detection results varied from 92 to 97% for the same index. Considering only the deforestation class, omission errors of the deforestation map varied from 15 to 22%, made of similar error contribution from forest mask update (6 to 10%) and from deforestation detection (9 to 12%). The commission errors for the deforestation class (22%) were mainly due to the forest mask update (16 to 17%) while the error contribution of deforestation detection is very low (5%).

Comparing both reference data sources (Table 4.2), overall accuracy of the deforestation map was greater when assessed from satellite image (84 to 90%) than from airborne video (73 to 81%). The same trend is observed based on the overall kappa (respectively 0.76 to 0.81 and 0.55 to 0.59). No omission error was found for the deforestation class using airborne video whereas the same index computed using satellite image reached 19 to 27%. In contrast, deforestation commission errors were found higher using airborne video (33 to 35%) than from satellite image (17%).

For the Mikeno sector, the deforestation map overall accuracy ranged from 79 to 82% and the overall kappa from 0.69 to 0.72

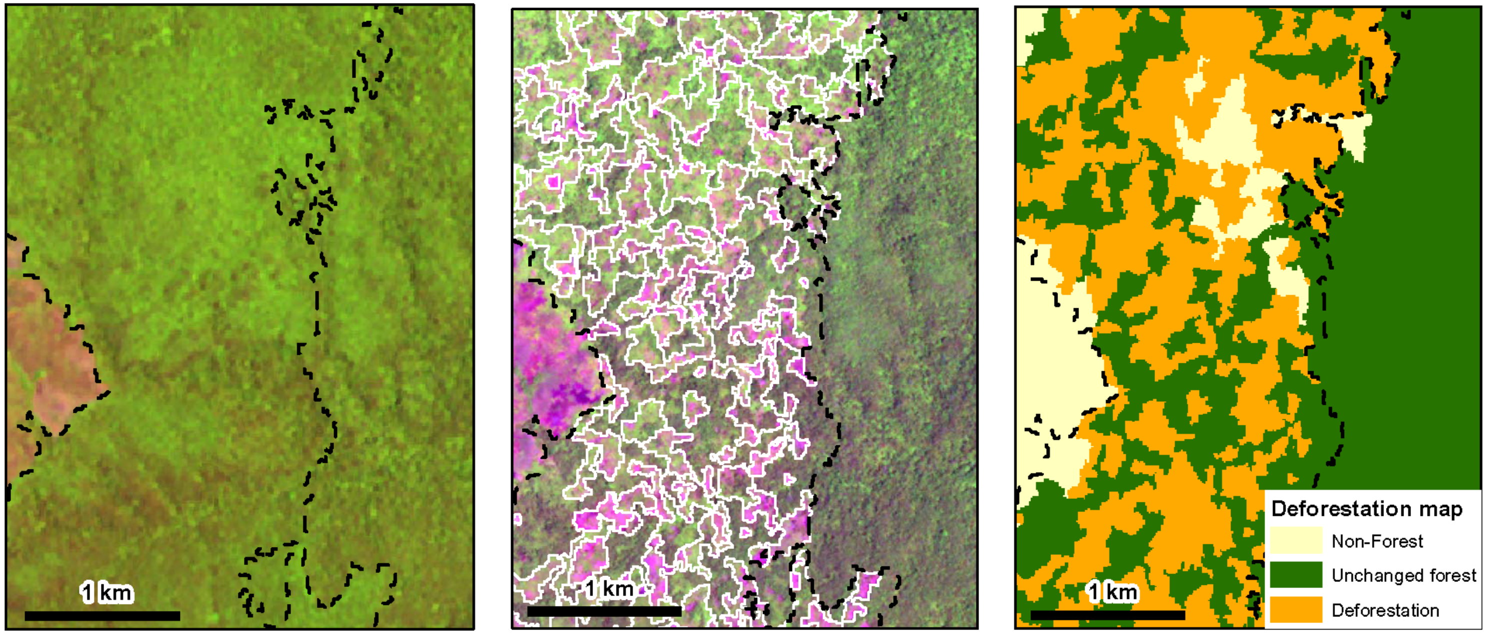

(a) (b) (c)

Figure 4.3: Extracts of satellite images acquired in (a) April 2000 and (b) February 2005 with delineated deforested areas over a active deforestation front in the Nyaleke-Mavivi region of the Semliki sector (RGB=SWIR-NIR-Red). Deforestation map (c) shows the different classes of labelled objects while super-objects are separated by black dashed lines.

Table 4.1: Performance indices for the Semliki deforestation map over the 2000-2005 period and separately for the forest mask update and the deforestation detection, in terms of number of objects (n=180) and of their corresponding areas.

	Deforestation map		Forest mask update		Deforestation detection	
Semliki	Object	Area	Object	Area	Object	Area
Overall accuracy (%)	80.6	86.8	85.0	89.4	92.2	96.7
Overall kappa	0.71	0.73	0.67	0.62	0.84	0.88
Deforestation: OE (%)	14.8	22.0	5.6	9.8	9.3	12.2
Deforestation: CE (%)	22.0	21.6	16.9	16.2	5.1	5.4

Table 4.2: Performance indices for the Semliki deforestation map over the 2000-2005 period according to the reference data source, i.e. satellite image and airborne video (respectively n=120 and n=60), in terms of number of objects and of their corresponding areas.

	Satellite image		Airborne video	
Semliki	Object	Area	Object	Area
Overall accuracy (%)	84.2	90.2	73.3	81.3
Overall kappa	0.76	0.81	0.59	0.55
Deforestation: OE (%)	18.6	27.1	0.0	0.0
Deforestation: CE (%)	16.7	16.9	35.3	33.4

(Table 4.3). Omission and commission errors for the deforestation class were similar (respectively 15 to 20% and 13%). The forest mask update is the main source of errors with an overall accuracy ranging from 81 to 85% while deforestation detection performed very well (96 to 97%). Errors of omission (10 to 11%) and commission (13%) were balanced for the forest mask update. For the deforestation detection, no commission error was observed whereas omission errors remained below 10%.

Table 4.3: Performance indices for the Mikeno deforestation map over the 2003-2004 period and separately for the forest mask update and deforestation detection, in terms of number of objects (n=180) and of their corresponding areas.

	Deforestation map		Forest mask update		Deforestation detection	
Mikeno	Object	Area	Object	Area	Object	Area
Overall accuracy (%)	79.4	81.8	81.1	84.7	97.1	95.6
Overall kappa	0.69	0.72	0.58	0.62	0.94	0.91
Deforestation: OE (%)	14.8	19.8	9.8	10.7	4.9	9.0
Deforestation: CE (%)	13.3	12.7	13.3	12.7	0.0	0.0

4.5.2 Deforestation rate maps

Two maps of deforestation rate were derived from the aggregation of the deforestation maps to more generalized zone corresponding to super-objects. These maps can be considered more robust than deforestation maps given that there is balance between omission and commission errors for the deforestation class. Quantitative results for each zone delineated on the deforestation rate maps are provided in Tables 4.4 and 4.5. The Semliki deforestation rate map over the 2000-2005 period concerns five zones showing annual deforestation rate ranging from 0.5 to 8.5% (Figure 4.4). From a forest surface of 49 000 ha in April 2000, about 2 400 ha were deforested by May 2005 with 1 600 and 800 ha respectively around and inside the Virunga National Park. Most of clear-cutted surfaces inside the park were found in the south-western part, the region of

Nyaleke-Mavivi (Figure 4.3). The Mikeno deforestation rate map (Figure 4.5) depicts large clear-cuts, about 900 ha deforested in few months. Most of the deforestation concerned the southern mid-altitude mountain forest of the park along a pioneer front showing an intensity gradient with rate ranging from 65 to 100%. As the deforestation process occurring between May and July 2004 was exceptional and very sudden, the deforestation rate can hardly be qualified as annual.

Table 4.4: Area estimates of the different classes and the derived annual rates for each zone from the deforestation rate map over the 2000-2005 period for the Semliki sector (Figure 4.4).

	Zone area a (ha)	Forest area b (ha in 2000)	Deforestation area c (ha)	Annual def. rate c/(b*5) (%)
1	2 160	1 810	770	8.5
2	24 970	2 550	1 030	1.9
3	15 010	11 280	320	0.6
4	2 620	14 290	160	1.4
5	4 130	3 560	110	0.6

Table 4.5: Area estimates of the different classes and the derived annual rates for each zone from the deforestation rate map over the 2003-2004 period for the Mikeno sector (Figure 4.5).

	Zone area a (ha)	Forest area b (ha in 2003)	Deforestation area c (ha)	Deforestation rate c/b (%)
1	370	370	370	100.0
2	300	300	240	80.0
3	210	210	140	66.7

4.6 Discussion

The proposed methodology was applied in various situations including different deforestation patterns, different time scales and

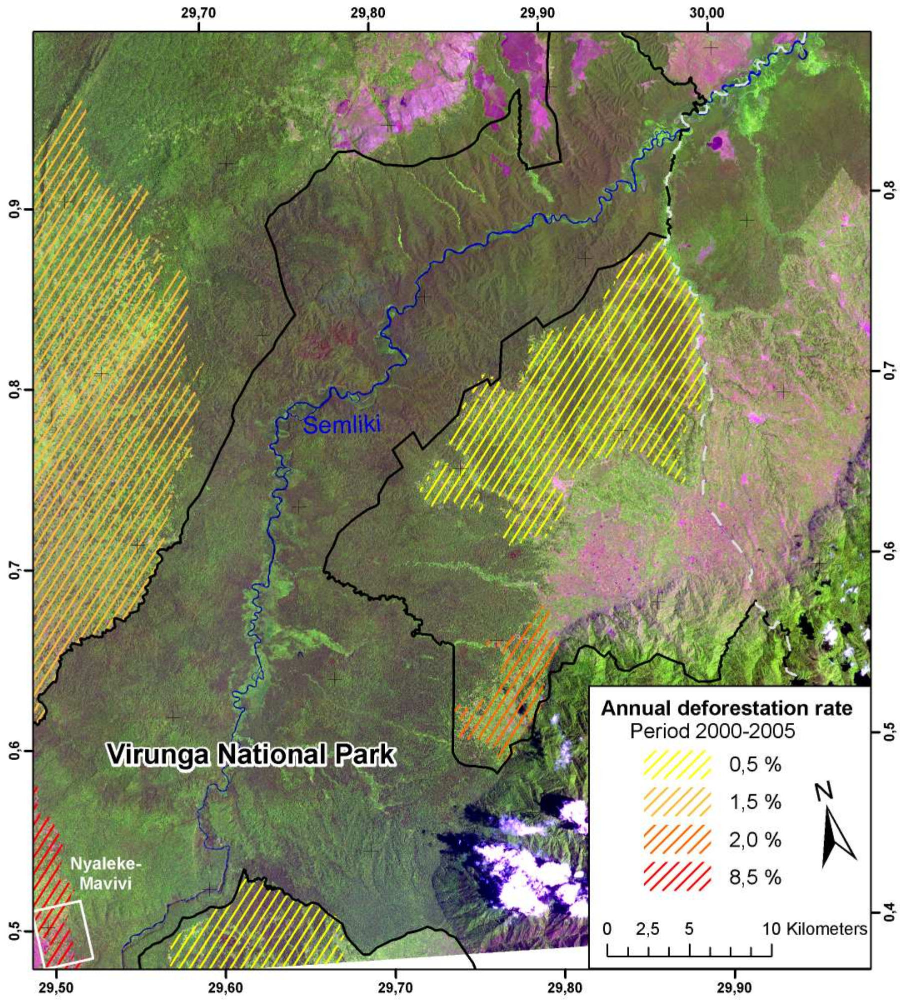

Figure 4.4: Deforestation rate map of the Semliki sector over the years 2000-2005 overlaid on the 2005 SPOT image (RGB=SWIR-NIR-Red)(grid in decimal degree).

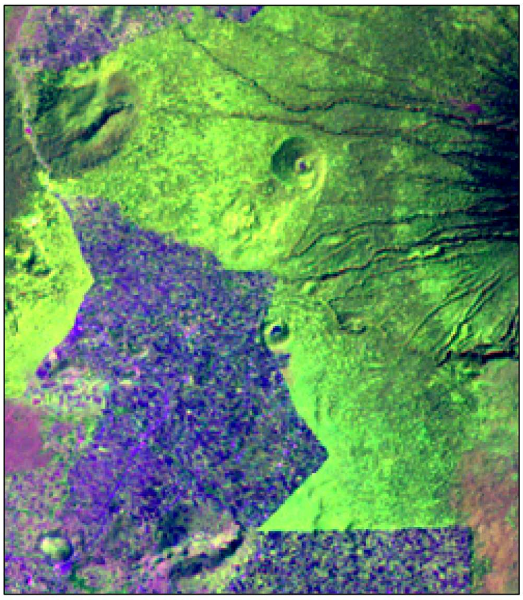

(a)

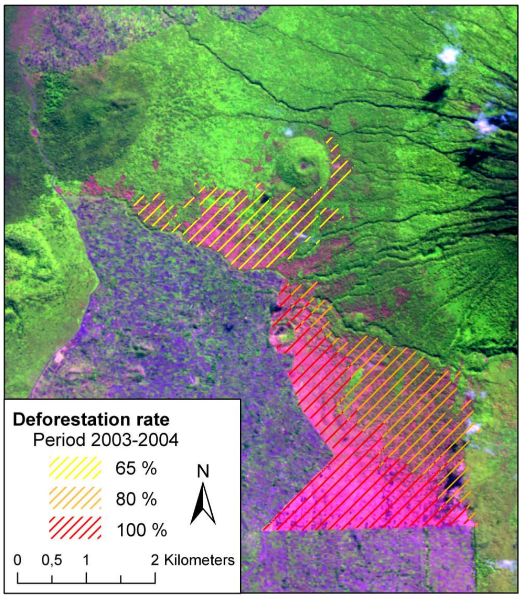

(b)

Figure 4.5: Subsets of (a) the 2003 Landsat image and (b) the deforestation rate map of the Mikeno sector over the years 2003-2004 on the 2004 SPOT image (RGB=SWIR-NIR-Red).

different data sources and was still found quite efficient. Deforestation patterns such as recent and less recent deforestation as well as large clear-cut or small encroachment were successfully identified. Very different change classes were observed. In case of recent deforestation, forests were merely converted to bare soils. This land cover class can be easily detected as its spectral signature is much contrasted with regards to the one of mature forest. However, in case of older deforestation, bare soils were first covered by pioneer herbaceous vegetation and then sometimes became a long-term fallow that might have spectral values close to forest spectral signature. This last deforestation pattern was also efficiently identified in this study thanks to the deforestation detection which compares multi-date signal independently of forest type. Reforestation could also be detected by this methodology by reversing the whole process. Indeed, by producing an updated forest mask for the end of the study period, the change detection algorithm can be applied for finding non forested areas at the beginning of the study period. But it was not been done here given that most of clear-cut parcels were not abandoned during the study period. Finally, the proposed method was applied on images from different sensors, namely Landsat-7, SPOT-4 and SPOT-5. Given the statistical nature of the change detection algorithm, no radiometric correction was required. The DN values of the satellite images were actually analyzed in relative term through the statistical process. This change detection technique is thus quite compatible with high spatial resolution multisource dataset.

The object-based approach was found very suitable for reducing the spectral heterogeneity of the forest and performing multi-scale analysis. First, the "salt and pepper" effect was significantly reduced by the segmentation. The main limitation of the object-based method is that very small deforested areas are not taken into account in the deforestation detection. Indeed, the scale parameter of the segmentation defines the minimum object size for the object delineation. Deforested areas below this size constraint are included in a larger object and can hardly be detected by the deforestation detection algorithm. The minimum object size was here consistent with the minimum size of deforestation processes. The methodology has proved its efficiency to map various deforestation patterns, from small encroachment to large clear-cut, with a single scale parameter for all objects of the scale-1 segmentation. Furthermore, the multiscale nature combining object and super-object was found very useful for the zoning of forest types to retrieve representative spectral signature for the forest mask update and aggregate deforestation detection results to map relevant features. That is why the delineation of super-object is crucial to define consistent zones of forest and deforestation. Based on appropriate segmentation parameters, the super-objects have efficiently included areas with same deforestation intensities.

According to the accuracy assessment, the forest mask update is the bottleneck of this method performance. However, these automated updating capabilities should be seen as a significant step towards operational high resolution monitoring. The automation of the forest mask update relies on some assumptions to deal with the complexity of spectral discrimination in heterogeneous landscape. More advanced classification methods are capable of taking into account such spectral variability, but this is often at the expense of time-consuming interactive classification. In several studies (Guild et al., 2004; Souza and Barreto, 2000), the accuracy of the forest mask was not assessed in spite of its important impact on the overall quality of deforestation detection.

The overall accuracies of deforestation detection algorithm achieved in both study areas were significantly higher (92 to 97%) than the few deforestation detection studies assessing their accuracy. Indeed, Guild et al. (2004) and Hayes and Sader (2001) have obtained respectively 79 and 85% overall accuracy for identifying deforestation using multi-date classification. However, these two methods detected different change types while this method only focused on deforestation. The deforestation detection results are also close to overall accuracy (93%) of the results obtained in Chapter 3 over temperate forests using a similar change detection method. It's worth noting that many methods have been applied for detecting deforestation but the lack of accuracy assessment limits the performances comparison.

The results obtained from both data sources, i.e. satellite image and airborne video, show systematic higher performances for the first source as expected. Indeed, the use of the same data for the analysis and the validation can overestimate the overall accuracy. However, the digital videos strengthened the robustness of the accuracy assessment as they were not used in the change detection process. Moreover, they are crucial sources of ground truth information given that field survey was not possible due to insecurity. These performance differences could also be partially explained by the earlier acquisition date of the second one compared to the first one and the absence of infrared bands in airborne video, useful for vegetation discrimination. However, these airborne videos were not acquired for the purpose of this accuracy assessment. Future assessment of forest monitoring system should make full advantage of these data by planning appropriate data acquisition.

Mapping deforestation and other land-cover changes over large regions is complicated for several reasons. First, deforested areas are generally small and rare over the whole study area. The representation of these areas is thus tricky for producing precise maps over large areas. Second, the information about exact location of deforested areas is less important than the mapping of the spatial dynamics and the intensity of the deforestation process. The categorical representation of scale-1 objects provide a static snapshot of a changing situation while mapping larger zones with quantitative deforestation rate information appeared much more relevant for monitoring deforestation processes. Deforestation rate map was then proposed as a general solution in order to represent different information about deforestation processes.

This study brought operational results to the Congolese authorities and conservation NGO requiring information about the evolution of deforestation fronts next to this famous protected area. Crucial information, such as front delineation and deforestation rates quantification, were provided by the deforestation rate map. This spatially-explicit representation of deforestation intensity is helpful for planning and monitoring these protected areas. These maps also highlighted the urgency to address land use planning issues in the Semliki sector which exhibits many population movements. In 2006, the population that caused the deforestation in the Nyaleke-Mavivi region has been peacefully relocated outside the park. In the near future, awareness campaigns highlighting land conversion problems in and near the park could be supported by these maps as communication documents.

4.7 Conclusions

An automated deforestation detection method has been developed for mapping deforestation rate using high resolution satellite images and existing forest map. This process combines the efficiency of multi-date and multiscale segmentation and of iterative statistical algorithm for change detection. In order to assess its robustness, the approach was tested for two case studies in the Virunga National Park located in DRCongo. Using stratified random sample based on two reference data sources, the deforestation map overall accuracies achieved from 79 to 87%. Deforestation rates were derived by aggregating deforestation detection results and then mapped over large zones. This innovative way of representing deforestation detection results from remote sensing has been found relevant for better describing deforestation processes into spatially-explicit maps.

The efficiency of the developed approach for identifying forest cover loss has been proved in several situations where deforestation patterns, time scales and data varied considerably. While this study was focused on the deforestation detection, the process of this methodology could be reversed to identify reforestation areas and even be applied to detect other land-cover changes. Whereas the deforestation detection algorithm has already provided high performances, the lower results for the forest mask definition suggests new improvements in future research.

Conclusions and perspectives

Forest monitoring based on satellite remote sensing is crucial for providing information about forest cover changes and reporting forest status. While existing change detection approaches are not quite appropriate to rapidly process the current flow of earth observation data, the recent advances in image segmentation have opened new opportunities for an object-based monitoring system.

An automated object-based forest change detection method has been developed in this thesis using high resolution satellite remote sensing. Based on the detailed characterization of spectral reflectance dynamics of forest cycle, this innovative approach combines different advanced tools including image segmentation, image differencing and a dedicated statistical procedure using multivariate iterative trimming. Designed and applied successfully in temperate ecosystems, this methodology was improved and found robust in tropical environment for different deforestation situations. The specific contributions of this thesis are presented in details in the following section.

Findings

This research has firstly contributed to characterize the spectral reflectance dynamics of forest cycle for better identifying disturbances related to changes in forest cover. The analysis of spectral reflectance and NDVI clearly demonstrated high spectral variation during the whole forest succession. By comparing multi-date satellite images using image differencing, this variation sometimes induces errors in change detection results when only one single spectral band or the NDVI is used. This study demonstrated the interest of multispectral analysis with all spectral bands for different temporal intervals between satellite images for more generic forest change detection.

Based on these results, a dedicated statistical change detection algorithm has been developed in this thesis using a multivariate iterative trimming. This algorithm can be considered as automated given that no predefined threshold for reflectance difference image is required. It can also be considered as generic as being based on a statistical approach and various object statistics. Although default parameter setting already provides satisfactory results, this algorithm can be optimised with respect to the considered applications by reducing either omission errors (for change survey), commission errors (for map updating) or balancing both errors (for carbon stock budget).

The multi-date segmentation approach was also found very efficient for change detection. While image segmentation generally combines spatial and spectral information, the developed object-based approach also includes the temporal component into the segmentation process. The resulting multi-date objects are consistent units to be analysed by the change detection algorithm. Moreover, image segmentation applied directly on the multi-date images was found better than a combination of different single-date object delineations which result in over-segmentation with many sliver polygons.

The robustness of this methodology has been proved by the design and the implementation of adequate validation protocols for assessing the change detection accuracy for different ecosystems, namely temperate and tropical. The method was found quite efficient when applied in various situations including different change types, different time scales and different satellite data. In order to compare object- and pixel-based methods, a specific approach was built on temperate forests combining both polygon-wise and pixel-wise validations. Based on this protocol, the developed object-based method was found more efficient than pixel-based methods for detecting forest changes. The reliability of the accuracy assessment relies on the combination of different reference data sources, which include one reference independent of the change detection process, as provided either by forest inventory or by airborne digital video. As there is still no standard for change detection accuracy assessment, this validation protocol is a first step for better quantitative comparison of change detection approaches.

Another important contribution of this thesis is the improvement of the method automation thanks to an initial step of forest mask update. Forest mask is indeed essential for feeding the change detection algorithm with an accurate delineation of the region of interest. This updating process efficiently combines single-date and multi-date analyses for delineating forest areas starting from existing forest maps and two satellite images acquired at different dates. Moreover, the integration of multiscale analysis for stratifying the forest/non-forest classification was also important for improving its performance.

Finally, this research has greatly contributed to provide innovative representation of change detection results thanks to the object-based and multiscale nature of the developed approach. While change mapping is generally difficult given that changes are rare and sparsely distributed, the deforestation rate map was found relevant for providing quantitative information on extent, location and intensity of deforestation processes. These spatially-explicit maps are also a meaningful and efficient way to support decision-making and forest management.

Perspectives

Object-based approaches are very promising for change detection. The recent improvements in image segmentation have largely contributed to the integration of such techniques in land-cover classification processes. These tools also offer opportunities to analyse the landscape at different scales, i.e. object sizes. Some conceptual studies have already assessed the potential of multiscale analysis, but these approaches generally rely on *a priori* information on the study region for defining relevant scales (Hall and Hay, 2003; Hay et al., 2005). The advantage of analysing different scales brings a new question about the accuracy of the change detection results. While the area accuracy was defined by the MMU until now, the objects analysis at one scale and the result representation at another scale, as done for the deforestation rate map, render complex the definition of accuracy. A multiscale analysis was already integrated in the developed method, but more investigation is needed for assessing the contribution of each scale in the precision of changed areas delineation. In order to compare different segmentation results, efficient tools are also required for providing quantitative and objective accuracy assessment of object boundaries. Due to the lack of such techniques, the multi-date segmentations using either two or three images acquired at different dates, respectively performed for the tropical and temperate regions, have not been quantitatively compared. The use of a three-date image segmentation in temperate regions was dictated by the need of direct method comparison with the pixel-based method using the RGB-NDVI technique. However, the visual assessment of the segmentation results suggested to apply it only on two images as for more images, changed areas are harder to be precisely delineated and can thus be easily included into larger unchanged objects. In this last case, the multi-date segmentation can be repeated independently for each pair of images. By bridging the gap between GIS and satellite images, object-based approaches become also useful for automated map updating procedures relying on GIS database. However, the developed tools should be integrated inside the updating process itself for ensuring the coherence of boundaries. As GIS data become largely widespread, they are also a relevant source of information for characterizing the nature of detected changes.

Operational forest monitoring systems can take advantage of the methodological advances of this research to deal with the increasing and continuous flow of satellite data. However, satellite images should be acquired over large areas and with high quality. First, satellite sensors providing large-scale images, such as DMC and AWiFS, should be preferred from high revisiting capabilities sensors as the time period between multi-date images is similar for larger areas. Second, the quality of satellite images relies on the data acquisition and the pre-processing steps. Whereas research is very active for finding more automated procedures, very few techniques are available for operational uses. Moreover, an important difficulty in tropical regions is the high cloud coverage which limits the monitoring capabilities. While visual cloud screening is a classical approach, more automated techniques are still needed for rapidly delineating and screening out these irrelevant regions. Another solution could be the combination of both optical images and radar images for respectively delineating forest regions and monitoring these areas. Given that radar images are rather noisy, the segmentation procedure should rely on optical images while the change detection algorithm could rely on radar data for more frequent data acquisition.

The developed generic approach can be extended to other kinds of data, other regions, or even for monitoring surface changes in non-forested areas. As a confirmation of the generalization of the thesis results, some methodological tools have already been integrated in large-scale monitoring studies. Indeed, deforestation in Central Africa has been accurately estimated (Duveiller et al., 2007) based on a processing chain which relies on the multi-date segmentation and the automated forest/non-forest classification developed in this thesis. This cost-effective method was found very efficient for rapidly processing many images extracts thanks to object-based techniques. Based on a sampling approach, such technique has the advantage of covering rapidly regional scale with a limited number of image samples to analyse but only provides estimates of forest cover changes for the whole region. In contrast, wall-to-wall mapping can provide both estimates and location of changes over the complete study area. While this kind of approach can be very time-consuming, the automated object-based approach developed in this thesis could significantly reduce this load. The sampling strategy can be sufficient for monitoring the global carbon balance but other applications such as biodiversity conservation need more local and precise information about forest reduction or expansion such as the change maps provided in this research. While very few change detection studies in the literature have provided change maps, this research has proposed a new way of representing change detection results into quantitative and spatially-explicit way. But more investigations are needed for extending these promising mapping techniques to other change types and other regions.

Publications related to this thesis

- Desclée, B., de Wasseige, C., Bogaert, P., and Defourny, P. (2007). Mapping tropical deforestation rate by automated object-based approach: case studies in the Virunga National Park (D.R. Congo). *International Journal of Applied Earth Observation and Geoinformation*, submitted.

- Desclée, B., Defourny, P. and Bogaert, P. (2007). Characterizing spectral reflectance dynamics over the whole conifer succession. *Canadian Journal of Remote Sensing*, in preparation.

- Duveiller, G., Defourny, P., Desclée, B. and Mayaux, P. (2007). Deforestation in Central Africa: estimates at regional, national and landscape levels by advanced processing of systematically-distributed Landsat extracts. *Remote Sensing of Environment*, accepted.

- Desclée, B., Bogaert, P., and Defourny, P. (2006). Forest change detection by statistical object-based method. *Remote Sensing of Environment*, **102**, 1–11.

- Desclée, B., de Wasseige, C., Bogaert, P., and Defourny, P. (2006). Tropical forest monitoring by object-based detection : towards an automated method in an operational perspective. In *Proceedings of the 1st International Conference on Object-based Image Analysis (OBIA 06)*, July 4-5, 2006, Salzburg, Austria.

- Duveiller, G., Defourny, P., Desclée, B., and Mayaux, P. (2006). A new approach to estimate tropical deforestation at sub-continental scale by object-oriented unsupervised classifications of Landsat imagery. In: *Proceedings of the 2nd International Symposium on Recent Advances in Quantitative Remote Sensing (RAQRS'II)*, September 22-29, 2006, Torrent (Valencia), Spain.

- Languy, M., de Wasseige, C., Desclée, B., Duveiller Bogdan, G., and Laime S. (2006). Changements d'occupation du sol en périphérie du Parc National des Virunga. In: Languy, M., de Merode, E. (Eds.), *Virunga; survie du premier Parc d'Afrique* (pp. 152-163) . Lannoo, Tielt, Belgium.

- Desclée B., Bogaert P. and Defourny P. (2004). Object-based method for automatic forest change detection, In: *Proceedings of the IEEE International Geoscience and Remote Sensing Symposium (IGARSS'04)*, September 20-24, 2004, Anchorage, Alaska.

Bibliography

Achard, F., Eva, H., Stibig, H., Mayaux, P., Gallego, J., Richards, T. and Malingreau, J. (2002). Determination of deforestation rates of the world's humid tropical forests. *Science*, **297**(5583):999–1002.

Adams, J., Sabol, D., Kapos, V., Filho, R., Roberts, D., Smith, M. O. and Gillespie, A. (1995). Classification of multispectral images based on fractions of endmembers: application to land-cover change in the Brazilian Amazôn. *Remote Sensing of Environment*, **52**:137–154.

Allen, T. and Kupfer, J. (2000). Application of Spherical Statistics to Change Vector Analysis of Landsat Data-Southern Appalachian Spruce-Fir Forests. *Remote Sensing of Environment*, **74**(3):482–493.

Almeida-Filho, R. and Shimabukuro, Y. (2002). Digital processing of a Landsat-TM time series for mapping and monitoring degraded areas caused by independent gold miners, Roraima State, Brazilian Amazon. *Remote Sensing of Environment*, **79**(1):42–50.

Alves, D., Pereira, J., De Sousa, C., Soares, J. and Yamaguchi, F. (1999). Characterizing landscape changes in central Rondonia using Landsat TM imagery. *International Journal of Remote Sensing*, **20**(14):2877–2882.

Anderson, L., Shimabukuro, Y., DeFries, R. and Morton, D. (2005). Assessment of deforestation in near real time over the Brazilian Amazon using multitemporal fraction images derived from terra MODIS. *IEEE Geoscience and Remote Sensing Letters*, **2**(3):315–318.

Anttila, P. (2002). Updating stand level inventory data applying growth models and visual interpretation of aerial photographs. *Silva Fennica*, **36**(2):549–560.

Asner, G., Bustamante, M. and Townsend, A. (2003). Scale dependence of biophysical structure in deforested areas bordering the Tapajo's National Forest, Central Amazon. *Remote Sensing of Environment*, **87**(4):507–520.

Asner, G., Keller, M., Pereira, R. and Zweede, J. (2002). Remote sensing of selective logging in Amazonia - Assessing limitations based on detailed field observations, Landsat ETM+, and textural analysis. *Remote Sensing of Environment*, **80**(3):483–496.

Asner, G. and Warner, A. (2003). Canopy shadow in IKONOS satellite observations of tropical forests and savannas. *Remote Sensing of Environment*, **87**(4):521–533.

Baatz, M. and Schäpe, A. (2000). Multiresolution Segmentation - an optimization approach for high quality multi-scale image segmentation. In Strobl, J., Blaschke, T. and Griesebner, G. (Editors), *Angewandte Geographische Informationsverarbeitung XII*, pp. 12–23. Wichmann-Verlag, Heidelberg.

Balmford, A., Bennun, L., Brink, B. t., Cooper, D., Côte, I. M., Crane, P., Dobson, A., Dudley, N., Dutton, I., Green, R. E., Gregory, R. D., Harrison, J., Kennedy, E. T., Kremen, C., Leader-Williams, N., Lovejoy, T. E., Mace, G., May, R., Mayaux, P., Morling, P., Phillips, J., Redford, K., Ricketts, T. H., Rodriguez, J. P., Sanjayan, M., Schei, P. J., van Jaarsveld, A. S. and Walther, B. A. (2005). The Convention on Biological Diversity's 2010 Target. *Science*, **307**(5707):212–213.

Bickel, P. (1965). On some robust estimates of location. *The Annals of Mathematical Statistics*, **36**(3):847–858.

Biging, G. S., Colby, D. R. and Congalton, R. G. (1998). *Remote sensing change detection: environmental monitoring methods and* *applications*, chapter Sampling systems for change detection accuracy assessment, pp. 281–308. Ann Arbor Press, Chelsea, MI.

Blaschke, T., Burnett, C. and Pekkarinen, A. (2004). *Remote Sensing Image Analysis: Including the Spatial Domain*, chapter Image Segmentation Methods for Object-based Analysis and Classification, pp. 211–236. Kluwer Academic Publishers, Netherlands.

Bruzzone, L. and Prieto, D. (2000a). An adaptive parcel-based technique for unsupervised change detection. *International Journal of Remote Sensing*, **21**(4):817–822.

Bruzzone, L. and Prieto, D. (2000b). Automatic analysis of the difference image for unsupervised change detection. *IEEE Transactions on Geoscience and Remote Sensing*, **38**(3):1171–1182.

Büttner, G., Feranec, J. and Jaffrain, G. (2002). Corine land cover update 2000. Technical report, European Environmental Agency, Copenhagen, Denmark.

Byrne, G., Crapper, P. and Mayo, K. (1980). Monitoring land-cover change by principal component analysis of multitemporal landsat data. *Remote Sensing of Environment*, **10**(3):175–184.

Cakir, H., Khorram, S. and Nelson, S. (2006). Correspondence analysis for detecting land cover change. *Remote Sensing of Environment*, **102**(3-4):306–317.

Canty, M., Nielsen, A. and Schmidt, M. (2004). Automatic radiometric normalization of multitemporal satellite imagery. *Remote Sensing of Environment*, **91**(3-4):441–451.

Carreiras, J., Pereira, J., Campagnolo, M. and Shimabukuro, Y. (2006). Assessing the extent of agriculture/pasture and secondary succession forest in the Brazilian Legal Amazon using SPOT VEGETATION data. *Remote Sensing of Environment*, **101**(3):283–298.

Chavez, P. and Kwarteng, A. (1989). Extracting spectral contrast in Landsat Thematic Mapper image data using selective Principal Componant Analysis. *Photogrammetric Engineering and Remote Sensing*, **55**(3):339–348.

Chavez, P. and MacKinnon, D. (1994). Automatic detection of vegetation changes in the southwestern United States using remotely sensed images. *Photogrammetric Engineering and Remote Sensing*, **60**(5):571–583.

Chavez Jr., P. (1996). Image-based atmospheric corrections revisited and improved. *Photogrammetric Engineering and Remote Sensing*, **62**:1025–1036.

Cohen, J. (1960). A coefficient of agreement for nominal scales. *Educational and Psychological Measurement*, **20**:37–46.

Cohen, W., Fiorella, M., Gray, J., Helmer, E. and Anderson, K. (1998). An efficient and accurate method for mapping forest clearcuts in the Pacific Northwest using Landsat imagery. *Photogrammetric Engineering and Remote Sensing*, **64**(4):293–300.

Cohen, W. B. and Fiorella, M. (1998). *Remote sensing change detection: environmental monitoring methods and applications*, chapter Comparison of methods for detecting conifer forest change with thematic mapper imagery, pp. 89–102. Ann Arbor Press, Chelsea, MI.

Collins, J. and Woodcock, C. (1996). An assessment of several linear change detection techniques for mapping forest mortality using multitemporal landsat TM data. *Remote Sensing of Environment*, **56**(1):66–77.

Collins, J. and Woodcock, C. (1999). Geostatistical estimation of resolution-dependent variance in remotely sensed images. *Photogrammetric Engineering and Remote Sensing*, **61**:41–50.

Coppin, P. and Bauer, M. (1994). Processing of multitemporal Landsat TM imagery to optimize Extraction of forest cover change features. *IEEE Transactions on Geoscience and Remote Sensing*, **32**(4):918–927.

Coppin, P. and Bauer, M. (1995). The potential contribution of pixel-based canopy change information to stand-based forest management in the northern U.S. *Journal of Environmental Management*, **44**:69–82.

Coppin, P. and Bauer, M. (1996). Digital change detection in forest ecosystems with remote sensing imagery. *Remote Sensing Reviews*, **13**:207–234.

Coppin, P., Jonckheere, I., Nackaerts, K., Muys, B. and Lambin, E. (2004). Digital change detection methods in ecosystem monitoring: a review. *International Journal of Remote Sensing*, **25**(9):1565–1596.

Coppin, P., Nackaerts, K., Queen, L. and Brewer, H. (2001). Operational monitoring of green biomass change for forest management. *Photogrammetric Engineering and Remote Sensing*, **67**(5):603–611.

Crist, E. and Cicone, R. (1984). A physically-based transformation of Thematic Mapper data The TM tasseled cap. *IEEE Transactions on Geoscience and Remote Sensing*, **22**:256–263.

Currit, N. (2005). Development of a remotely sensed, historical land-cover change database for rural Chihuahua, Mexico. *International Journal of Applied Earth Observation and Geoinformation*, **7**(3):232–247.

Dai, X. and Khorram, S. (1998). The effects of image misregistration on the accuracy of remotely sensed change detection. *IEEE Transactions on Geoscience and Remote Sensing*, **36**(5):1566–1577.

Davis, L. S. (1975). A survey of edge detection techniques. *Computer Graphics Image Process*, **4**:248–270.

de Wasseige, C. and Defourny, P. (2002). Retrieval of tropical forest structure characteristics from bi- directional reflectance of SPOT images. *Remote Sensing of Environment*, **83**(3):362–375.

de Wasseige, C. and Defourny, P. (2004). Remote sensing of selective logging impact for tropical forest management. *Forest Ecology and Management*, **188**(1-3):161–173.

de Wasseige, C., Languy, M. and Defourny, P. (2005). Changing the course of events on the ground. *SPOT Magazine*, **40**:11–13.

Deer, P. (1998). *Digital change detection in remotely sensed imagery using fuzzy set theory.* Ph.D. thesis, Department of Geography and Department of Computer Science, University of Adelaide, Australia.

DeFries, R., Houghton, R., Hansen, M., Field, C., Skole, D. and Townshend, J. (2002). Carbon emissions from tropical deforestation and regrowth based on satellite observations for the 1980s and 1990s. *Proceedings of the National Academy of Sciences*, **99**(22):14256–14261.

Di Gregorio, A. (2005). *Land Cover Classification System (LCCS), version 2: Classification Concepts and User Manual.* Food and Agriculture Organization of the United Nations (FAO), Rome, Italy.

Di Maio Mantovani, A. and Setzer, A. (1997). Deforestation detection in the Amazon with an AVHRR-based system. *International Journal of Remote Sensing*, **18**(2):273–286.

Dorren, L., Maier, B. and Seijmonsbergen, A. (2003). Improved Landsat-based forest mapping in steep mountainous terrain using object-based classification. *Forest Ecology and Management*, **183**(1-3):31–46.

Duveiller, G., Defourny, P., Desclée, B. and Mayaux, P. (2007). Deforestation in Central Africa: estimates at regional, national and landscape levels by advanced processing of systematically-distributed Landsat extracts. *Remote Sensing of Environment*, **accepted**.

FAO (2000). FRA 2000: on definitions of forest and forest change. Fao, forestry working paper 33, Food and Agriculture Organization of the United Nations, Rome.

FAO (2001). Global forest resources assessment 2000. Report fao, forestry paper 140, Food and Agriculture Organization of the United Nations, Rome.

FAO (2006). Global forest resources assessment 2005. Report fao, forestry paper 147, Food and Agriculture Organization of the United Nations, Rome.

Fiorella, M. and Ripple, W. (1993). Analysis of conifer forest regeneration using Landsat Thematic Mapper data. *Photogrammetric Engineering and Remote Sensing*, **59**(9):1383–1388.

Flanders, D., Hall-Beyer, M. and Pereverzoff, J. (2003). Preliminary evaluation of eCognition object-based software for cut block delineation and feature extraction. *Canadian Journal of Remote Sensing*, **29**(4):441–452.

Foody, G. (2002). Status of land cover classification accuracy assessment. *Remote Sensing of Environment*, **80**(1):185–201.

Foody, G. (2003). Remote sensing of tropical forest environments: towards the monitoring of environmental resources for sustainable development. *International Journal of Remote Sensing*, **24**(20):4035–4046.

Franklin, S., Lavigne, M., Wulder, M. and McCaffrey, T. (2002). Large-area forest structure change detection: An example. *Canadian Journal of Remote Sensing*, **28**(4):588–592.

Franklin, S., Moskal, L., Lavigne, M. and Pugh, K. (2000). Interpretation and classification of partially harvested forest stands in the Fundy Model Forest using multitemporal Landsat TM digital data. *Canadian Journal of Remote Sensing*, **26**:318–333.

Franklin, S. E., Jagielko, C. B. and Lavigne, M. B. (2005). Sensitivity of the Landsat enhanced wetness difference index (EWDI) to temporal resolution. *Canadian Journal of Remote Sensing*, **31**(2):149–152.

Fu, K. S. and Mui, J. K. (1981). A survey on image segmentation. *Pattern Recognitio*, **13**:3–16.

Fung, T. and LeDrew, E. (1988). The determination of optimal threshold levels for change detection using various accuracy indice. *Photogrammetric Engineering and Remote Sensing*, **54**(10):1449–1454.

Gao, B. C. (1996). NDWI - A normalized difference water index for remote sensing of vegetation liquid water from space. *Remote Sensing of Environment*, **58**(3):257–266.

Geist, H. (2006). *Our earth's changing land: an encyclopedia of land-use and land-cover change*. Greenwood Press.

Geist, H. and Lambin, E. (2002). Proximate causes and underlying driving forces of tropical deforestation. *Bioscience*, **52**(2):143–150.

Gerylo, G., Hall, R., Franklin, S. and Smith, L. (2002). Empirical relations between Landsat TM spectral response and forest stands near fort simpson, Northwest Territories, Canada. *Canadian Journal of Remote Sensing*, **28**(1):68–79.

Gholz, H., Nakane, K. and Shimoda, H. (1997). *The use of remote sensing in the modelling of forest productivity*. Kluwer Academic Publishers.

Gopal, S. and Woodcock, C. (1996). Remote sensing of forest change using artificial neural networks. *IEEE Transactions on Geoscience and Remote Sensing*, **34**(2):398–404.

Greenberg, J., Kefauver, S., Stimson, H., Yeaton, C. and Ustin, S. (2005). Survival analysis of a neotropical rainforest using multitemporal satellite imagery. *Remote Sensing of Environment*, **96**(2):202–211.

Guild, L., Cohen, W. and Kauffman, J. (2004). Detection of deforestation and land conversion in Rondonia, Brazil using change detection techniques. *International Journal of Remote Sensing*, **25**(4):731–750.

Guyot, G., Guyon, D. and Riom, J. (1989). Factors affecting the spectral response of forest canopies- A review. *Geocarto International*, **4**:3–18.

Hall, J. (2001). Criteria and indicators of sustainable forest management. *Environmental Monitoring and Assessment*, **67**(1-2):109–119.

Hall, O. and Hay, G. J. (2003). A multiscale object-specific approach to digital change detection. *International Journal of Applied Earth Observation and Geoinformation*, **4**(4):311–327.

Hansen, M. and DeFries, R. (2004). Detecting long-term global forest change using continuous fields of tree-cover maps from 8-km advanced very high resolution radiometer (AVHRR) data for the years 1982-99. *Ecosystems*, **7**(7):695–716.

Haralick, R. M. and Shapiro, L. G. (1985). Survey, image segmentation techniques. *Computer Vision, Graphics, and Image Processing*, **29**:100–132.

Hardisky, M., Klemas, V. and Smart, R. (1983). The influence of soil salinity, growth form, and leaf moisture on the spectral radiance of Spartina alterniflora canopies. *Photogrammetric Engineering and Remote Sensing*, **49**:77–83.

Hay, G., Castilla, G., Wulder, M. and Ruiz, J. (2005). An automated object-based approach for the multiscale image segmentation of forest scenes. *International Journal of Applied Earth Observation and Geoinformation*, **7**:339–359.

Hayes, D. and Sader, S. (2001). Comparison of change-detection techniques for monitoring tropical forest clearing and vegetation regrowth in a time series. *Photogrammetric Engineering and Remote Sensing*, **67**(9):1067–1075.

Healey, S., Cohen, W., Yang, Z. and Krankina, O. (2005). Comparison of Tasseled Cap-based Landsat data structures for use in forest disturbance detection. *Remote Sensing of Environment*, **97**(3):301–310.

Healey, S., Yang, Z., Cohen, W. and Pierce, D. (2006). Application of two regression-based methods to estimate the effects of partial harvest on forest structure using Landsat data. *Remote Sensing of Environment*, **101**(1):115–126.

Heikkonen, J. and Varjo, J. (2004). Forest change detection applying Landsat Thematic Mapper difference features: A comparison of different classifiers in boreal forest conditions. *Forest Science*, **50**(5):579–588.

Häme, T. (1991). Spectral interpretation of changes in forest using satellite scanner images. *Acta Forestalia Fennica*, **222**:111 pp.

Helsinki: The Society of Forest in Finland – The Finnish Forest Research Institute.

Häme, T., Heiler, I. and Miguel-Ayanz, J. (1998). An unsupervised change detection and recognition system for forestry. *International Journal of Remote Sensing*, **19**(6):1079–1099.

Hoaglin, D., Mosteller, F. and Tukey, J. (1983). *Understanding Robust and Exploratory Data Analysis*. Wiley, New York.

Horler, D. and Ahern, F. (1986). Forestry information content of Thematic Mapper data. *International Journal of Remote Sensing*, **7**:405–428.

Huber, P. (1972). The 1972 Wald lecture robust statistics: a review. *The Annals of Mathematical Statistics*, **43**(4):1041–1067.

IPCC (2001). *Climate Change 2001: The Scientific Basis*. Cambridge: Cambridge University Press.

Ishii, H. and McDowell, N. (2002). Age-related development of crown structure in coastal Douglas-fir trees. *Forest Ecology and Management*, **169**(3):257–270.

Jakubauskas, M. and Price, K. (1997). Empirical relationships between structural and spectral factors of Yellowstone lodgepole pine forests. *Photogrammetric Engineering and Remote Sensing*, **63**(12):1375–1381.

Jensen, J., Qiu, F. and Ji, M. (1999). Predictive modelling of coniferous forest age using statistical and artificial neural network approaches applied to remote sensor data. *International Journal of Remote Sensing*, **20**(14):2805–2822.

Jha, C. and Unni, N. (1994). Digital change detection of forest conversion of a dry tropical indian forest region. *International Journal of Remote Sensing*, **15**(13):2543–2552.

Jin, S. and Sader, S. (2005a). Comparison of time series tasseled cap wetness and the normalized difference moisture index in detecting forest disturbances. *Remote Sensing of Environment*, **94**(3):364–372.

Jin, S. and Sader, S. (2005b). MODIS time-series imagery for forest disturbance detection and quantification of patch size effects. *Remote Sensing of Environment*, **99**(4):462–470.

Jolly, A., Guyon, D. and Riom, J. (1996). Use of middle-infrared Landsat Thematic Mapper data for representation of clearcuts in the Landes region. *International Journal of Remote Sensing*, **17**(18):3615–3645.

Kasischke, E. S., Goetz, S., Hansen, M. C., Ustin, S. L., Ozdogan, M., Woodcock, C. E. and Rogan, J. (2004). *Remote sensing for natural resources management and environmental monitoring*, volume 4 of *Manual of remote sensing*, chapter Temperate and boreal forests, pp. 147–238. John Wiley & Sons, Inc., 3rd edition.

Kass, M., Witkin, A. and Terzopoulos, D. (1988). Snakes: Active contour models. *International Journal of Computer Vision*, **1**(4):321–331.

Kauth, R. and Thomas, G. (1976). The tasselled cap - A graphic description of the spectral-temporal development of agricultural crops as seen by Landsat. In *Proceedings of the Symposium on Machine Processing of Remotely Sensed Data, Purdue University, West Lafayette, Ind.*

Kayitakiré, F., Giot, P. and Defourny, P. (2002). Automated delineation of the forest stands using digital color orthophotos: Case study in Belgium. *Canadian Journal of Remote Sensing*, **28**(5):629–640.

Kayitakiré, F., Hamel, C. and Defourny, P. (2006). Retrieving forest structure variables based on image texture analysis and IKONOS-2 imagery. *Remote Sensing of Environment*, **102**(3-4):390–401.

Kimes, D., Holben, B., Nickeson, J. and McKee, W. (1996). Extracting forest age in a Pacific Northwest Forest from thematic mapper and topographic data. *Remote Sensing of Environment*, **56**(2):133–140.

Kotz, S., Johnson, N. and Read, C. (1988). *Encyclopedia of statistical sciences*. Wiley, New York.

Kurz, W. A., Apps, M., Banfield, E. and Stinson, G. (2002). Forest carbon accounting at the operational scale. *Forestry Chronicle*, **78**(5):672–679.

Languy, M. and de Merode, E. (Editors) (2006). *Virunga; survie du premier Parc d'Afrique*. Lannoo, Tielt, Belgium.

Lanly, J. (1982). Tropical Forest Resources. Report fao, forestry paper 30, Food and Agriculture Organization of the United Nations, Rome.

Latham, J. (2001). AFRICOVER East Africa. *LUCC Newsletter*, **7**:15–16.

Le Hégarat-Mascle, S. and Seltz, R. (2004). Automatic change detection by evidential fusion of change indices. *Remote Sensing of Environment*, **91**(3-4):390–404.

Lee, S. (1995). A trimmed mean of location of an AR(infinity) stationary process. *Journal of Statistical Planning and Inference*, **48**(2):131–140.

Liang, S., Fallah-Adl, H., Kalluri, S., Jaja, J., Kauffman, Y. and Townshend, J. (1997). An operational atmospheric correction algorithm for Landsat Thematic Mapper imagery over the land. *Journal of Geophysical Research*, **102**(17):173–186.

Lillesand, T., Kiefer, R. and Chipman, J. (2004). *Remote sensing and image interpretation*. Wiley, New York, 5th edition.

Loveland, T. and DeFries, R. (2004). *Ecosystems and land-use change*, chapter Observing and monitoring land use and land cover change, pp. 231–246. Number 153 in Geophysical monograph. American Geophysical Union.

Lu, D., Batistella, M. and Moran, E. (2004a). Multitemporal spectral mixture analysis for Amazonian land-cover change detection. *Canadian Journal of Remote Sensing*, **30**(1):87–100.

Lu, D., Mausel, P., Batistella, M. and Moran, E. (2005). Land-cover binary change detection methods for use in the moist tropical region of the Amazon: a comparative study. *International Journal of Remote Sensing*, **26**(1):101–114.

Lu, D., Mausel, P., Brondizio, E. and Moran, E. (2004b). Change detection techniques. *International Journal of Remote Sensing*, **25**(12):2365–2407.

Lu, D., Mausel, P., Brondizio, E. and Moran, E. (2004c). Relationships between forest stand parameters and Landsat TM spectral responses in the Brazilian Amazon Basin. *Forest Ecology and Management*, **198**(1-3):149–167.

Lucas, R., Honzak, M., Amaral, I., Curran, P. and Foody, G. (2002). Forest regeneration on abandoned clearances in central Amazonia. *International Journal of Remote Sensing*, **23**(5):965–988.

Lunetta, R., Johnson, D., Lyon, J. and Crotwell, J. (2004). Impacts of imagery temporal frequency on land-cover change detection monitoring. *Remote Sensing of Environment*, **89**(4):444–454.

Lyon, J., Yuan, D., Lunetta, R. and Elvidge, C. (1998). A change detection experiment using vegetation indices. *Photogrammetric Engineering and Remote Sensing*, **64**(2):143–150.

Malila, W. (1980). Change vector analysis : an approach for detecting forest changes with Landsat. In *Proceedings of the 6th annual Symposium on Machine Processing of Remotely Sensed Data*, pp. 326–335. Purdue University, West Lafayette, Indiana (Ann Arbor, ERIM).

Malingreau, J. and Tucker, C. (1988). Large-scale deforestation in the southeastern amazon basin of Brazil. *Ambio*, **17**(1):49–55.

McDonald, A. J., Gemmell, F. M. and Lewis, P. E. (1998). Investigation of the utility of spectral vegetation indices for determining information on coniferous forests. *Remote Sensing of Environment*, **66**(3):250–272.

Meinel, G. and Neubert, M. (2004). A comparison of segmentation programs for high resolution remote sensing data. In *Proceedings of the XXth ISPRS Congress*. Istanbul, Turkey.

Michener, W. and Houhoulis, P. (1997). Detection of vegetation changes associated with extensive flooding in a forested ecosystem. *Photogrammetric Engineering and Remote Sensing*, **63**(12):1363–1374.

Middleton, E., Chan, S., Rusin, R. and Mitchell, S. (1997). Optical properties of black spruce and jack pine needles at BOREAS sites in Saskatchewan, Canada. *Canadian Journal of Remote Sensing*, **23**(2):108–119.

Miller, A., Bryant, E. and Birnie, R. (1998). Analysis of land cover changes in the Northern Forest of New England using multitemporal Landsat MSS data. *International Journal of Remote Sensing*, **19**(2):245–265.

Mäkelä, H. and Pekkarinen, A. (2001). Estimation of timber volume at the sample plot level by means of image segmentation and Landsat TM imagery. *Remote Sensing of Environment*, **77**(1):66–75.

Morisette, J., Khorram, S. and Mace, T. (1999). Land-cover change detection enhanced with generalized linear models. *International Journal of Remote Sensing*, **20**(14):2703–2721.

Morton, D., DeFries, R., Shimabukuro, Y., Anderson, L., Espirito-Santo, F., Hansen, M. and Carroll, M. (2005). Rapid Assessment of Annual Deforestation in the Brazilian Amazon Using MODIS Data. *Earth Interactions*, **9**:1–22.

Muchoney, D. and Haack, B. (1994). Change detection for monitoring forest defoliation. *Photogrammetric Engineering and Remote Sensing*, **60**(10):1243–1251.

Munoz, X., Freixenet, J., Cufi, X. and Marti, J. (2003). Strategies for image segmentation combining region and boundary information. *Pattern Recognition Letters*, **24**(1-3):375–392.

Nackaerts, K., Vaesen, K., Muys, B. and Coppin, P. (2005). Comparative performance of a modified change vector analysis in forest change detection. *International Journal of Remote Sensing*, **26**(5):839–852.

Nelson, R. (1983). Detecting forest canopy change due to insect activity using Landsat MSS. *Photogrammetric Engineering and Remote Sensing*, **49**(9):1303–1314.

Nielsen, A., Conradsen, K. and Simpson, J. (1998). Multivariate alteration detection (MAD) and MAF postprocessing in multispectral, bitemporal image data: New approaches to change detection studies. *Remote Sensing of Environment*, **64**(1):1–19.

Niemeyer, I. (2006). Object-based change detection – an unsupervised approach. In *Proceedings of the 1st International Conference on Object-based Image Analysis (OBIA 2006)*. Salzburg University, Austria.

Nilson, T., Kuusk, A., Lang, M. and Lukk, T. (2003). Forest reflectance modeling: Theoretical aspects and applications. *Ambio*, **32**(8):535–541.

Nilson, T. and Peterson, U. (1994). Age-dependence of forest reflectance - Analysis of main driving factors. *Remote Sensing of Environment*, **48**(3):319–331.

Pal, N. and Pal, S. (1993). A review on image segmentation techniques. *Pattern Recognition*, **26**(9):1277–1294.

Petit, C., Scudder, T. and Lambin, E. (2001). Quantifying processes of land-cover change by remote sensing: resettlement and rapid land-cover change in southeastern Zambia. *International Journal of Remote Sensing*, **22**:3435–3456.

Pussa, K., Liira, J. and Peterson, U. (2005). The effects of successional age and forest site type on radiance of forest clear-cut communities. *Scandinavian Journal of Forest Research*, **20**:79–87.

Radke, R., Andra, S., Al Kofahi, O. and Roysam, B. (2005). Image change detection algorithms: A systematic survey. *Ieee Transactions on Image Processing*, **14**(3):294–307.

Rametsteiner, E. and Simula, M. (2003). Forest certification–An instrument to promote sustainable forest management? *Journal of Environmental Management*, **67**(1):87–98.

Rautiainen, M., Stenberg, P., Nilson, T. and Kuusk, A. (2004). The effect of crown shape on the reflectance of coniferous stands. *Remote Sensing of Environment*, **89**(1):41–52.

Richards, J. (1993). *Remote sensing digital image analysis. An introduction*. Springer-Verlag, Berlin, 2nd edition.

Richards, J. (2006). *Remote sensing digital image analysis. An introduction*. Springer-Verlag.

Ridd, M. and Liu, J. (1998). A comparison of four algorithms for change detection in an urban environment. *Remote Sensing of Environment*, **63**(2):95–100.

Roberts, D., Batista, G., Pereira, J., Waller, E. and Nelson, B. (1998). *Lunetta, R.S. and Elvidge, C. D.*, chapter Change identification using multitemporal spectral mixture analysis: applications in eastern Amazônia, pp. 137–161. Ann Arbor Press, Chelsea, MI.

Rogan, J. and Chen, D. (2004). Remote sensing technology for mapping and monitoring land-cover and land-use change. *Progress in Planning*, **61**:301–325.

Rogan, J., Franklin, J. and Roberts, D. (2002). A comparison of methods for monitoring multitemporal vegetation change using Thematic Mapper imagery. *Remote Sensing of Environment*, **80**(1):143–156.

Rogan, J., Miller, J., Stow, D., Franklin, J., Levien, L. and Fischer, C. (2003). Land-cover change monitoring with classification trees using Landsat TM and ancillary data. *Photogrammetric Engineering and Remote Sensing*, **69**(7):793–804.

Rogerson, P. (2002). Change detection thresholds for remotely sensed images. *Journal of Geographical Systems*, **4**(1):85–97.

Rosenfield, G. and Fitzpatrick-Lins, K. (1986). A coefficient of agreement as a measure of thematic classification accuracy. *Photogrammetric Engineering and Remote Sensing*, **52**:223–227.

Rosin, P. (2002). Thresholding for change detection. *Computer Vision and Image Understanding*, **86**(2):79–95.

Roy, P. and Tomar, S. (2001). Landscape cover dynamics pattern in Meghalaya. *International Journal of Remote Sensing*, **22**(18):3813–3825.

Sader, S. (1995). Spatial characteristics of forest clearing and vegetation regrowth as detected by Landsat thematic mapper imagery. *Photogrammetric Engineering and Remote Sensing*, **61**(9):1145–1151.

Sader, S., Hayes, D., Hepinstall, J., Coan, M. and Soza, C. (2001). Forest change monitoring of a remote biosphere reserve. *International Journal of Remote Sensing*, **22**(10):1937–1950.

Sader, S. and Winne, J. (1992). RGB-NDVI color composites for visualizing forest change dynamics. *International Journal of Remote Sensing*, **13**(16):3055–3067.

Saksa, T., Uuttera, J., Kolstrom, T., Lehikoinen, M., Pekkarinen, A. and Sarvi, V. (2003). Clear-cut detection in boreal forest aided by remote sensing. *Scandinavian Journal of Forest Research*, **18**(6):537–546.

Sala, O. E., Chapin, F. S., Armesto, J. J., Berlow, E., Bloomfield, J., Dirzo, R., Huber-Sanwald, E., Huenneke, L. F., Jackson, R. B., Kinzig, A., Leemans, R., Lodge, D. M., Mooney, H. A., Oesterheld, M., Poff, N. L., Sykes, M. T., Walker, B. H., Walker, M. and Wall, D. H. (2000). Global biodiversity scenarios for the year 2100. *Science*, **287**(5459):1770–1774.

Sanchez-Azofeifa, G., Harriss, R. and Skole, D. (2001). Deforestation in Costa Rica: A quantitative analysis using remote sensing imagery. *Biotropica*, **33**(3):378–384.

Saura, S. (2002). Effects of minimum mapping unit on land cover data spatial configuration and composition. *International Journal of Remote Sensing*, **23**(22):4853–4880.

Schott, J., Salvaggio, C. and Volchok, W. (1988). Radiometric scene normalization using pseudoinvariant features. *Remote Sensing of Environment*, **26**:1–7.

Schroeder, T., Cohen, W., Song, C., Canty, M. and Yang, Z. (2006). Radiometric correction of multi-temporal Landsat data for characterization of early successional forest patterns in western Oregon. *Remote Sensing of Environment*, **103**(1):16–26.

Singh, A. (1989). Digital change detection techniques using remotely-sensed data. *International Journal of Remote Sensing*, **10**(6):989–1003.

Sivanpillai, R., Smith, C., Srinivasan, R., Messina, M. and Ben Wu, X. (2006). Estimation of managed loblolly pine stand age and density with Landsat ETM+ data. *Forest Ecology and Management*, **223**(1-3):247–254.

Skakun, R., Wulder, M. and Franklin, S. (2003). Sensitivity of the Thematic Mapper Enhanced Wetness Difference Index (EWDI) to detect mountain pine beetle red-attack damage. *Remote Sensing of Environment*, **86**(4):433–443.

Soille, P. and Pesaresi, M. (2002). Advances in mathematical morphology applied to geoscience and remote sensing. *IEEE Transactions on Geoscience and Remote Sensing*, **40**(9):2042–2055.

Song, C. and Woodcock, C. (2003). Monitoring forest succession with multitemporal Landsat images: Factors of uncertainty. *IEEE Transactions on Geoscience and Remote Sensing*, **41**(11):2557–2567.

Song, C., Woodcock, C. and Li, X. (2002). The spectral/temporal manifestation of forest succession in optical imagery - The potential of multitemporal imagery. *Remote Sensing of Environment*, **82**(2-3):285–302.

Song, C., Woodcock, C., Seto, K., Lenney, M. and Macomber, S. (2001). Classification and change detection using Landsat TM data: When and how to correct atmospheric effects? *Remote Sensing of Environment*, **75**(2):230–244.

Souza, C. and Barreto, P. (2000). An alternative approach for detecting and monitoring selectively logged forests in the Amazon. *International Journal of Remote Sensing*, **21**(1):173–179.

Spanner, M., Pierce, L., Peterson, D. and Running, S. (1990). Remote sensing of temperate coniferous forest leaf area index. The influence of canopy closure, understory vegetation and background reflectance. *International Journal of Remote Sensing*, **11**(1):95–111.

Stehman, S. (2005). Comparing estimators of gross change derived from complete coverage mapping versus statistical sampling of remotely sensed data. *Remote Sensing of Environment*, **96**(3-4):466–474.

Steininger, M. (1996). Tropical secondary forest regrowth in the Amazon: Age, area and change estimation with Thematic Mapper data. *International Journal of Remote Sensing*, **17**(1):9–27.

Steininger, M., Tucker, C., Townshend, J., Killeen, T., Desch, A., Bell, V. and Ersts, P. (2001). Tropical deforestation in the Bolivian Amazon. *Environmental Conservation*, **28**(2):127–134.

Sunar, F. (1998). An analysis of changes in a multi-date data set: a case study in the Ikitelli area, Istanbul, Turkey. *International Journal of Remote Sensing*, **19**(2):225–235.

Townshend, J. and Justice, C. (1995). Spatial variability of images and the monitoring of changes in the normalized difference vegetation index. *International Journal of Remote Sensing*, **16**(12):2187–2195.

Tucker, C. and Townshend, J. (2000). Strategies for monitoring tropical deforestation using satellite data. *International Journal of Remote Sensing*, **21**(6-7):1461–1471.

Turner, B., Villar, S., Foster, D., Geoghegan, J., Keys, E., Klepeis, P., Lawrence, D., Mendoza, P., Manson, S., Ogneva-Himmelberger, Y., Plotkin, A., Salicrup, D., Chowdhury, R., Savitsky, B., Schneider, L., Schmook, B. and Vance, C. (2001).

Deforestation in the southern Yucatan peninsular region: an integrative approach. *Forest Ecology and Management*, **154**(3):353–370.

Uotila, A. and Kouki, J. (2005). Understorey vegetation in spruce-dominated forests in eastern Finland and Russian Karelia: Successional patterns after anthropogenic and natural disturbances. *Forest Ecology and Management*, **215**(1-3):113–137.

Varjo, J. (1996). Controlling continuously updated forest data by satellite remote sensing. *International Journal of Remote Sensing*, **17**(1):43–67.

Vermote, E., Tanre, D., Deuze, J., Henman, M. and Morcrette, J. (1997). Second simulation of the satellite signal in the solar spectrum (6S), An overview. *IEEE Transactions on Geoscience and Remote Sensing*, **35**(3):675–686.

Vincent, L. and Soille, P. (1991). Watersheds in digital spaces: An efficient algorithm based on immersion simulations. *IEEE Transactions on Pattern Analysis and Machine Intelligence*, **13**:583–589.

Volcani, A., Karnieli, A. and Svoray, T. (2005). The use of remote sensing and GIS for spatio-temporal analysis of the physiological state of a semi-arid forest with respect to drought years. *Forest Ecology and Management*, **215**(1-3):239–250.

Walter, V. (2004). Object-based classification of remote sensing data for change detection. *Isprs Journal of Photogrammetry and Remote Sensing*, **58**(3-4):225–238.

Wilson, E. and Sader, S. (2002). Detection of forest harvest type using multiple dates of Landsat TM imagery. *Remote Sensing of Environment*, **80**(3):385–396.

Woodcock, C., Macomber, S., Pax-Lenney, M. and Cohen, W. (2001). Monitoring large areas for forest change using Landsat: Generalization across space, time and Landsat sensors. *Remote Sensing of Environment*, **78**(1-2):194–203.

Wulder, A., Skakun, R., Kurz, W. and White, J. (2004). Estimating time since forest harvest using segmented Landsat ETM+ imagery. *Remote Sensing of Environment*, **93**(1-2):179–187.

Zhan, X., Sohlberg, R., Townshend, J., DiMiceli, C., Carroll, M., Eastman, J., Hansen, M. and DeFries, R. (2002). Detection of land cover changes using MODIS 250 m data. *Remote Sensing of Environment*, **83**(1-2):336–350.

Zhang, Q., Devers, D., Desch, A., Justice, C. and Townshend, J. (2005). Mapping tropical deforestation in Central Africa. *Environmental Monitoring and Assessment*, **101**(1-3):69–83.

Titres récents de la collection :

2004

Département de biologie appliquée et des productions agricoles

N°43. Yankam Njonou, Rabelais, Analyse économique de la réponse du marché du blé différencié aux instruments de l'organisation commune des marchés du secteur des céréales : Le cas de la France.

N°47. Collard, François, Characterization of frutctosamine 3-kinase related protein.

N°49. Ruibal Mendieta, Nike Luisa, Lipids and minerals in spelt (Triticum aestivum ssp. spelta) and common wheat (T. aestivum ssp. vulgare): Chemical and nutritional distinction between both cereals.

Département de chimie appliquée et des bio-industries

N°41. Kanczewska, Justyna, Regulation of the plant plasma membrane H+-ATPase by phosphorylation and 14-3-3 proteins.

N°42. Liégeois, Catherine, Pour un meilleur contrôle du statut pro-oxydant/ antioxydant des matières premières de la bière. Etude de la contribution des différentes étapes de fabrication du moût aux teneurs en trans-2-nonénal des bières vieillies.

N°44. Counet, Christine, Détermination des structures chimiques des polyphénols du chocolat et étude de leurs principales propriétés fonctionnelles.

N°46. Lefebvre, Benoît, Plant H+-ATPase targeting to the plasma membrane is not by default and requires cytosolic structural determinants.

N°50. Dries Jan, Development and comparison of different multifunctional permeable reactive barrier (MPRB) concepts for the treatment of groundwater contaminated by pollutant mixtures.

N°51. Cranenbrouck, La culture monoxénique, un outil privilégié pour la systématique des champignons mycorhiziens à arbuscules et l'étude de leurs relations symbiotiques avec la plante hôte.

N°52. Callewaert Maïté, Surface modification by stimuli-responsive polymers : from model systems to stainless steel cleanability.

Département des sciences du milieu et de l'aménagement du territoire

N°45. Javaux, Mathieu, Solute transport in a heterogeneous unsaturated subsoil: experiments and modeling.

N°48. Fontenelle, Jean-Philippe, Dynamiques agraires, irrigation et institutions dans le delta du Fleuve rouge (Viêt-nam).

2005

Département de biologie appliquée et des productions agricoles

N°53. Nkunzimana, Tharcisse, Une filière agro-industrielle en mutation. Cas de la filière théicole au Burundi.

N°55. Meunier, Alexandre, Detection of rhizomania in Belgium: Diversity and characterization of Beet necrotic yellow vein virus RNAs-2 and –3.

N°56. Grissa, Kaouthar, Étude de la dynamique des populations et du contrôle des acariens ravageurs dans les vergers de pommiers tunisiens.

N°62. Rubayiza, Aloys, Authentication and quality control of coffee by fluorescence and Raman spectroscopy.

N°68. Odjo, Sunday Pierre, Modélisation en équilibre général non séparable et analyse de réformes agricoles et commerciales au Bénin.

N°69. Célestin, Dario Styve, Stabilisation du secteur caféier en Haïti par la promotion de la concurrence et la mise en œuvre d'un plan d'assurance pour la gestion des risques agricoles.

Département de chimie appliquée et des bio-industries

N° 57. Vermeulen, Catherine, Synthèse et caractérisation organoleptique de thiols polyfonctionnels ~ Recherche de leur présence dans la bière.

N°58. Van Wilder, Valérie, Phosphorylation des aquaporines de la membrane plasmique de maïs.

N°64. Bertinchamps, Fabrice, Total oxidation of chlorinated VOCs on supported oxide catalysts.

N°65. Demoulin, Olivier, Dynamic aspects of the surface of a palladium on alumina catalyst used in combustion of methane.

N°67. Trincal, Mathieu, Grx5p, a mitochondrial glutaredoxin required for mitochondrial DNA maintenance.

N°70. Dury, Frédéric, Coupling of the deoxygenation of benzoic acid with the oxidation of propylene as a new tool to elucidate the architecture of Mo-based oxide catalysts.

Département des sciences du milieu et de l'aménagement du territoire

N°54. Romanowicz, Agnieszka Aleksandra, The impacts of environmental change on water resources: A case study in the Dyle catchment (Belgium) in support of the implementation of the Water Framework Directive.

N°59. Delfosse, Thomas, Acid Neutralisation and Sulphur Retention in S-Impacted Andosols

N°60. Titeux, Hugues, Transfert de carbone organique dissous et de métaux dans des sols forestiers acides: influence du fonctionnement de la litière et des réserves minérales du sol.

N°61. Blaes, Xavier, Crop monitoring by advanced SAR remote sensing techniques : modelling and experimental analysis.

N°63. Farcy, Christine, L'aménagement forestier à la croisée des chemins. Éléments de réponse au défi posé par les nouvelles attentes d'une société en mutation.

N°66. Jonard, Mathieu, Dynamique des litières foliaires en peuplements purs et mélangés de chêne et de hêtre : Retombées foliaires et premières étapes de la décomposition.

2006

Département de biologie appliquée et des productions agricoles

N°71. Muratori, Frédéric, Reconnaissance des facteurs cuticulaires de l'hôte et conséquences sur l'exploitation des colonies par le parasitoïde de pucerons, *Aphidius rhopalosiphi* (Hymenoptera: Aphidiinae).

N°72. Condori Ali, Paulino Bruno, Analyse comparative et modélisation de la croissance et du développement de tubercules andins dans les Andes en Bolivie.

N°75. Doucet, Diane, Development of a model and similarities with a benyvirus.

N°76. Nkwembe Unsital, Guy-Bernard, La problématique de la pauvreté des ménages agricoles ruraux et urbains dans la périphérie de la ville de Kinshasa. Essai d'analyse du phénomène et de ses implications sur la sécurité alimentaire.

N°78. Ndayiragjie, Alexis, Relations entre métabolisme des polyamines et la résistance au stress salin chez le riz (*Oryza sativa* L.).

N°80. Secheli Ringot, Diana, Risk analysis of ochratoxin A and developpement of a decontamination procedure based on the biosorption of ochratoxin A onto yeast industry derivatives.

N°82. Abboudi, Tarik, The indispensable amino acid requirements for maintenance in Atlantic salmon fry.

N°83. Martins da Silva, Evaldo, Polyphenols from the Amazonian plant *Inga edulis*: process optimization for the production of purified extracts with high antioxidant capacity.

N°84. Fadlaoui, Aziz, Modélisation bioéconomique de la conservation des ressources génétiques animales.

N°85. Kambale Valimunzigha, Charles, Étude du comportement physiologique et agronomique de la tomate (*Solanum lycopersicum* L.) en réponse à un stress hydrique précoce.

N°86. Lepoint, Pascale, Speciation within the African Coffee Wilt Pathogen.

N°88. Mushagalusa Nachigera, Gustave, Competitive relationships in potato/maize intercropping: involvement of root system architecture

N°89. Nyamangyoku Ishibwela, Obedi, Ferrous iron toxicity: Mechanisms of resistance and impact on nutrient elements at the vegetative stage in cultivated rices (*Oryza sativa* L., *Oryza glaberrima* Steud and interspecific hybrids)

Département de chimie appliquée et des bio-industries

N°73. Pety de Thozée, Cédric, Implication of the ER quality control in the degradation of the yeast plasma membrane Pdr5 ^{L183P} ABC transporter.

N°79. Gurdak, Elzbieta, Supramolecular organization of collagen layers adsorbed on polymers.

N°87. Janssens, Xavier, Monitoring and predicting elusive species colonisation – Application to the otter in the Cévennes National Park (France).

Département des sciences du milieu et de l'aménagement du territoire

N°74. Kayitakire, François, Forest stand characterisation using very high resolutions satellite remote sensing

N°77. Van der Velde, Marijn, Agricultural and climatic impacts on the groundwater resources of a small island: measuring and modelling water and solute transport in soil and groundwater on Tongatapu.

N°81. Degen, Thomas, Dynamique initiale de la végétation herbacée et de la régénération ligneuse dans le cas de trouées, au sein d'une hêtraie (*Luzulo-Fagetum*).

2007

Département de chimie appliquée et des bio-industries

N°90. Eyers, Laurent, Characterization of bacterial populations of 2,4,6-trinitrotoluene (TNT) contaminated soils and isolation of a *Pseudomonas aeruginosa* strain with TNT denitration activities.

N°91. Dupré de Boulois, Hervé, Role of arbuscular mycorrhizal fungi on the accumulation of radiocaesium by plants.

Pour plus d'informations, visitez http://edoc.bib.ucl.ac.be/